

Tonopah Test Range Air Monitoring: CY2014 Meteorological, Radiological, and Airborne Particulate Observations

prepared by

George Nikolich, Craig Shadel, Jenny Chapman, Steve Mizell,
Greg McCurdy, Vicken Etyemezian, and Julianne J. Miller

submitted to

Nevada Field Office
National Nuclear Security Administration
U.S. Department of Energy
Las Vegas, Nevada

October 2015

Publication No. 45263

Reference herein to any specific commercial product, process, or service by trade name, trademark, manufacturer, or otherwise, does not necessarily constitute or imply its endorsement, recommendation, or favoring by the United States Government or any agency thereof or its contractors or subcontractors.

Available for sale to the public from:

U.S. Department of Commerce
National Technical Information Service
5301 Shawnee Rd.
Alexandria, VA 22312
Phone: 800.553.6847
Fax: 703.605.6900
Email: orders@ntis.gov
Online ordering: <http://www.osti.gov/ordering.htm>

Available electronically at <http://www.osti.gov/bridge>

Available for a processing fee to the U.S. Department of Energy and its contractors, in paper, from:

U.S. Department of Energy
Office of Scientific and Technical Information
P.O. Box 62
Oak Ridge, TN 37831-0062
Phone: 865.576.8401
Fax: 865.576.5728
Email: reports@adonis.osti.gov

Tonopah Test Range Air Monitoring: CY2014 Meteorological, Radiological, and Airborne Particulate Observations

prepared by

George Nikolich, Craig Shadel, Jenny Chapman, Steve A. Mizell,
Greg McCurdy, Vicken Etyemezian, and Julianne J. Miller

Division of Hydrologic Sciences
Desert Research Institute
Nevada System of Higher Education

Publication No. 45263

submitted to

Nevada Field Office
National Nuclear Security Administration
U.S. Department of Energy
Las Vegas, Nevada

October 2015

The work upon which this report is based was supported by the U.S. Department of Energy under Contract #DE-NA0000939. Approved for public release; further dissemination unlimited.

THIS PAGE INTENTIONALLY LEFT BLANK

ABSTRACT

In 1963, the U.S. Department of Energy (DOE) (formerly the Atomic Energy Commission [AEC]), implemented Operation Roller Coaster on the Tonopah Test Range (TTR) and an adjacent area of the Nevada Test and Training Range (NTTR) (formerly the Nellis Air Force Range). This test resulted in radionuclide-contaminated soils at Clean Slate I, II, and III. This report documents observations made during ongoing monitoring of radiological, meteorological, and dust conditions at stations installed adjacent to Clean Slate I and Clean Slate III and at the TTR Range Operations Control center. The primary objective of the monitoring effort is to determine if winds blowing across the Clean Slate sites are transporting particles of radionuclide-contaminated soils beyond both the physical and administrative boundaries of the sites. Results for the calendar year (CY) 2014 monitoring are: (1) the gross alpha and gross beta values from the monitoring stations are approximately equivalent to the highest values observed during the CY2014 reporting at the surrounding Community Environmental Monitoring Program (CEMP) stations; (2) only naturally occurring radionuclides were identified in the gamma spectral analyses; (3) the ambient gamma radiation measurements indicate that the average annual gamma exposure is similar at all three monitoring stations and periodic intervals of increased gamma values appear to be associated with storm fronts passing through the area; and (4) the concentrations of both resuspended dust and saltated sand particles generally increase with increasing wind speed. Differences in the observed dust concentrations are likely the result of differences in the soil characteristics immediately adjacent to the monitoring stations. Neither the resuspended particulate radiological analyses nor the ambient gamma radiation measurements suggest wind transport of radionuclide-contaminated soils.

THIS PAGE INTENTIONALLY LEFT BLANK

CONTENTS

ABSTRACT.....	iii
LIST OF FIGURES	vi
LIST OF TABLES.....	viii
LIST OF ACRONYMS	ix
INTRODUCTION	1
MONITORING STATIONS LOCATIONS AND CAPABILITIES.....	4
BSNE SAND TRAP INSTALLATION.....	9
WEATHER CONDITIONS AND OTHER ENVIRONMENTAL PARAMETERS	13
RADIOLOGICAL ASSESSMENT OF AIRBORNE PARTICULATES.....	21
COMPARISON OF GLASS-FIBER AND CELLULOSE-FIBER FILTERS.....	25
GAMMA RADIATION OBSERVATIONS	26
OBSERVATIONS OF SOIL TRANSPORT BY SALTATION.....	31
OBSERVATIONS OF SOIL TRANSPORT BY SUSPENSION	34
PM ₁₀ TO PM _{2.5} RATIO.....	38
APRIL 25, 2014, WIND EVENT	40
DISCUSSION.....	42
CONCLUSIONS.....	43
RECOMMENDATIONS	44
REFERENCES	45
APPENDIX A: QUALITY ASSURANCE PROGRAM	A-1
APPENDIX B: SUMMARIES OF METEOROLOGICAL DATA	B-1
APPENDIX C: DAILY AVERAGE METEOROLOGICAL AND ENVIRONMENTAL DATA FOR TTR MONITORING STATIONS 400, 401, AND 402 DURING CY2014.....	C-1

LIST OF FIGURES

1.	Location of monitoring stations at the Tonopah Test Range (TTR) in the north end of the Nevada Test and Training Range in southern Nevada.....	2
2.	The TTR environmental monitoring stations are located on the south side of the Sandia National Laboratory compound (Station 400) and the north ends of the Clean Slate I (Station 402) and III (Station 401) contamination areas.....	3
3.	Station 400 is a trailer mounted radiological and meteorological measurement system located near the Range Operations Center (ROC) in the Sandia National Laboratories (SNL) compound on the TTR.....	5
4.	The solar powered air sampler, saltation sensor, and meteorological tower (background, center, and foreground, respectively) at Station 401 are located along the north fence that bounds the Clean Slate III contamination area.....	6
5.	The solar powered air sampler, saltation sensor, and meteorological tower (center right, foreground left, and center left, respectively) at Station 402 are located along the north fence that bounds the Clean Slate I contamination area.....	7
6.	Sand and dust particles are carried into the BSNE Sand Trap by fast moving air.....	10
7.	Northeast view at Station 401. In the foreground is one of three BSNE Sand Trap installations at TTR Clean Slate III.....	11
8.	Equipment locations along the fence line at TTR Clean Slate III, monitoring station 401.....	12
9.	Equipment locations along the fence line at TTR Clean Slate I, monitoring station 402.....	12
10.	Ambient air temperature for Station 400 for CY2014.....	13
11.	Ambient air temperature for Station 401 for CY2014.....	14
12.	Ambient air temperature for Station 402 for CY2014. The data gap in August was because of equipment failure at the station.....	14
13.	Average ambient air temperature for Stations 400, 401, and 402 CY2014.....	15
14.	Average ambient soil temperature for Stations 400, 401, and 402 for CY2014.....	16
15.	Comparison of average air and average soil temperatures by regression illustrates the close relationship between the two parameters at Station 401.....	16
16.	Total daily precipitation for Stations 400, 401, and 402 for CY2014.....	17
17.	Cumulative precipitation for Stations 400, 401, and 402 for CY2014.....	17
18.	Soil volumetric water content for Stations 400, 401, and 402 for CY2014.....	19
19.	Annual wind roses for Stations 400, 401, and 402 for CY2014. Left panel: all winds. Right panel: winds greater than 24 km/hr (15 mph).....	20

21.	The mean annual gross alpha concentrations for the TTR samples collected on glass-fiber filters (blue) are higher than the mean annual gross alpha concentrations for samples collected at most of the CEMP stations (green).....	23
22.	The mean annual gross beta concentrations for the TTR samples collected on glass-fiber filters (blue) are in the same range or lower than the mean annual gross beta concentrations for samples collected at the CEMP stations (green).....	24
23.	The CY2014 PIC gamma data for the TTR monitoring stations.	27
24.	The CY2014 PIC gamma data and precipitation for TTR Station 400.....	29
25.	The CY2014 PIC gamma data for the CEMP station at Warm Springs Summit and the TTR stations, highlighting coincident times of increased values.	30
26.	Diagram of the saltation process. Suspension of smaller particles ejected by the impact of a particle landing after saltation is depicted on the left.	32
27.	Average saltation counts generally increase rapidly as the wind speed increases above 20 mph at both TTR air monitoring Stations 401 and 402.	33
28.	Regression of PM ₁₀ against saltation counts by wind speed class.	34
29.	Wind speed frequency by wind class for Stations 400,401, and 402 for CY2014.	36
30.	Same as Figure 29 but with logarithmic <i>y</i> -axis.....	36
31.	PM ₁₀ trends as a function of wind speed for stations 400, 401, and 402 for CY2014...	37
32.	PM ₁₀ trends as a function of wind speed for stations 400, 401, and 402 for CY2014...	37
33.	PM _{2.5} as a function of wind speed for stations 400, 401, and 402 for CY2014.....	39
34.	Ratio of PM ₁₀ to PM _{2.5} trends as a function of wind speed for stations 400, 401, and 402 for CY2014.	39
35.	Wind and dust episode April 25, 2014, Station 400.	40
36.	Wind and dust episode April 25, 2014, Station 401.	41
37.	Wind and dust episode April 25, 2014, Station 402.	41

LIST OF TABLES

1.	Location coordinates for the TTR air monitoring stations.....	5
2.	Radiological, meteorological, and environmental sensors deployed at the TTR air monitoring stations.....	8
3.	Gross alpha results for TTR sampling stations 2014.	22
4.	Gross beta results for TTR sampling stations 2014.	22
5.	Mean annual gross alpha and gross beta concentrations for 2014 reported at CEMP stations that surround the TTR.	23
6.	The number of CY2014 particulate samples in which naturally occurring radionuclides were identified by gamma spectroscopy varied by radionuclide and between stations.	24
7.	Gamma exposure rate at the TTR measured by the PIC detectors.	26
8.	Gamma exposure rate measured with PICs at CEMP stations in the TTR region.	28
9.	Average saltation particle impact counts by wind speed class at TTR air monitoring Stations 401 and 402.	32
10.	Summary of wind and PM ₁₀ data for Stations 400, 401, and 402 for CY2014.	35

LIST OF ACRONYMS

AEC	Atomic Energy Commission
BSNE	Big Spring Number Eight
CAU	Corrective Action Unit
CEMP	Community Environmental Monitoring Program
CS I	Clean Slate I, also known as Clean Slate 1
CS II	Clean Slate II, also known as Clean Slate 2
CS III	Clean Slate III, also known as Clean Slate 3
CY	Calendar year
DOE	Department of Energy
DRI	Desert Research Institute
FY	Fiscal year
GOES	Geostationary Operational Environmental Satellite
GZ	Ground zero
NNSA/NFO	National Nuclear Security Administration, Nevada Field Office
NRC	Nuclear Regulatory Commission
NTTR	Nevada Test and Training Range
PIC	Pressurized ionization chamber
PM	Particulate matter
ROC	Range Operations Center
RSL	Radiological Services Laboratory
SNL	Sandia National Laboratories
TDR	Time domain reflectometry
TTR	Tonopah Test Range
VWC	Volumetric water content
WRCC	Western Regional Climate Center

THIS PAGE INTENTIONALLY LEFT BLANK

INTRODUCTION

In May and June 1963 the U.S. Department of Energy (DOE) (formerly the Atomic Energy Commission [AEC]) implemented Operation Roller Coaster to evaluate the dispersal of radionuclides when nuclear devices were subjected to chemical explosions while in storage or transit (Dick *et al.*, 1963; Johnson and Edwards, 1996). The operation consisted of four tests, Double Tracks conducted in Stonewall Flat on the Nevada Test and Training Range (NTTR) and Clean Slate I, II, and III conducted in Cactus Flat on the Tonopah Test Range (TTR). Both test areas are southeast of Tonopah, Nevada, in Nye County (Figures 1 and 2).

The primary purpose of the Clean Slate tests was to study dispersion of plutonium from nonnuclear explosions of plutonium weapons (DOE, 1996). The Clean Slate tests involved one weapon containing plutonium and several simulated weapons containing uranium (Dick *et al.*, 1963; Johnson and Edwards, 1996). For each test, data collection was distributed along arcs within a quarter-circle, wedge-shaped area that emanated from the test ground zero (GZ) and centered on a radius that extended from GZ to the south or southeast (Dick *et al.*, 1963; Johnson and Edwards, 1996), the expected downwind directions. Data collection during the tests focused on plutonium and uranium because of their radiological toxicity (Dick *et al.*, 1963). Subsequent surveys to characterize radionuclide-contaminated soils focused on the detection of plutonium through the measurement of the plutonium daughter product, americium-241 (Proctor and Hendricks, 1995). Americium-241 can be more readily measured than the alpha-emitting plutonium isotopes because americium-241 emits gamma rays.

Immediate post-shot cleanup at each test involved disposing of contaminated debris in a pit at GZ, scraping the surface soil around GZ to a depth of several inches, and placing the soil in the disposal pit or mounding it over the contaminated debris. The mound of contaminated materials was covered with additional soil and compacted and watered (Johnson and Edwards, 1996) and fences were constructed around the contamination at each site. Based on soil survey data collected during 1973, a second fence was constructed at the approximate limit of 40 pCi/g of plutonium in soil (Duncan *et al.*, 2000).

Aerial surveys of Operation Roller Coaster contamination areas were conducted in 1977 (EG&G, 1979) and 1993 (Proctor and Hendricks, 1995). These surveys used gamma detectors to identify americium-241. Based on the 1977 survey, the total area of diffuse plutonium for all Operation Roller Coaster sites was estimated to be 20 million square meters (4,942.11 acres). The 1993 survey estimated the maximum concentration at the Clean Slate I GZ to be between 200 and 400 pCi/g. At Clean Slate II and III, the maximum concentrations at GZ were reported to be in excess of 2,000 pCi/g. Contamination was reported outside the outer perimeter fence at all three Clean Slate sites. At Clean Slate III, plutonium concentration outside of the fence did not exceed 200 pCi/g. However, the concentrations reported outside the fences at Clean Slate I and II were greater than 200 pCi/g but less than 400 pCi/g (Proctor and Hendricks, 1995).

After soil remediation reduced the concentration of transuranics, which include plutonium and americium, to less than or equal to 200 pCi/g, Double Tracks was closed in 1996 (Duncan *et al.*, 2000). Soil contamination at Clean Slate I was remediated in 1997 so that the concentration of transuranics was less than or equal to 400 pCi/g (SNL, 2012). Clean Slate II and III have not been remediated.

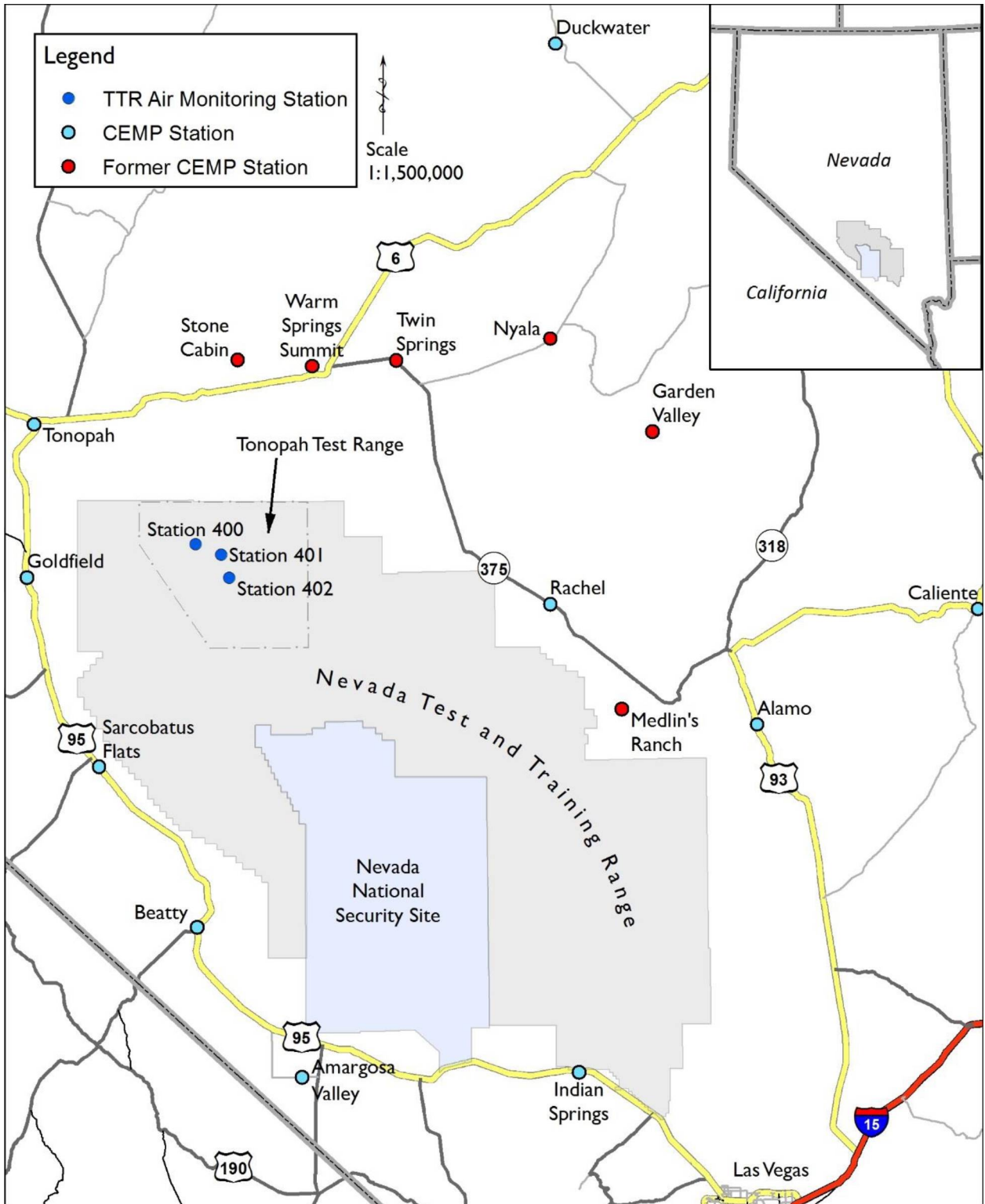


Figure 1. Location of monitoring stations at the Tonopah Test Range (TTR) in the north end of the Nevada Test and Training Range in southern Nevada. Also shown are current and former Community Environmental Monitoring Stations (CEMP) for which monitoring data are available.



Figure 2. The TTR environmental monitoring stations are located on the south side of the Sandia National Laboratory compound (Station 400) and the north ends of the Clean Slate I (Station 402) and III (Station 401) contamination areas.

In 2008, at the request of the DOE National Nuclear Security Administration, Nevada Field Office (NNSA/NFO), the Desert Research Institute (DRI) constructed and deployed two portable environmental monitoring stations at the TTR as part of the Environmental Restoration Project Soils Activities. A third station was deployed in 2011. The DRI has operated these stations continuously since installation. The primary objective of the monitoring stations is to evaluate whether there is wind transport of radiological contaminants, specifically plutonium, from the Soils Corrective Action Units (CAUs) associated with Operation Roller Coaster and if so, under what conditions such transport occurs. Instrumentation currently in use is intended to quantify radiological constituents in the air to a height of six to eight feet above the local ground surface. The objective of this annual report is to document the operation of the TTR monitoring stations during calendar year 2014 (CY2014), present the data collected, interpret the results in the context of the monitoring objectives, and provide recommendations as needed.

MONITORING STATIONS LOCATIONS AND CAPABILITIES

As part of its work under the Soils Activity, DRI operates three portable monitoring stations at the TTR. Stations 400 and 401 were installed in May and June 2008, respectively. Station 402 was installed in May 2011. The monitoring stations were installed to facilitate the assessment of wind transport of plutonium from the surficial soil contamination sites that resulted from the Clean Slate tests. Wind direction, access, and power availability were key considerations in selecting the specific monitoring station locations. Wind data for the Tonopah Airport (Engelbrecht *et al.*, 2008) indicated that the predominant wind directions in the area were from the northwest and south-southeast. Wind direction data collected from the TTR monitoring stations substantiate the assessment of Engelbrecht *et al.* (2008).

Station 400 is located at the Sandia National Laboratories (SNL) Range Operations Center (ROC). Station coordinates are given in Table 1. The ROC, adjacent TTR airfield, and surrounding work area are downwind of the Clean Slate contamination sites when winds are out of the south-southeast. At a distance of eight to nine kilometers (five to six miles), these facilities are the closest, regularly manned work locations to the Clean Slate contamination sites. Therefore, Station 400 facilitates the characterization of radiological conditions in the TTR work areas that may result from wind transport of radionuclide-contaminated soils at the Clean Slate sites and provides data to compare radiological conditions at the ROC with conditions at the Clean Slate sites. Station 400 was originally located just north of the center of the SNL compound, approximately 145 m (475 ft) west-northwest of the ROC. In the summer of 2012, the station was moved approximately 200 m (650 ft) to the southeast at the request of SNL. In the new location, Station 400 is approximately 90 m (300 ft) south of the ROC near the southeast corner of the SNL compound (Figure 2). Sandia National Laboratories provides line power to operate the equipment at Station 400, which consists of a meteorological tower and air sampling equipment installed on a 2.1 m x 4.3 m (7 ft x 14 ft) trailer (Figure 3).

Table 1. Location coordinates for the TTR air monitoring stations.

Station	Latitude	Longitude
Station 400 – original	37° 47' 15" N	116° 45' 26" W
Station 400 – current	37° 47' 10" N	116° 45' 21" W
Station 401	37° 45' 39" N	116° 40' 58" W
Station 402	37° 42' 33" N	116° 39' 32" W



Figure 3. Station 400 is a trailer mounted radiological and meteorological measurement system located near the Range Operations Center (ROC) in the Sandia National Laboratories (SNL) compound on the TTR.

Stations 401 and 402 are located at the demarcation fence on the northwest perimeter of the Clean Slate III and Clean Slate I sites, respectively (Figure 2). These locations were chosen because they place the monitoring instrumentation in proximity to the contamination sites and on the downwind side of the sites during south-southeast winds, one of the two predominant wind directions through the area. Both Stations 401 and 402 are solar powered with battery backup power and the batteries are recharged by solar panels. Table 1 gives the coordinates for these monitoring stations. At Stations 401 and 402, the air samplers, solar panels, and the batteries used to power the samplers are on trailers. This arrangement requires that the meteorological towers be installed on free-standing tripods that are separate from the trailer (Figures 4 and 5).

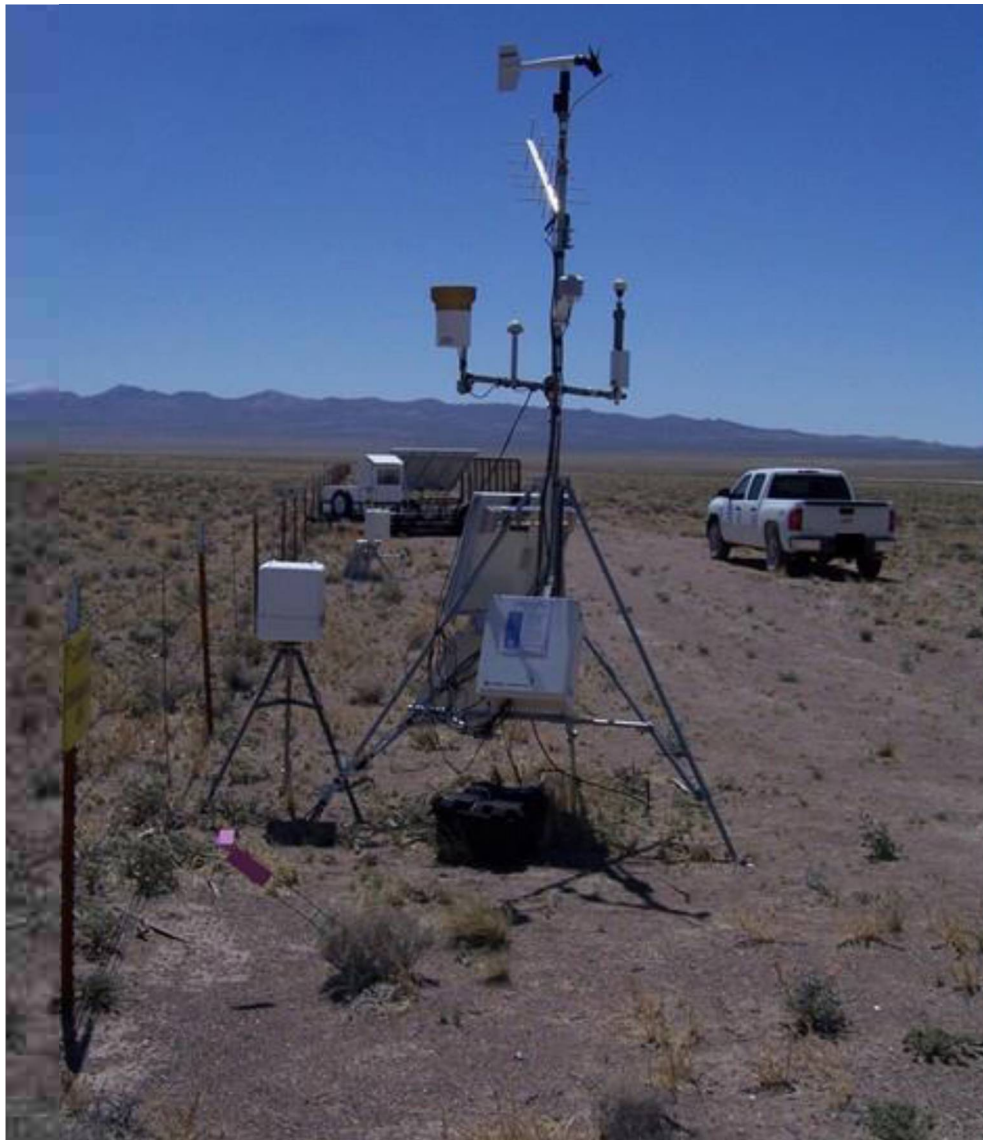


Figure 4. The solar powered air sampler, saltation sensor, and meteorological tower (background, center, and foreground, respectively) at Station 401 are located along the north fence that bounds the Clean Slate III contamination area.



Figure 5. The solar powered air sampler, saltation sensor, and meteorological tower (center right, foreground left, and center left, respectively) at Station 402 are located along the north fence that bounds the Clean Slate I contamination area.

The fundamental design of these stations is similar to that used in the Community Environmental Monitoring Program (CEMP) (NSTec, 2013). The Quality Assurance Program is also patterned after that used by CEMP (Appendix A). The equipment deployed provides data on radiological, meteorological, and environmental conditions. Table 2 lists the parameters measured and the approximate date of the initial data collection at each of the three monitoring stations. Plutonium was the principal radionuclide released into the

Table 2. Radiological, meteorological, and environmental sensors deployed at the TTR air monitoring stations. The dates refer to the first occurrence of data collection for that parameter at the given station.

Instrument/Measurement	Station 400	Station 401	Station 402
Wind speed	5/27/2008	6/10/2008	5/18/2011
Wind direction	5/27/2008	12/22/2009	5/18/2011
Precipitation	5/27/2008	12/22/2009	5/18/2011
Temperature	5/27/2008	6/10/2008	5/18/2011
Relative humidity	5/27/2008	6/10/2008	5/18/2011
Solar radiation	5/27/2008	na	5/18/2011
Barometric pressure	5/27/2008	na	5/18/2011
Soil temperature	5/27/2008	12/22/2009	5/18/2011
Soil moisture content	5/27/2008	12/22/2009	5/18/2011
Airborne particle size profiler	5/27/2008	6/10/2008	5/18/2011
Airborne particle collector	5/27/2008	7/30/2008	8/23/2011
Saltation sensor	na	8/9/2011	8/9/2011
Gamma radiation PIC	5/27/2008	12/22/2009	12/15/2011
MiniVol TM ¹	5/27/2008	na	na
Data logger	5/27/2008	6/10/2008	5/18/2011
GOES transmitter	5/27/2008	12/22/2009	5/18/2011
BSNE Sand Traps	na	4/01/2014	4/01/2014

¹ Samples have never been collected from the MiniVolTM collectors.

na = not available.

environment during the Clean Slate experiments. It attaches to small soil particles and may be suspended in the air and transported from the site along with windblown dust. Americium-241, a daughter product of plutonium-241 that releases gamma energy during decay, is much easier to detect than the alpha particle released during plutonium decay. Therefore, two radiological data collection systems are deployed at each of the monitoring stations. Gamma energy is measured using a pressurized ionization chamber (PIC) (Hi-Q, San Diego, California) and airborne particulates are collected for radiological analysis. Continuous flow, low-volume (flow rate is approximately 0.05663 m³ [2 ft³] per minute) air samplers (MetOne, Grants Pass, Oregon) are used to collect airborne particulates.

Glass-fiber filters with a pore size of 0.3 µm and diameter of 10 cm (4 inch) are used. Prior to CY2013, Stations 401 and 402 used cellulose-fiber filters with a pore size of 20 µm to 25 µm. The conversion to all glass-fiber filters was made to ensure that the smaller-sized particulates to which plutonium might be attached are collected. Filters are retrieved every two weeks and are delivered to the Radiological Services Laboratory (RSL) at the University of Nevada, Las Vegas, for analyses.

The total mass of collected dust is submitted for gross alpha, gross beta, and gamma spectroscopy analyses in an effort to assess the magnitude of radionuclides associated with the suspended dust. Gamma spectroscopy is performed to determine if americium-241, the daughter product of plutonium-241, is present. If americium-241 is detected, then alpha spectroscopy is performed to determine the quantity of plutonium-241 present. Because plutonium particles tend to attach to small soil particles, suspension or resuspension of dust from contaminated soil sites by wind and transport by rainfall runoff are the likely mechanisms for transporting radiological contaminants beyond the physical and administrative boundaries of each site. The effort reported here is focused on possible transport by wind resuspension. Additionally, inhaling plutonium-contaminated dust particles is the most likely mechanism for human exposure. Suspension and transport of contaminated dust is controlled by local meteorological and other environmental conditions, such as wind speed and soil moisture content. Many meteorological parameters influence these conditions. Electronic sensors measure meteorological and other environmental conditions every three seconds. These measurements are averaged or totaled, as appropriate, and stored in the on-site data logger every 10 minutes. The maximum and minimum value of each parameter are also saved on the data logger. These values are used to evaluate data quality. The data loggers are downloaded during site visits every two weeks. To assess instrument performance and provide rapid updates of observations, hourly averages of the 10-minute data are transmitted to the Western Regional Climate Center (WRCC) via the Geostationary Operational Environmental Satellite (GOES) system. At the WRCC, data are quality checked and archived for interpretation. A gap in automatic data collection occurred at Station 402 during the first part of August 2014. This was because of a battery failure at the station damaging the charge controller and the time required to obtain replacement parts.

In addition to the automatic sensors, two MiniVolsTM (Air Metrics, Eugene, Oregon) are deployed at Station 400. These samplers are intended to be run in the event of a nearby wildfire or during extreme dust storms because they are set up to facilitate analyses that distinguish organic and inorganic constituents. The MiniVolsTM are manually activated, low-volume air samplers equipped with Teflon-filter media. No events caused the MiniVolsTM to be activated in 2014, so no data were collected from these instruments.

BSNE SAND TRAP INSTALLATION

On April 1, 2014, DRI installed BSNE (Big Spring Number Eight; Custom Products and Consulting LLC, Big Spring, Texas) dust samplers to monitor dust and soil transport by saltation at Clean Slate I and Clean Slate III. The BSNEs are isokinetic wind aspirated samplers that collect a large portion of sand that enters the opening regardless of wind speed (Figure 6). The inlet height is set fairly low at 15 cm (6 inches) to collect the maximum amount of erodible soil material transported by saltation. The samplers are roughly oriented at 160 degrees from north, in the direction of dominant winds as indicated by wind rose diagrams. Two collectors are installed at each mounting rod (Figure 7). One of the collectors is pointed toward the contaminated area in order to collect material likely to have been transported from the Clean Slate site. The other collector is pointed in the opposite direction and is used to collect the material moving across the undisturbed area. This physical setup and orientation allows determination of the net movement of soil material from the Clean Slate sites.

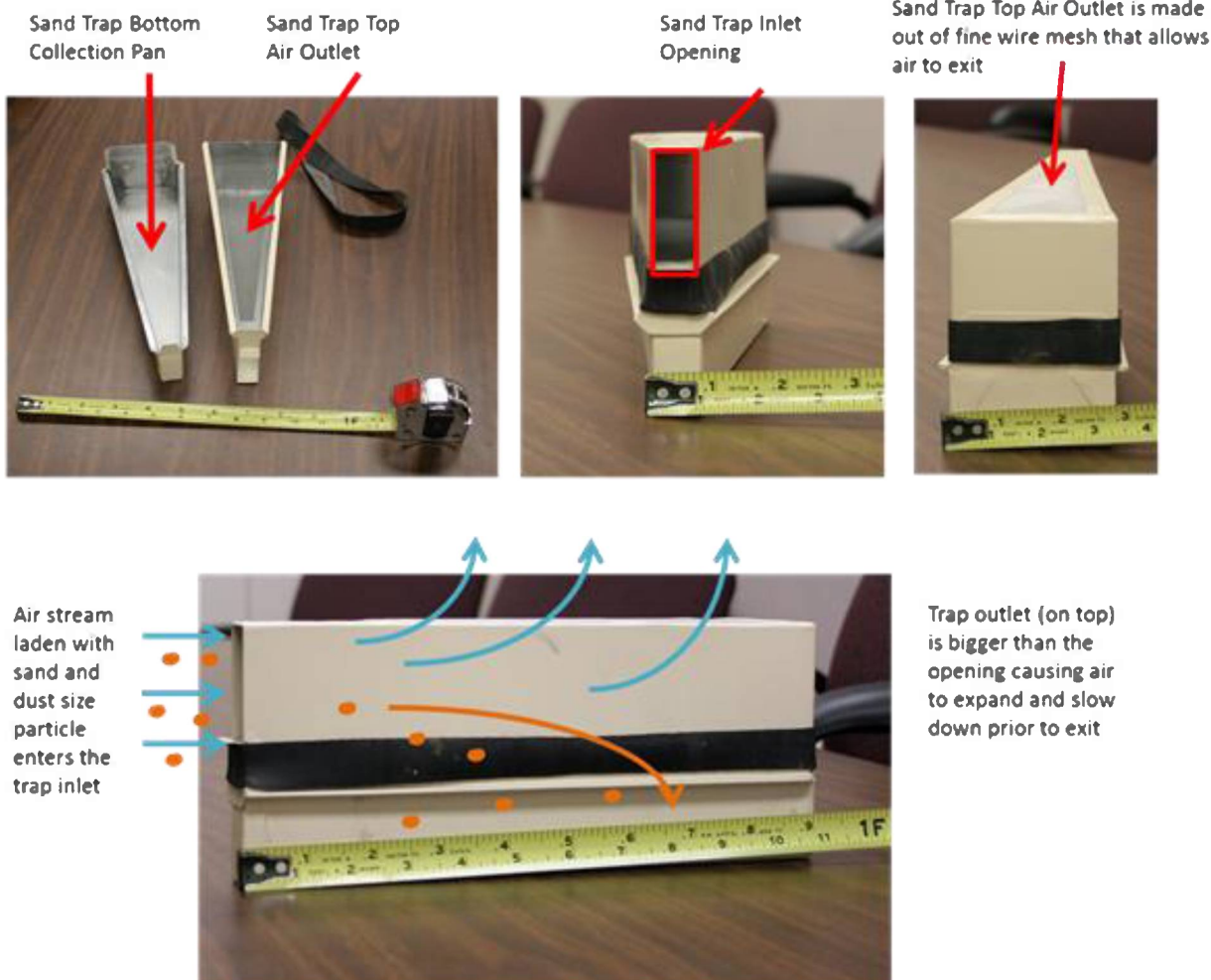


Figure 6. Sand and dust particles are carried into the BSNE Sand Trap by fast moving air. As the air slows down, momentum is lost and the particles settle on the bottom of the collection pan. Some dust particles may be small enough to be carried out by air through the wire mesh at the top of the trap.



Figure 7. Northeast view at Station 401. In the foreground is one of three BSNE Sand Trap installations at TTR Clean Slate III. The Clean Slate III boundary fence is to the right. Behind the sand trap is the saltation sensor and meteorological station with additional sand traps located along the fence line.

Three replicate BSNE dust samplers with two collectors each were installed at both Clean Slate I and Clean Slate III (Figures 8 and 9) along the fence line to assess spatial variability in soil transport by saltation. These samplers are passive and field operators check the sampler mass loading during the biweekly site visits. The DRI is developing a procedure in conjunction with other DOE contractors to collect and analyze the soil trapped in the BSNEs. The expectation is that a three- to four-month collection period will be used to better understand seasonal and geographic trends, though this will depend on the period of time needed to collect sufficient mass for analysis. The information collected will help determine if contaminated material reaches the fence line and the amount of net soil migration over time.

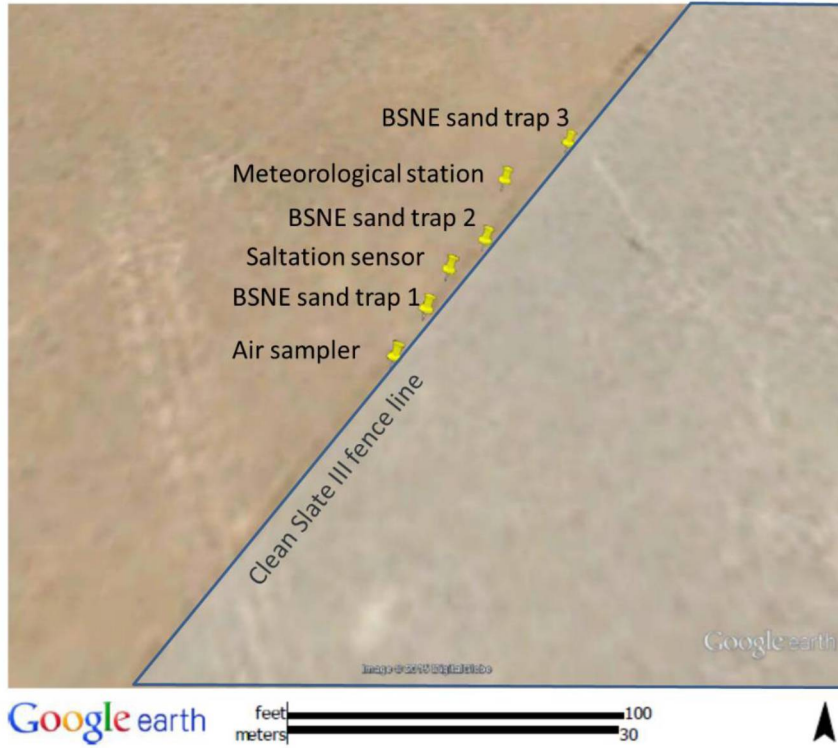


Figure 8. Equipment locations along the fence line at TTR Clean Slate III, monitoring station 401.

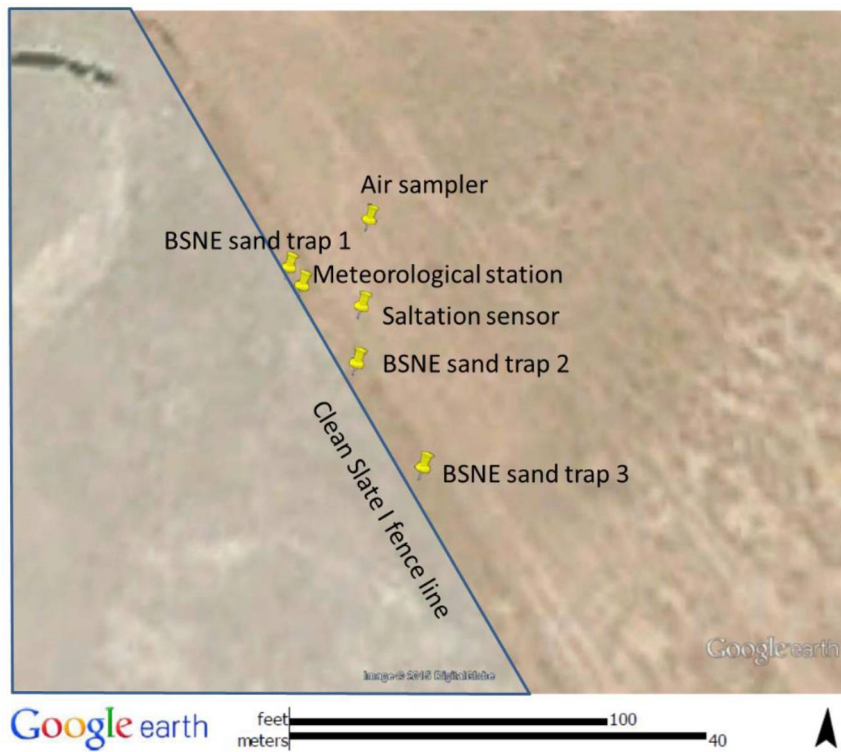


Figure 9. Equipment locations along the fence line at TTR Clean Slate I, monitoring station 402.

WEATHER CONDITIONS AND OTHER ENVIRONMENTAL PARAMETERS

Summary tables of the meteorological data recorded at the stations are in Appendix B and daily average meteorological and environmental data are plotted in Appendix C. These data are summarized and discussed below. Air temperature trends recorded during the year at Stations 400, 401, and 402 between January 1, 2014, and December 31, 2014, are shown in Figures 10 through 12. The three traces shown in the figures depict the maximum, average, and minimum daily temperature based on hourly average measurements. The maximum temperature during summer was between 38 °C and 39 °C (99 °F to 100 °F) and the minimum temperature during winter was between -18 °C and -13 °C (0 °F to 8 °F). On average, the maximum daily air temperature at Station 400 is approximately 10 °C (14 °F) above the daily average air temperature and the minimum daily air temperature is approximately 10 °C (14 °F) below the average, giving an average diurnal temperature swing of approximately 20 °C (28 °F). The diurnal temperature swing at Stations 401 and 402 is smaller at approximately 16 °C (34 °F).

Air temperature trends between all three stations are very similar (Figure 13), which is expected considering the close proximity and relatively small change in elevation between the three stations. The average air temperature at Station 400 is higher than Stations 401 and 402, possibly because Station 400 is located near several buildings and paved roads that absorb more heat during the day.

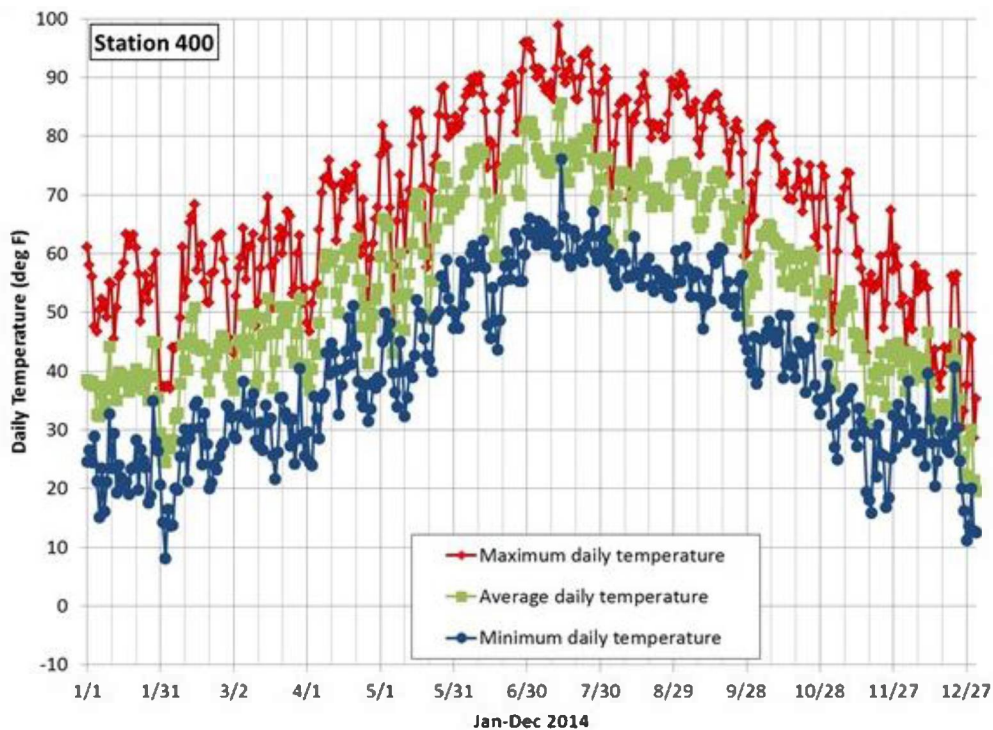


Figure 10. Ambient air temperature for Station 400 for CY2014.

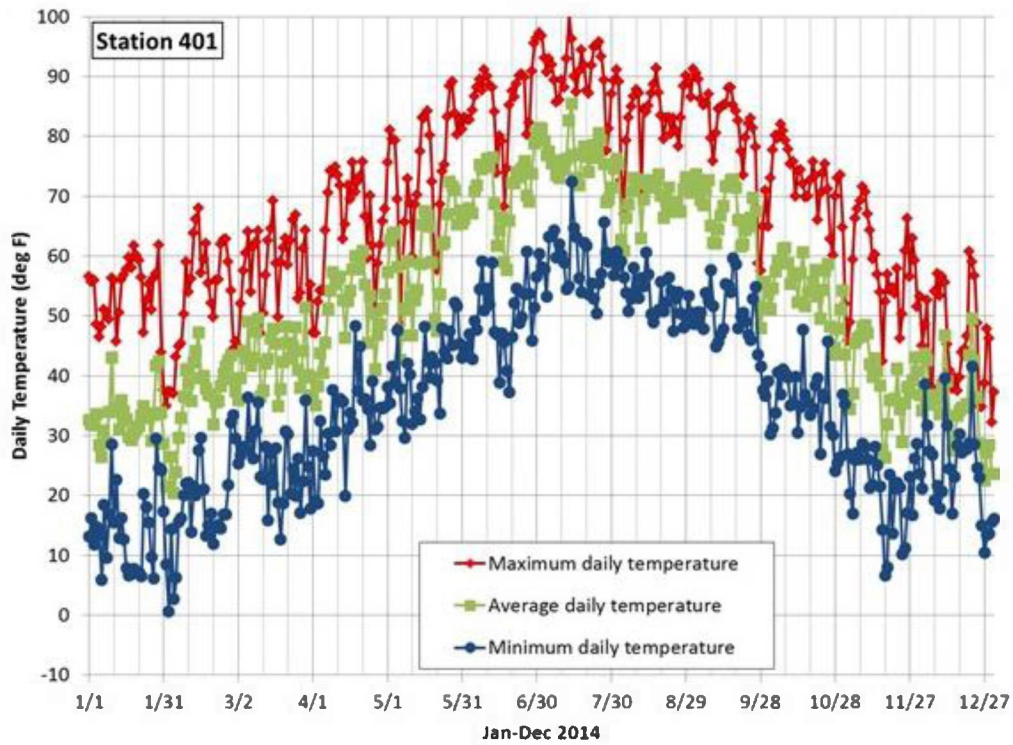


Figure 11. Ambient air temperature for Station 401 for CY2014.

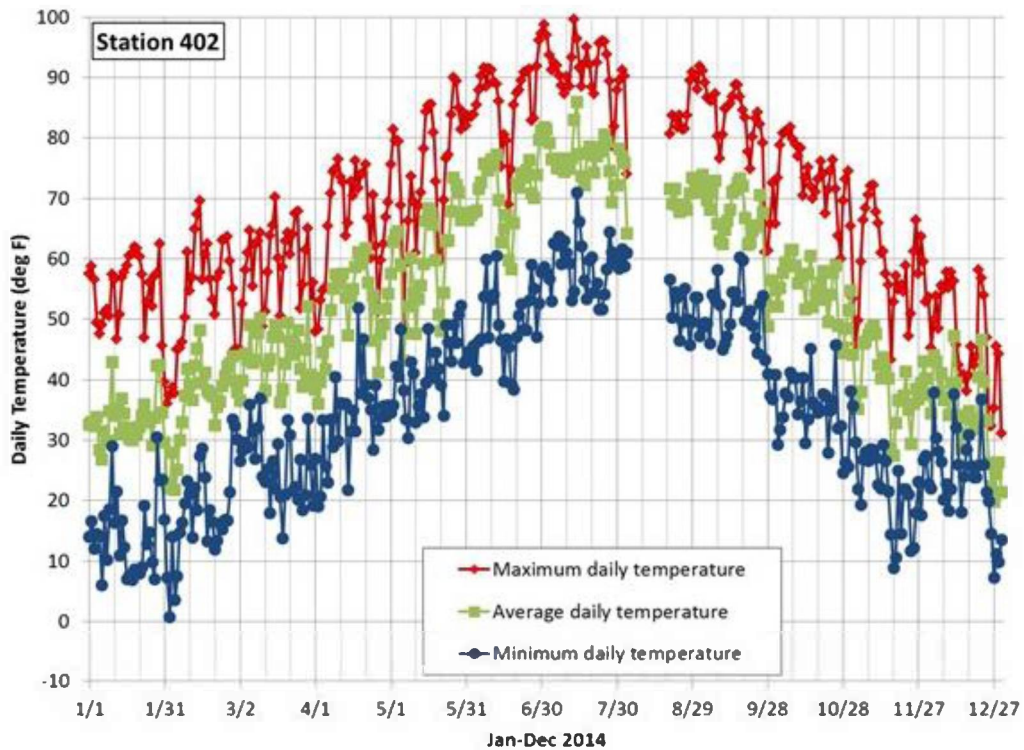


Figure 12. Ambient air temperature for Station 402 for CY2014. The data gap in August was because of equipment failure at the station.

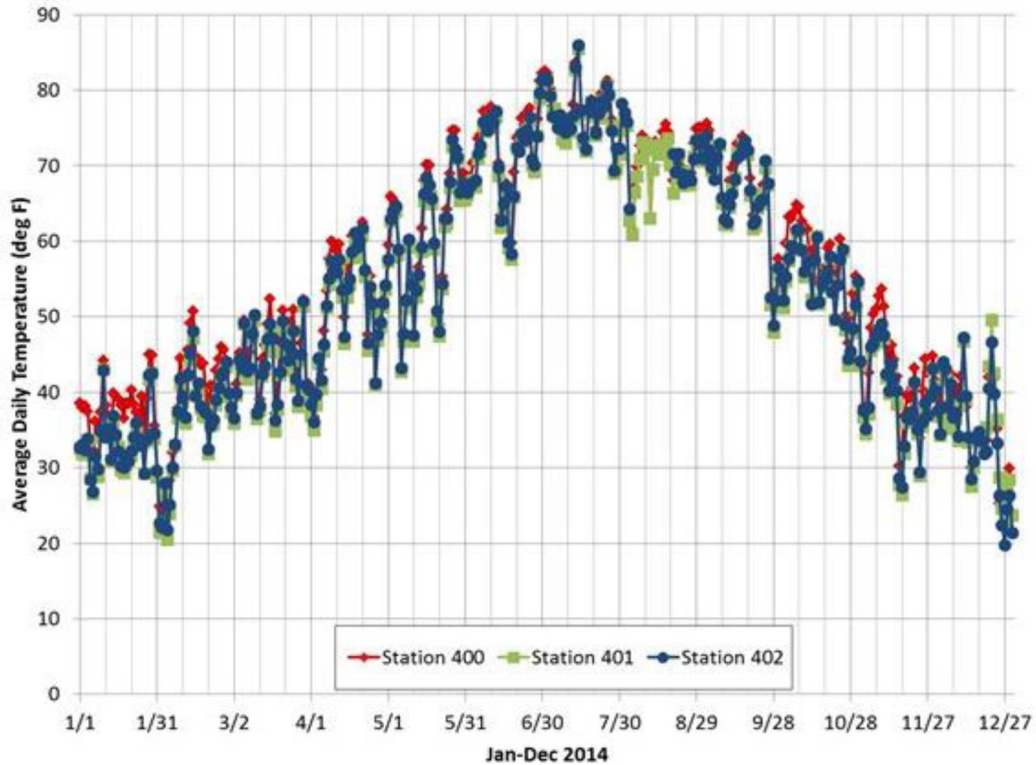


Figure 13. Average ambient air temperature for Stations 400, 401, and 402 CY2014.

The daily average soil temperature for all three TTR stations is shown in Figure 14. Soil temperature is measured using temperature probes made of thermocouple wire that have been buried at a depth of 10 to 13 cm (4 to 5 in). Generally there are minor differences in soil temperature readings between the stations. These minor differences may be explained in part by differences in local soil thermal conductivity, soil moisture, vegetation cover, and variations in probe burial depth. Station 400 generally indicates higher soil temperature compared with Stations 401 and 402. The gravel ground cover at Station 400 loses moisture more rapidly than the fine-grained soils at Stations 401 and 402. The absence of soil moisture at Station 400 would permit a stronger response of soil temperature to air temperature compared with the responses observed at Stations 401 and 402 where soil moisture is more readily retained. Data from Station 401 (Figure 15) illustrates the close relationship between soil temperature and air temperature. The intercept of the regression equation indicates that the soil temperature tends to be warmer by almost 3.3 °C (6 °F) than the air temperature, perhaps because of direct solar heating of the soil.

Total daily precipitation for Stations 400, 401, and 402 in the period between January 1, 2014, and December 31, 2014, is shown in Figure 16. The maximum total daily precipitation occurred on September 8, 2014, with Stations 400, 401, and 402 receiving 19 mm (0.75 in), 25 mm (0.99 in), and 35 mm (1.38 in), respectively, on that day. Total cumulative precipitation for Stations 400, 401, and 402 in the period between January 1, 2014, and December 31, 2014, is shown in Figure 17. Total precipitation for the calendar year varied between 131.6 mm (5.18 in) for Station 400 and 146.3 mm (5.76 in) for Station 401. Precipitation during 2014 at Station 402 was 135.9 mm (5.35 in). Most rainfall events were widespread enough to be recorded by all three stations.

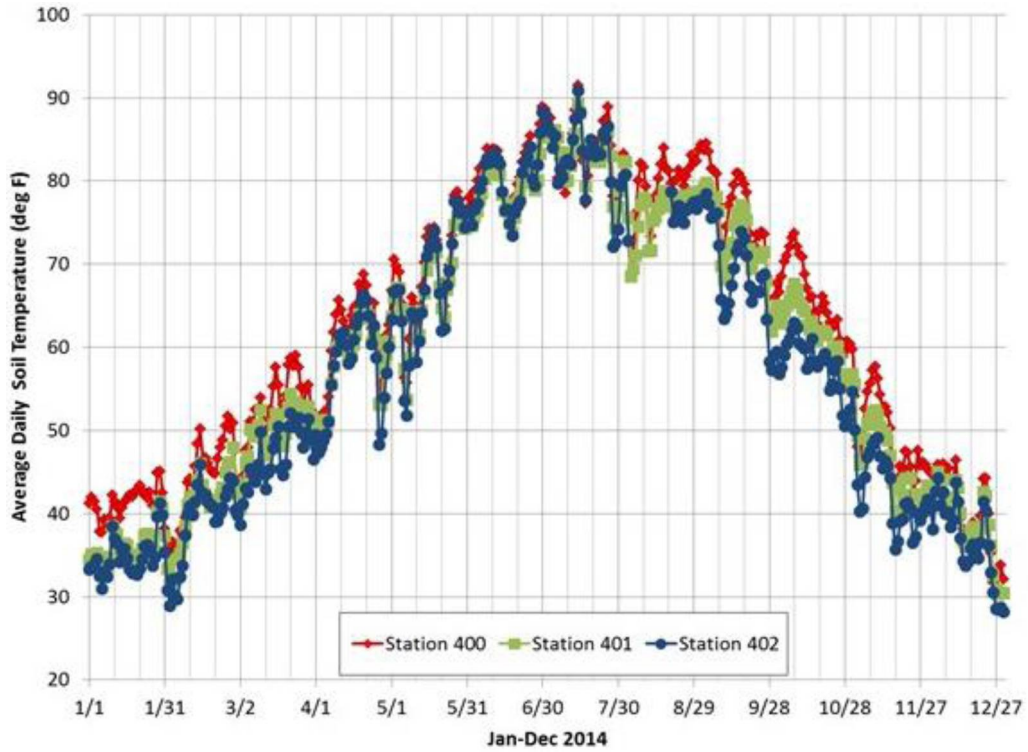


Figure 14. Average ambient soil temperature for Stations 400, 401, and 402 for CY2014.

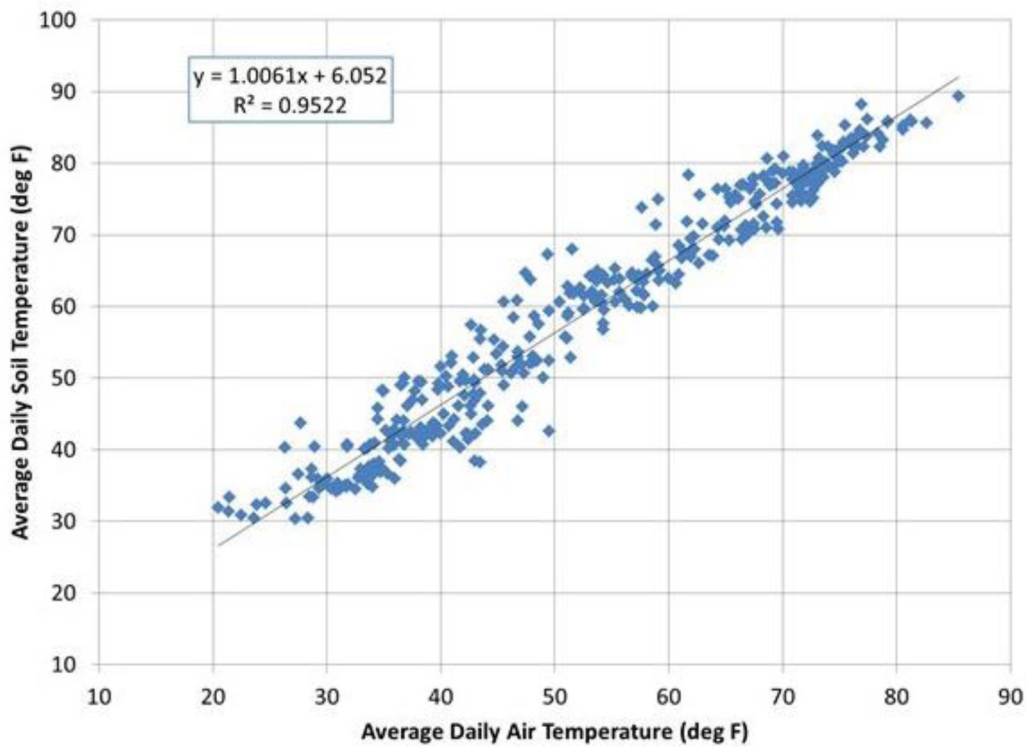


Figure 15. Comparison of average air and average soil temperatures by regression illustrates the close relationship between the two parameters at Station 401.

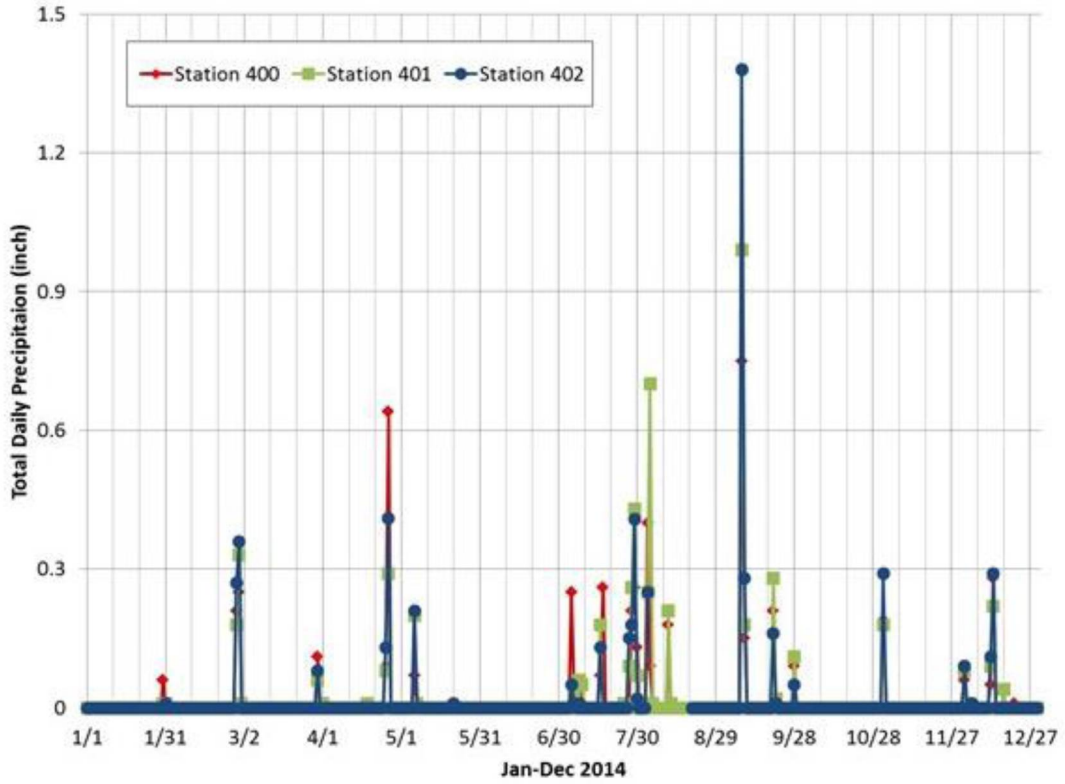


Figure 16. Total daily precipitation for Stations 400, 401, and 402 for CY2014.

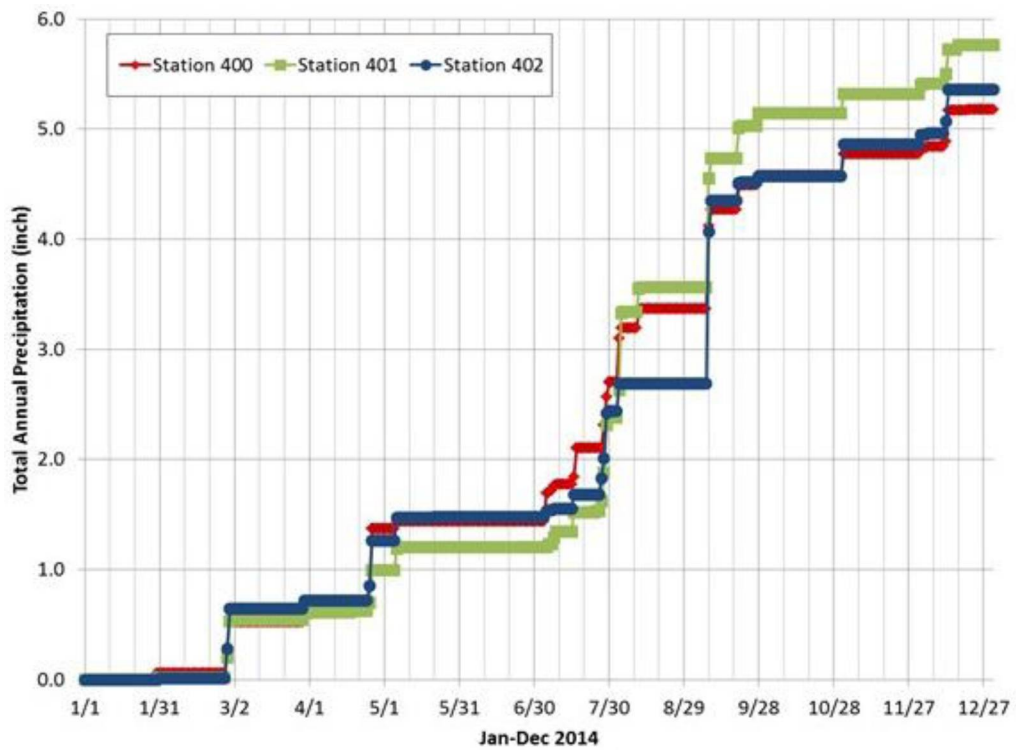


Figure 17. Cumulative precipitation for Stations 400, 401, and 402 for CY2014.

Total precipitation for all three stations during CY2014 averages 137.9 mm (5.43 in), which is slightly over the historic average annual precipitation of 129.03 mm (5.08 in) measured at the Tonopah Airport from 1954 through 2014 (www.wrcc.dri.edu/cgi-bin/cliMAIN.pl?nv8170, accessed April 24, 2015). The CY2014 average total annual precipitation is approximately double that measured at the stations in CY2013 (67.6 mm, 2.6 in). Because nonheated rain gages are used at the three stations, snowfall may be underestimated if the gages froze or if snow was blown out of the gage before it melted, but with the majority of precipitation during warmer months, snow losses should be small for CY2014.

Soil volumetric water content was monitored at all three stations in the top 5 cm (2 in) of soil using time domain reflectometry (TDR) probes. The TDR probes provide an estimate of soil water content based on direct measurement of soil conductivity. The TDR indicates the relative changes in soil water content associated with rain events and drying periods. The water content of this top layer of soil is most relevant to soil migration when soil is exposed to high winds. Sufficiently high soil moisture content is expected to diminish the soil material available for wind transport because moisture helps bind the soil particles together. Figure 18 shows the volumetric water content (VWC) of the top soil layer at Stations 400, 401, and 402 in the period between January 1, 2014, and December 31, 2014. Increases in soil VWC coincide with precipitation events and subsequent decreases in VWC correspond to drying periods. Because of lower air and soil temperatures, springtime rain events experience longer drying periods. Soils had the lowest water content in June and July 2014 and the highest at the beginning of August following a series of rain events. However, soil VWC alone is not a reliable indicator of the potential for dust generation. For example, short intense rain events may break up the soil crust and release fine soil particles for transport when exposed to wind instead of increase soil stability because of the additional moisture. It is also important to consider that soils are usually at their lowest water content between June and August, when winds are not as strong as during March and April when most dust events occur.

Wind is a major mechanism that drives soil migration at the TTR. Therefore, it is important to monitor wind in conjunction with real-time particulate matter (PM) concentrations in order to determine the conditions under which dust transport by wind occurs. Annual wind rose diagrams (Figure 19 and 20) have been developed for all three stations for CY2014. In Figure 19, each station has two wind roses that cover the same time period. The one on the left shows all wind speeds and their contribution to the overall wind rose and the one on the right shows only winds above 24 km/hr (15 miles per hour [mph]). In general, winds above 24 km/hr (15 mph) result in elevated PM₁₀ (particulate matter of aerodynamic diameter of less than 10 micrometers) concentrations in the air. The PM₁₀ concentration is an indicator of small particles that are suspended in the air and can be easily inhaled. As seen in Figure 19, the most prevalent winds are from the south or northwest, especially for wind speeds above 24 km/hr (15 mph). The geographic context of the wind can be seen in Figure 20.

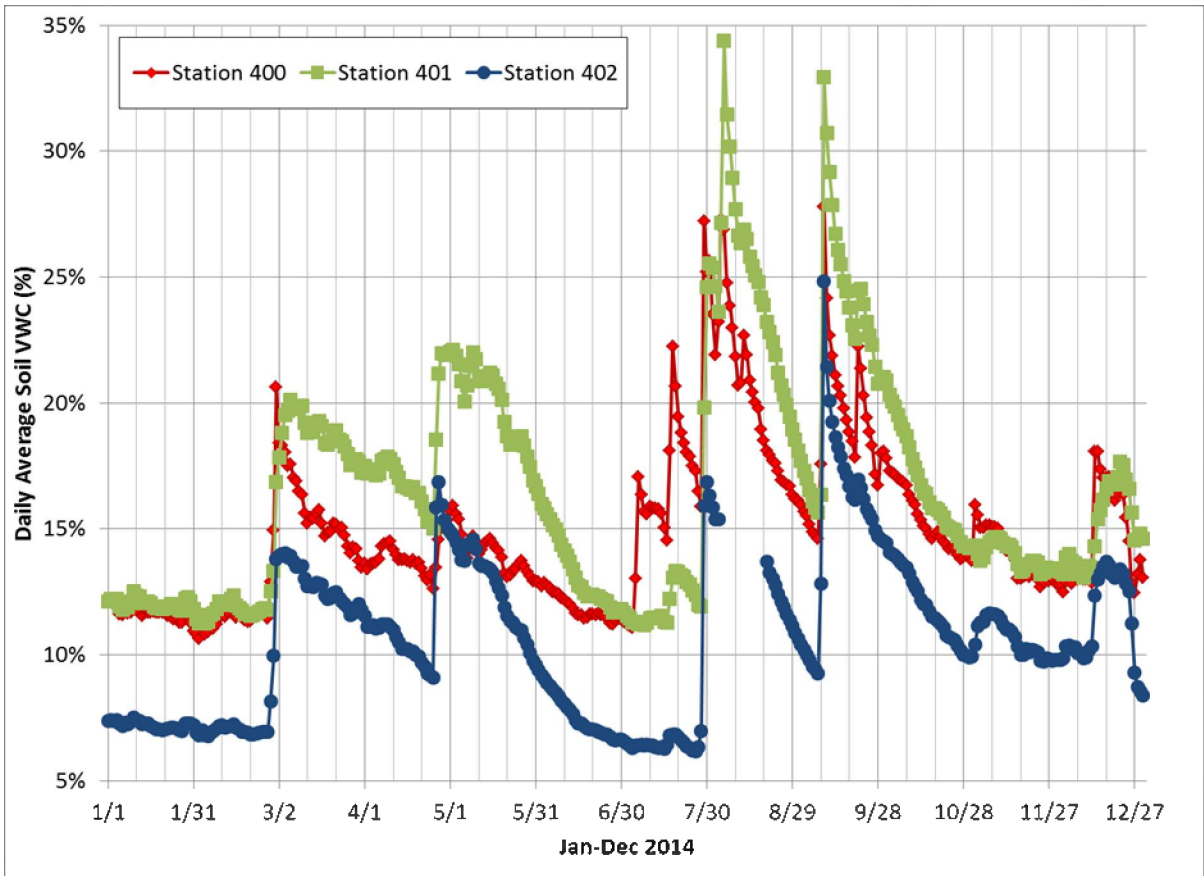


Figure 18. Soil volumetric water content for Stations 400, 401, and 402 for CY2014.

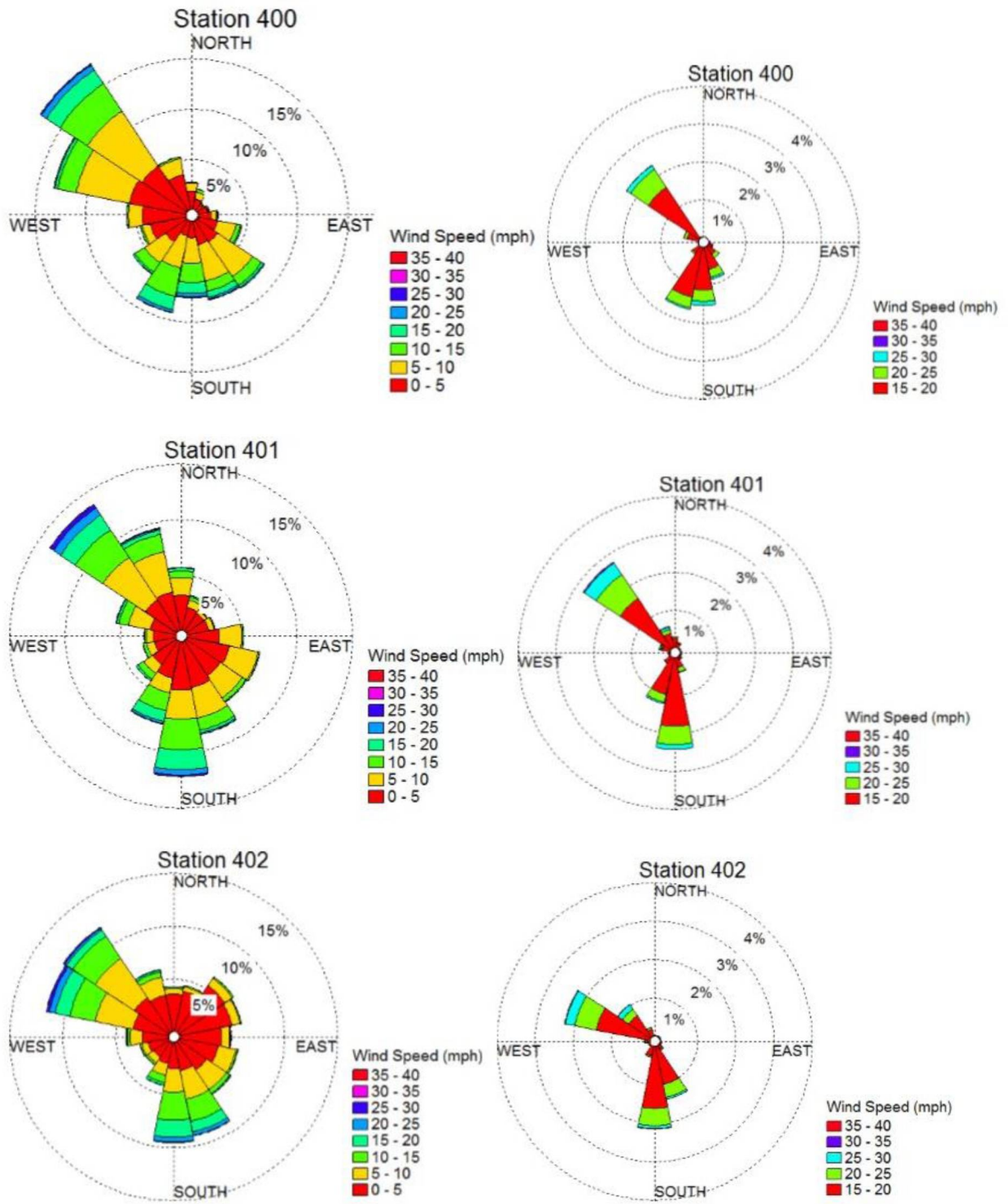


Figure 19. Annual wind roses for Stations 400, 401, and 402 for CY2014. Left panel: all winds. Right panel: winds greater than 24 km/hr (15 mph).

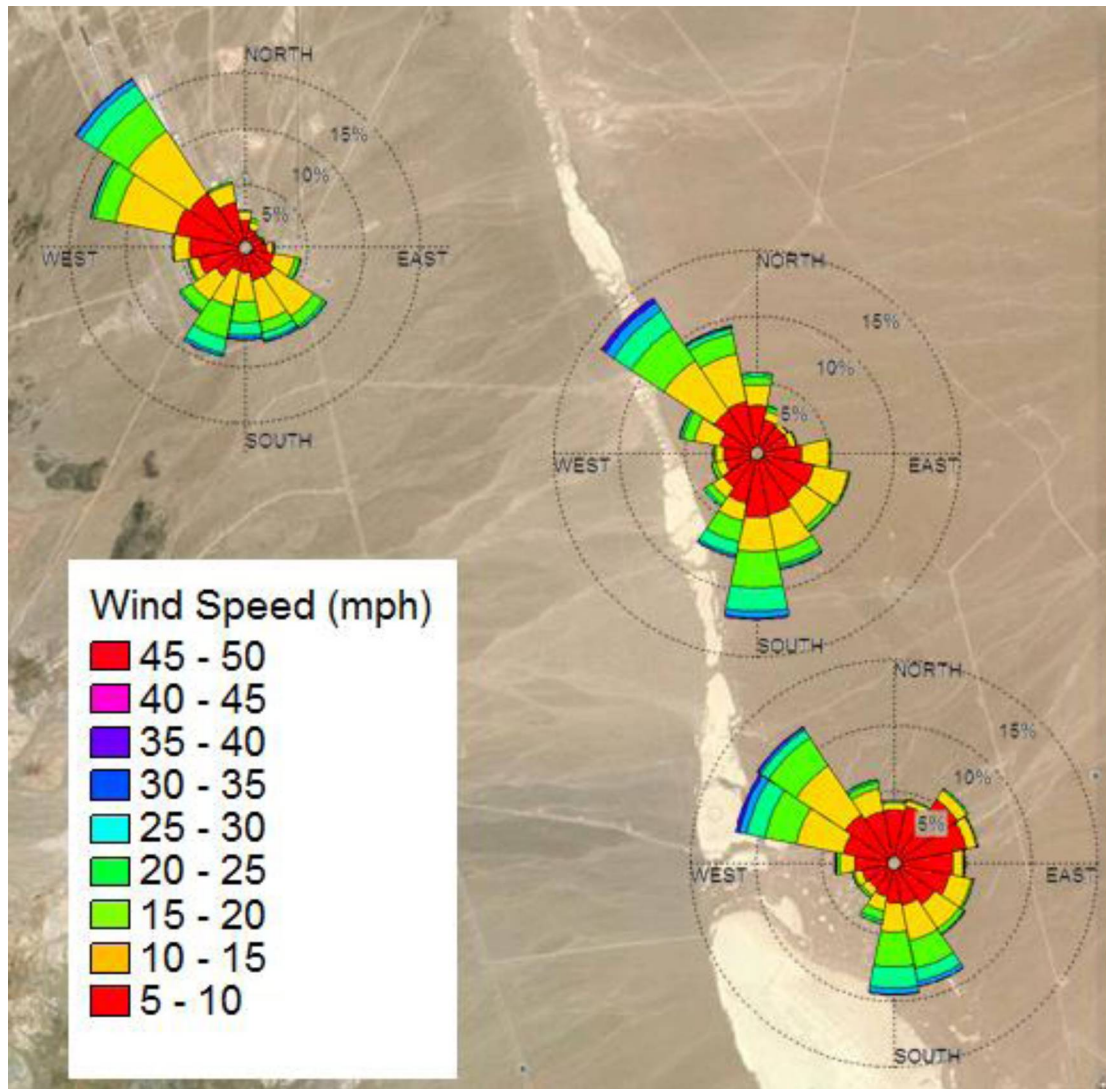


Figure 20. Annual wind rose diagrams for the TTR stations shown in map view.

RADIOLOGICAL ASSESSMENT OF AIRBORNE PARTICULATES

Airborne dust particles are collected continuously using Hi-Q™ samplers located at each of the TTR air monitoring stations. A glass-fiber filter (diameter: 10 cm [4 in]; pore size: 0.3 μm) was used at all stations during CY2014. Prior to CY2014, cellulose-fiber filters (diameter: 10 cm [4 in]; pore size: 20 μm to 25 μm) were used at Stations 401 and 402. A cellulose-fiber filter was also used for a duplicate air sampler installed at Station 400 and operated from May 2013 through May 2014 to compare filter performance and related analytical results. Previous monitoring reports (Mizell *et al.*, 2014) observe that gross alpha and gross beta measurements are significantly lower for samples collected with cellulose-fiber filters compared with glass-fiber filters. This is attributed to the finer pore size of the glass-fiber filter, which captures more particles.

The Hi-Q™ air sampling equipment draws ambient air through the filters at a rate of approximately 56.6 lpm (2 cfm) and is designed to maintain the same flow rate as dust gathers on the filter. The total volume of air passed through the filter and the total hours of operation are recorded when filters are recovered from the monitoring stations and new filters are deployed every two weeks. Filters are weighed before and after deployment to determine the mass of particulates collected. Sample filters are accumulated and periodically submitted to the RSL at the University of Nevada, Las Vegas, for gross alpha, gross beta, and gamma spectroscopy assessment. The gross alpha and gross beta observations for CY2014 are summarized below in Tables 3 and 4, respectively.

Filters collected during CY2014 were deployed between December 23, 2013, and December 23, 2014. This generated 26 air particulate filter samples for Station 400. Only 24 particulate samples were collected from Stations 401 and 402 because of denial of access in April. The results from samples collected with cellulose-fiber filters from the second air sampler at Station 400 will only be used for the filter comparison study, which is described in a following section. The mean annual gross alpha activity (Table 3) for the glass-fiber filter samples ranged from 1.41×10^{-15} $\mu\text{Ci/mL}$ at Station 401 to 1.66×10^{-15} $\mu\text{Ci/mL}$ at Station 402. The mean annual gross beta activity (Table 4) for the glass-fiber filter samples ranged from 1.46×10^{-14} $\mu\text{Ci/mL}$ at Station 401 to 1.94×10^{-14} $\mu\text{Ci/mL}$ at Station 402.

Table 3. Gross alpha results for TTR sampling stations 2014.

Sampling Location	Number of samples	Concentration ($\times 10^{-15}$ $\mu\text{Ci/mL}$ [3.7×10^{-5} Becquerel (Bq/m^3)])			
		Mean	Standard Deviation	Minimum	Maximum
Station 400(G)	26	1.60	0.79	0.28	3.50
Station 400(C)	11	1.35	0.46	0.73	2.48
Station 401(G)	24	1.41	0.67	0.22	2.59
Station 402(G)	24	1.66	0.77	0.62	2.90

NOTES: Bq = Becquerel; m^3 = cubic meter; $\mu\text{Ci}/\text{ml}$ = microcurie per milliliter; TTR = Tonopah Test Range; (G) = glass-fiber filter; (C) = cellulose-fiber filter; glass-fiber filters retain particulates greater than $0.3 \mu\text{m}$; cellulose-fiber filters retain particulates greater than $20 \mu\text{m}$.

Table 4. Gross beta results for TTR sampling stations 2014.

Sampling Location	Number of samples	Concentration ($\times 10^{-14}$ $\mu\text{Ci/mL}$ [3.7×10^{-4} Becquerel (Bq/m^3)])			
		Mean	Standard Deviation	Minimum	Maximum
Station 400(G)	26	1.79	0.35	1.08	2.36
Station 400(C)	11	0.76	0.26	0.51	1.57
Station 401(G)	24	1.46	0.28	0.95	1.92
Station 402(G)	24	1.94	0.37	1.32	2.60

NOTES: Bq = Becquerel; m^3 = cubic meter; $\mu\text{Ci}/\text{ml}$ = microcurie per milliliter; TTR = Tonopah Test Range; (G) = glass-fiber filter; (C) = cellulose-fiber filter; glass-fiber filters retain particulates greater than $0.3 \mu\text{m}$; cellulose-fiber filters retain particulates greater than $20 \mu\text{m}$.

Table 5 gives the CY2014 gross alpha and gross beta concentrations reported for CEMP stations surrounding the TTR. Glass-fiber filters are used in the air samplers at the CEMP stations, so the comparison below is limited to the glass-fiber filter samples from the TTR. Mean annual gross alpha concentrations at the TTR monitoring stations are higher than the values at all of the surrounding CEMP stations with the exception of Sarcobatus Flats (Figure 21). The maximum gross alpha value for 2014 of $3.5 \times 10^{-15} \mu\text{Ci}/\text{mL}$ was recorded at both Sarcobatus Flats and TTR Station 400. The mean annual gross beta concentrations at the CEMP stations (Figure 22) are higher than those measured at the TTR stations with the exception of TTR Station 402 being higher than Beatty and Tonopah. All of the TTR maximum gross beta measurements are lower than the maximums measured at the CEMP stations.

Table 5. Mean annual gross alpha and gross beta concentrations for 2014 reported at CEMP stations that surround the TTR.

Sampling Location	Gross alpha ($\times 10^{-15} \mu\text{Ci}/\text{mL}$)			Gross beta ($\times 10^{-14} \mu\text{Ci}/\text{mL}$)		
	Mean	Minimum	Maximum	Mean	Minimum	Maximum
Alamo	1.38	0.51	3.24	2.00	1.34	2.84
Beatty	0.91	0.25	1.35	1.92	1.11	2.91
Goldfield	1.02	0.63	2.83	1.97	1.28	3.34
Rachel	0.95	0.40	1.65	1.98	1.24	2.78
Sarcobatus Flats	1.71	0.67	3.50	2.10	1.19	3.74
Tonopah	0.90	0.50	1.93	1.81	1.12	3.01

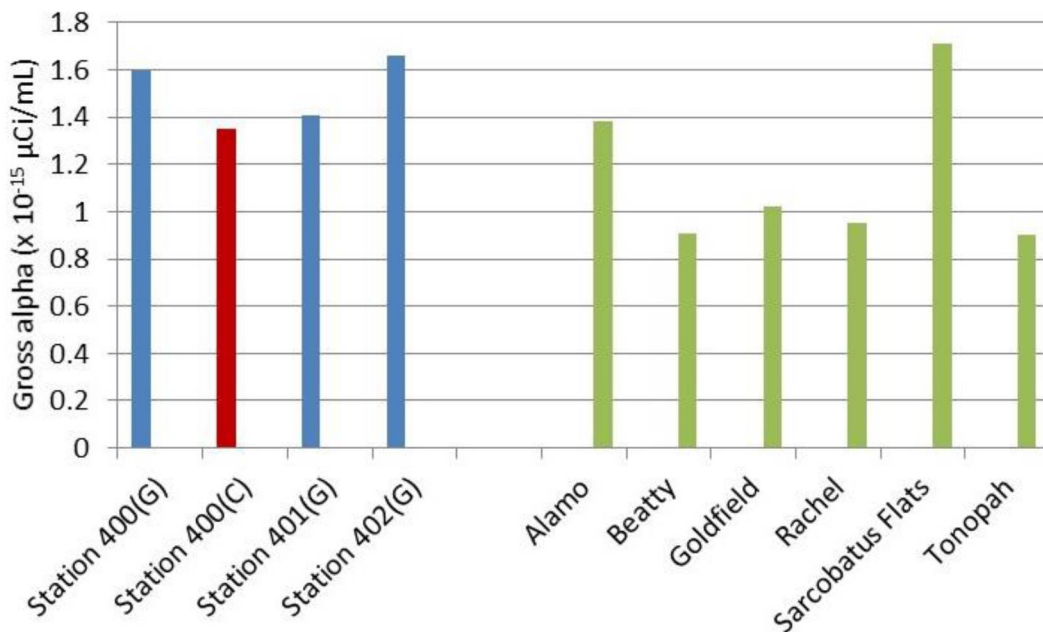


Figure 21. The mean annual gross alpha concentrations for the TTR samples collected on glass-fiber filters (blue) are higher than the mean annual gross alpha concentrations for samples collected at most of the CEMP stations (green). The mean of the TTR samples collected on cellulose-fiber filters is shown in red.

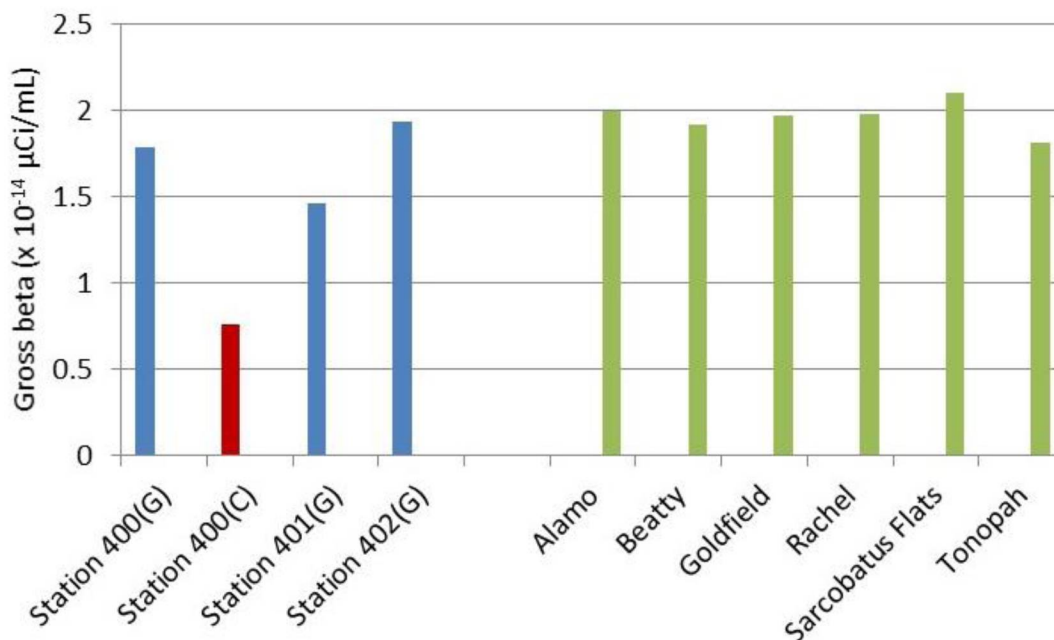


Figure 22. The mean annual gross beta concentrations for the TTR samples collected on glass-fiber filters (blue) are in the same range or lower than the mean annual gross beta concentrations for samples collected at the CEMP stations (green). The mean of the TTR samples collected on cellulose-fiber filters is shown in red.

Gamma spectroscopy identified only naturally occurring radionuclides in the particulate samples collected from TTR air monitoring Stations 400, 401, and 402 during CY2014 (Table 6). The detected radionuclides occurred with varying frequency. Beryllium-7 and lead-210 were the most commonly detected. No anthropogenic, gamma-emitting radionuclides were detected. No indicators of plutonium-239 or plutonium-240 were detected.

Table 6. The number of CY2014 particulate samples in which naturally occurring radionuclides were identified by gamma spectroscopy varied by radionuclide and between stations.

Ion	Number of samples		
	Station 400	Station 401	Station 402
Beryllium-7 (Be-7)	24	23	24
Lead-210 (Pb-210)	10	5	11
Potassium-40 (K-40)	1	4	1
Protactinium-234m (Pa-234m)	1	0	0

COMPARISON OF GLASS-FIBER AND CELLULOSE-FIBER FILTERS

Cellulose-fiber filters were used in the air particulate samplers from the date of installation until March 23, 2011, when glass-fiber filters were installed at Station 400 located in the Sandia ROC compound on the TTR. The switch from cellulose- to glass-fiber filters occurred as interest in the radionuclide characteristics of the inhalable fraction (PM₁₀) of airborne particulates increased. Cellulose-fiber filters have a pore size of 20 to 25 micrometer (μm) that will pass the PM₁₀, whereas the glass-fiber filters have a pore size of 0.3 μm and will retain the majority of the PM₁₀. Between May 29, 2013, and May 28, 2014, airborne particulate samples were collected on both glass- and cellulose-fiber filters to provide comparable samples. Sample mass, gross alpha activity, and gross beta activity were used to compare the effectiveness of the two sample filters (Mizell and Shadel, in review). Samples were collected and new filters were deployed approximately every 14 days, which resulted in 26 paired samples for the comparison.

Because the glass-fiber filters have a smaller pore size, they were expected to collect more particulate material, and therefore have greater sample mass. The average sample mass collected on the glass-fiber filters, 0.0217 grams (g), was approximately 1.5 times the average sample mass collected on the cellulose-fiber filters, 0.0144 g (Mizell and Shadel, in review). On four occasions, the mass on the cellulose-fiber filter was greater than the mass on the glass-fiber filter. A nonparametric matched-pair sign test (Helsel and Hirsch, 1995) was performed to evaluate the probability that samples collected on the different filter media represent the same sample-mass populations. At $\alpha = 0.01$, there is 0.00 probability that the mass collected on the glass- and cellulose-fiber filters represent the same population. Therefore, the null hypothesis is rejected and the glass- and cellulose-fiber filters are statistically determined to represent different sample-mass populations. Samples collected on glass-fiber filters represent a population with greater mass.

Because the glass-fiber filters retain more mass and a greater amount of small particles, they were expected to result in higher gross alpha and gross beta activities. The average gross alpha activity on glass-fiber filters, 1.95×10^{-15} μCi/mL, was approximately 1.43 times greater than the average gross alpha activity on cellulose-fiber filters, 1.36×10^{-15} μCi/mL (Mizell and Shadel, in review). Similarly, the average gross beta activity on glass-fiber filters, 1.90×10^{-14} μCi/mL, was almost twice the average gross beta activity on cellulose-fiber filters, 0.97×10^{-14} μCi/mL. Although the gross alpha data suggest that the glass-fiber filter results are greater than the cellulose-fiber filter results, there are nine sample pairs in which the gross alpha activity for the cellulose-fiber filters is greater or the same as on the glass-fiber filters. In contrast, the gross beta activity for the glass-fiber filters is always greater than for the paired cellulose-fiber filter. Using the nonparametric matched-pair sign test (Helsel and Hirsch, 1995), it was determined that at the significance level of $\alpha = 0.01$, the probability that the gross alpha activity for the glass- and cellulose-fiber filter data sets represent the same gross-alpha-activity population is approximately 10 percent. This low probability leads to the conclusion that the two filters produce gross alpha results that represent different populations. The nonparametric matched-pair sign test (Helsel and Hirsch, 1995) results in the same conclusion for the gross beta activities. These statistical tests indicate that the radiological characteristics for the glass-fiber filter samples are statistically different from those obtained for the cellulose-fiber filter samples.

A linear regression analysis was performed to determine if gross alpha and gross beta activities equivalent to a glass-fiber filter sample could be estimated from the measured cellulose-fiber filter activity. This analysis produced a regression coefficient (R^2) of 0.0395 for the gross alpha data and 0.5025 for the gross beta data (Mizell and Shadel, in review). There is little correlation between the glass- and cellulose-fiber filter values for the gross alpha values and a fair correlation for the gross beta values. The cellulose sample gross alpha activity cannot be used to estimate a likely glass-fiber filter equivalent value. The glass-fiber filter equivalent can be estimated with fair reliability from the gross beta activity of a cellulose-fiber filter.

These statistical analyses (Mizell and Shadel, in review) indicate that the glass-fiber filters produce air particulate samples with greater mass and higher gross alpha and gross beta activities. Additionally, linear regression results in a glass-fiber filter equivalent gross alpha activity estimate with very low confidence and glass-fiber filter equivalent gross beta activity estimate with only fair confidence, which indicates that glass-fiber equivalent concentrations cannot reliably be estimated from past samples collected using cellulose-fiber filters.

GAMMA RADIATION OBSERVATIONS

Gamma radiation is measured using a PIC detector. A PIC detector is generally deployed to detect gamma radiation events that substantially exceed ambient radiation levels as a result of human activities. In the absence of such activities, ambient gamma radiation rates are recorded. These radiation values vary naturally among locations and reflect differences in altitude and latitude (cosmic radiation) and radioactivity in the soil (terrestrial radiation). Additionally, slight variations in gamma radiation at a single location may be because of changes in weather (UNSCEAR, 2000).

The PIC data collected at the TTR air monitoring stations measure gamma radiation exposure every three seconds. These measurements are averaged every 10 minutes before being recorded in the station database. The 10-minute average gamma values for CY2014 recorded at TTR monitoring Stations 400, 401, and 402 are presented in Table 7 and Figure 23. Shown with the gamma record from each PIC are: the mean of all CY2014 10-minute gamma values at that station and the PIC mean plus and minus two standard deviations.

Table 7. Gamma exposure rate at the TTR measured by the PIC detectors.

Sampling Location	Average of 10-minute Gamma Exposure Rate ($\mu\text{R/hr}$)			
	Mean	Standard Deviation	Minimum	Maximum
Station 400	19.16	0.39	16.14	26.85
Station 401	20.25	0.82	18.12	26.02
Station 402	20.74	0.66	18.79	25.39

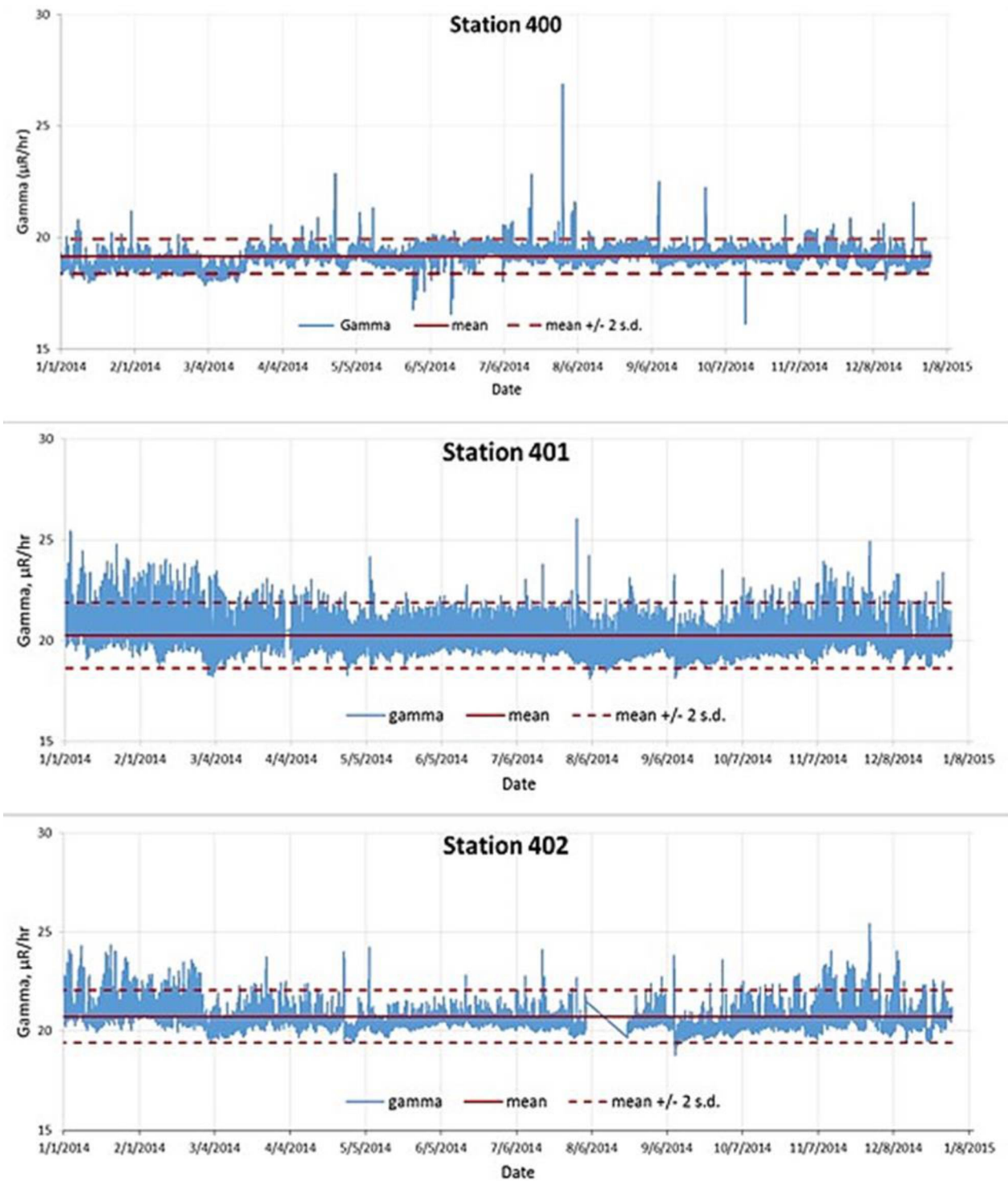


Figure 23. The CY2014 PIC gamma data for the TTR monitoring stations. The data gap at Station 402 in August was because of equipment failure at the station.

The average gamma exposure rates for the CEMP stations in the region are generally lower than the TTR stations with the exception of the CEMP station at Warm Springs Summit (Table 8). The 2013 annual report (Mizell *et al.*, 2014) examined atmospheric conditions coinciding with increases in gamma radiation. Observed meteorological conditions associated with intervals of increased gamma values commonly included increasing wind speeds, wind direction changes, increasing barometric pressure, increasing humidity, decreasing air temperature, and precipitation. These conditions also indicate a passing storm front, which suggests an association between storm front passage and intervals of increased gamma values. Additionally, high dust counts observed prior to the intervals of increased gamma values are likely the result of the winds associated with these storm fronts. The 2013 analysis concluded that the observed intervals of increased gamma values were not associated with wind transport of radionuclide-contaminated soil material.

A comparison of the CY2014 gamma measurements for Station 400 with precipitation measured at the monitoring station (Figure 24) reveals that many of the short-term gamma increases coincide with precipitation events. Comparisons between the stations and with the gamma record from the CEMP station at Warm Springs Summit also find coincidence between the timing of the gamma increases (Figure 25). These observations suggest that many of the higher gamma values are associated with precipitation or other widespread weather events, not migration of contaminated material from the Clean Slate sites.

Table 8. Gamma exposure rate measured with PICs at CEMP stations in the TTR region.

Sampling Location	Average of 10-minute Gamma Exposure Rate ($\mu\text{R/hr}$)			
	Mean	Standard Deviation	Minimum	Maximum
Alamo	13.23	0.37	12.13	17.28
Beatty	16.44	0.28	15.27	18.94
Goldfield	14.67	0.41	11.94	18.47
Rachel	14.98	0.55	10.63	18.27
Sarcobatus Flats	16.82	0.40	10.63	21.36
Tonopah	15.8	0.35	14.02	20.42
Warm Springs Summit	19.33	0.48	18.08	23.77

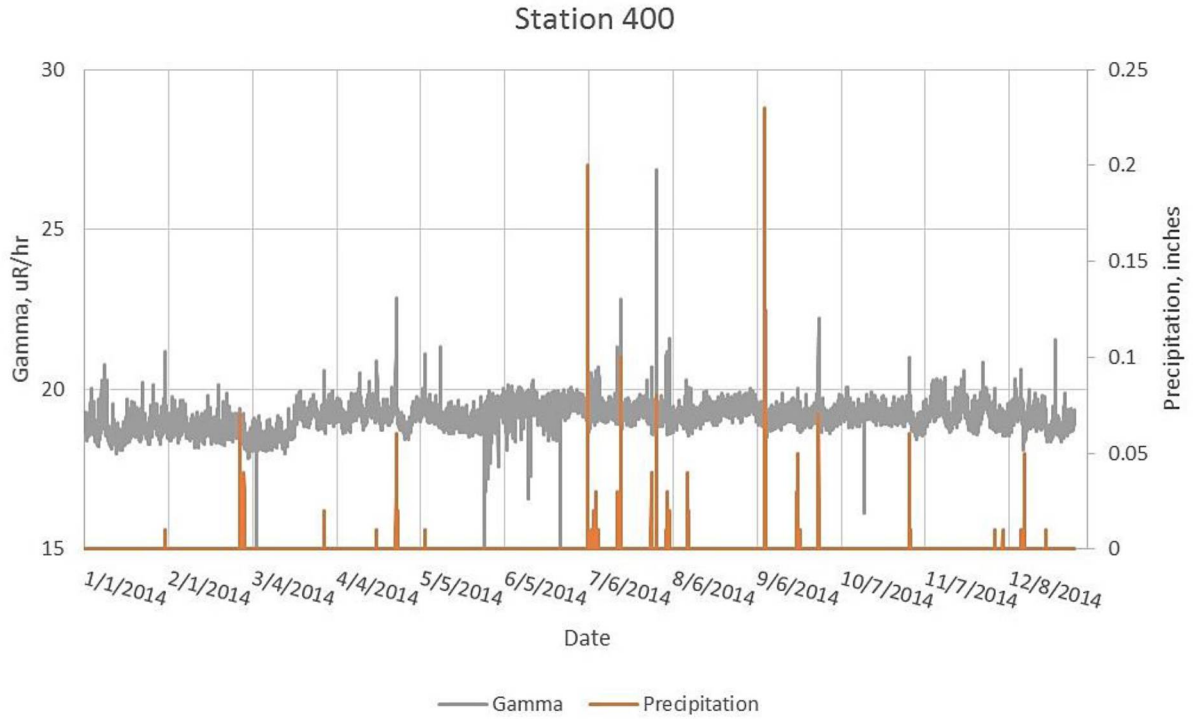


Figure 24. The CY2014 PIC gamma data and precipitation for TTR Station 400.

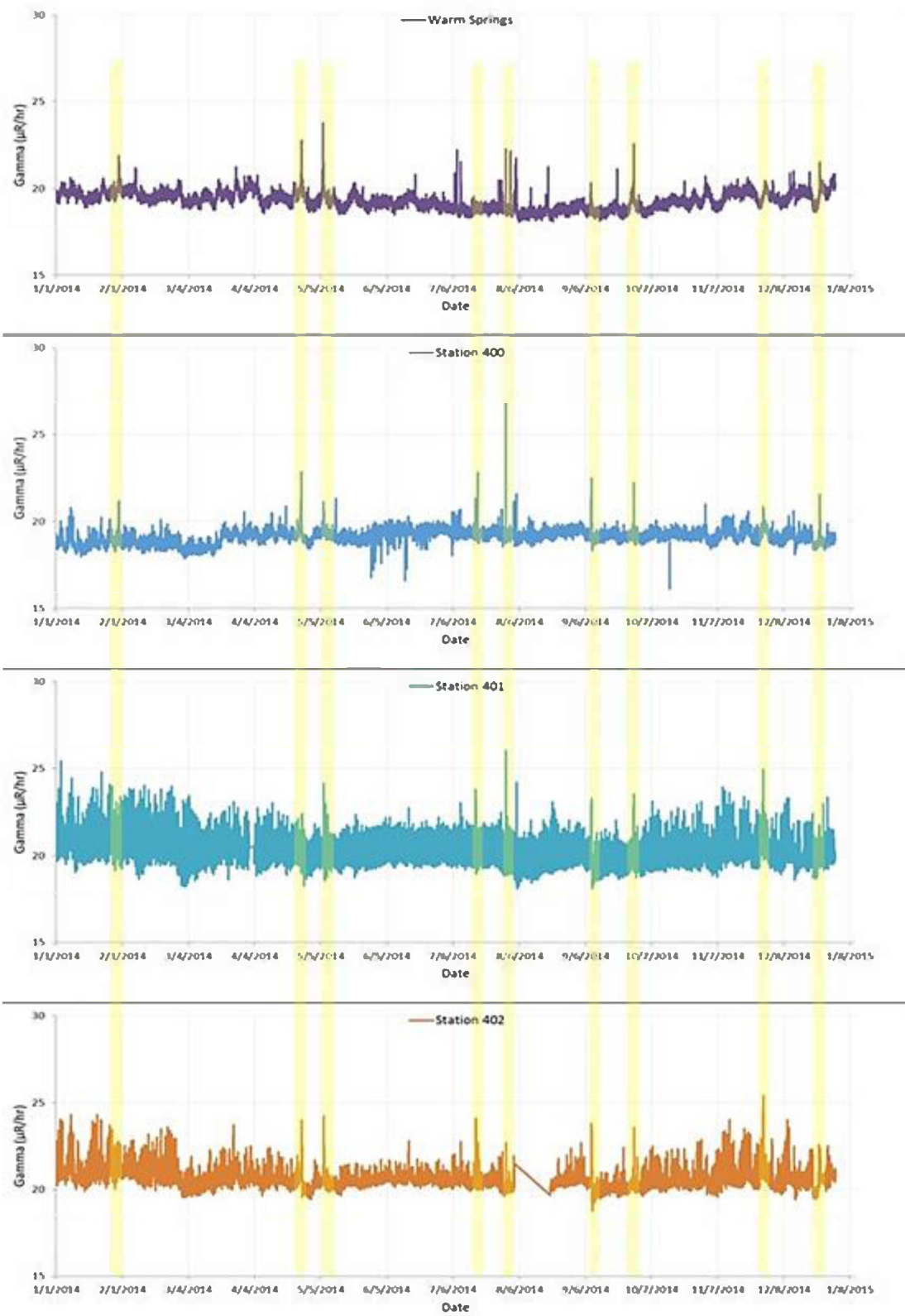


Figure 25. The CY2014 PIC gamma data for the CEMP station at Warm Springs Summit and the TTR stations, highlighting coincident times of increased values.

OBSERVATIONS OF SOIL TRANSPORT BY SALTATION

Saltation is the mechanism by which larger soil particles are transported across the ground surface. Generally, saltation involves particle sizes greater than approximately 50 μm . Particles are dislodged and carried a small distance in the air before falling to the ground (Figure 26). Transport paths usually follow a parabolic trajectory; the particles essentially bounce across the ground. The amount of time the particles are in the air and the distances traveled are functions of wind speed and particle mass. Saltation is important because the impact of saltated particles dislodges smaller particles and ejects them into the air where the smaller particles are transported by suspension.

The Sensit H11-LINTM (Sensit, Inc., Redlands, California) is deployed at TTR air monitoring Stations 401 and 402 to measure the motion of soil particles saltating across the ground surface. The sensing area, which is set 10 cm (4 in) above the ground surface, wraps completely around the vertically oriented instrument and is capable of registering impacts from any direction. The sensing area is made of piezoelectric material that converts particle impacts to electrical impulses that are registered and summed over 10-minute intervals and subsequently stored on the station data logger. The saltation sensors are located in proximity to the meteorological towers at each station in areas that are free of recent disturbance and vegetation that might interfere with their operation. Windblown plant debris, such as tumbleweed, is cleared from the sensor area as needed. Rain drop impact dislodges soil particles and ejects particles and may result in spurious impact counts on the saltation sensors during precipitation events. Therefore, saltation sensor data that are coincident with precipitation are not considered during data analysis.

Sand particle saltation is strongly dependent on wind speed. The relationship between wind speed and saltation particle counts was investigated by determining the average number of particle counts/10-minute interval for wind speeds categorized in 8 km/hr (5-mph) wind speed classes (Table 9) after removing those intervals influenced by rain for the reasons described above. Figure 27 shows that the relationship between wind speed and saltation particle count is not linear. As wind speed increases past a threshold value (approximately 24 to 32 km/hr or 15 to 20 mph), the particle counts respond by increasing roughly exponentially. Below the 32 km/hr (20 mph) wind class, both Stations 401 and 402 show similarly low saltation counts. At wind speeds above 32 km/hr (20 mph), the saltation counts at Station 401 are notably greater than observed at Station 402, though the shape of the curves is similar. There could be a real difference in supply of saltation-sized particles between the sites or the difference in saltation counts could be a localized effect that depends on the placement of the Sensit. Data from the multiple BSNE traps can be used to assess variability between the sites.

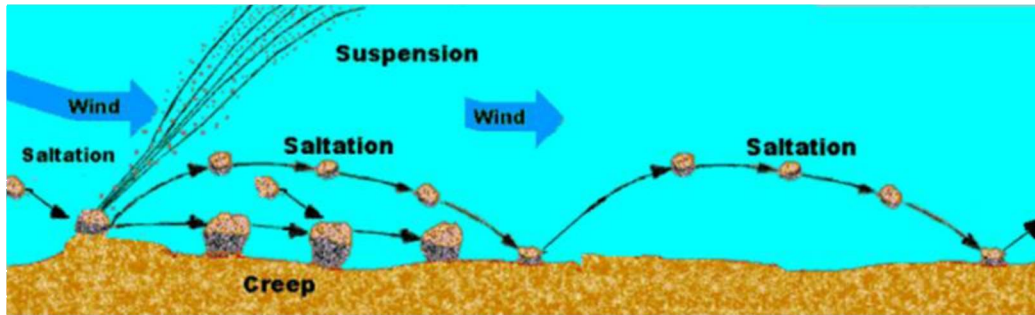


Figure 26. Diagram of the saltation process. Suspension of smaller particles ejected by the impact of a particle landing after saltation is depicted on the left.

Table 9. Average saltation particle impact counts by wind speed class at TTR air monitoring Stations 401 and 402.

Wind Speed Class (mph)	Duration (hours)	Average Wind Speed (mph)	Average Particle Counts (count/10-min)
Station 401			
0 – 5	4157.5	2.59	0.00
5 – 10	2580.8	6.88	0.08
10 – 15	1204.0	11.90	0.36
15 – 20	537.5	16.80	0.87
20 – 25	160.5	21.60	2.36
25 – 30	59.2	26.64	13.35
30 – 35	4.5	30.71	99.85
>35	0.2	35.10	367.00
Total	8704.2		
Station 402			
0 – 5	4318.7	2.53	0.23
5 – 10	2123.3	6.83	1.53
10 – 15	1059.7	11.89	1.26
15 – 20	465.2	16.81	1.93
20 – 25	146.5	21.71	4.87
25 – 30	45.3	26.64	12.89
30 – 35	2.7	31.36	57.81
Total	8161.3		

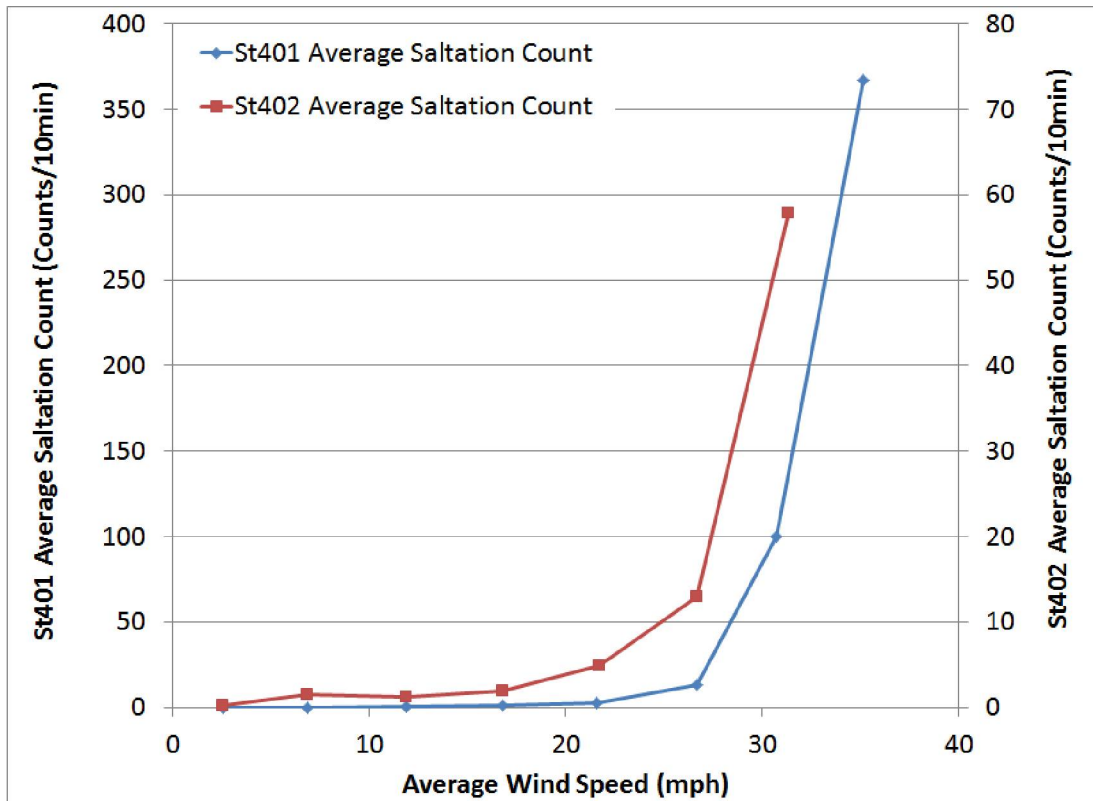


Figure 27. Average saltation counts generally increase rapidly as the wind speed increases above 20 mph at both TTR air monitoring Stations 401 and 402.

Because saltated particles are likely to dislodge and eject smaller particles from the soil surface, the relationship between saltation particle counts and PM_{10} concentrations is important. A correlation analysis was performed to investigate this relationship. The strong correlation between high saltation values and high PM_{10} values indicates that saltation (driven by strong winds) contributes to the fine dust emissions. The PM_{10} concentration can also be generated by the resuspension of dust deposited on the soil surface by winds below the saltation threshold, in which case the PM_{10} concentration is not associated with saltation counts. Such resuspension without saltation is often supply limited, with the PM_{10} concentration elevated for a short time and then decreasing even though the wind remains strong. Figure 28 shows the correlation between saltation counts and PM_{10} concentration at Stations 401 and 402. At both stations, there is a strong linear correlation between saltation counts and PM_{10} concentration in 2014. Although there is a strong, apparently linear, relationship between saltation and PM_{10} concentration at both stations, the difference in slopes indicate that saltation counts can be used to indicate when PM_{10} concentrations are likely to be elevated but cannot be used to precisely predict the value of PM_{10} concentrations, certainly not through a general (not site-specific) relationship. This is probably because of a high degree of spatial variation in saltation counts, even within an area that is nominally homogeneous in terms of sand and dust transport character.

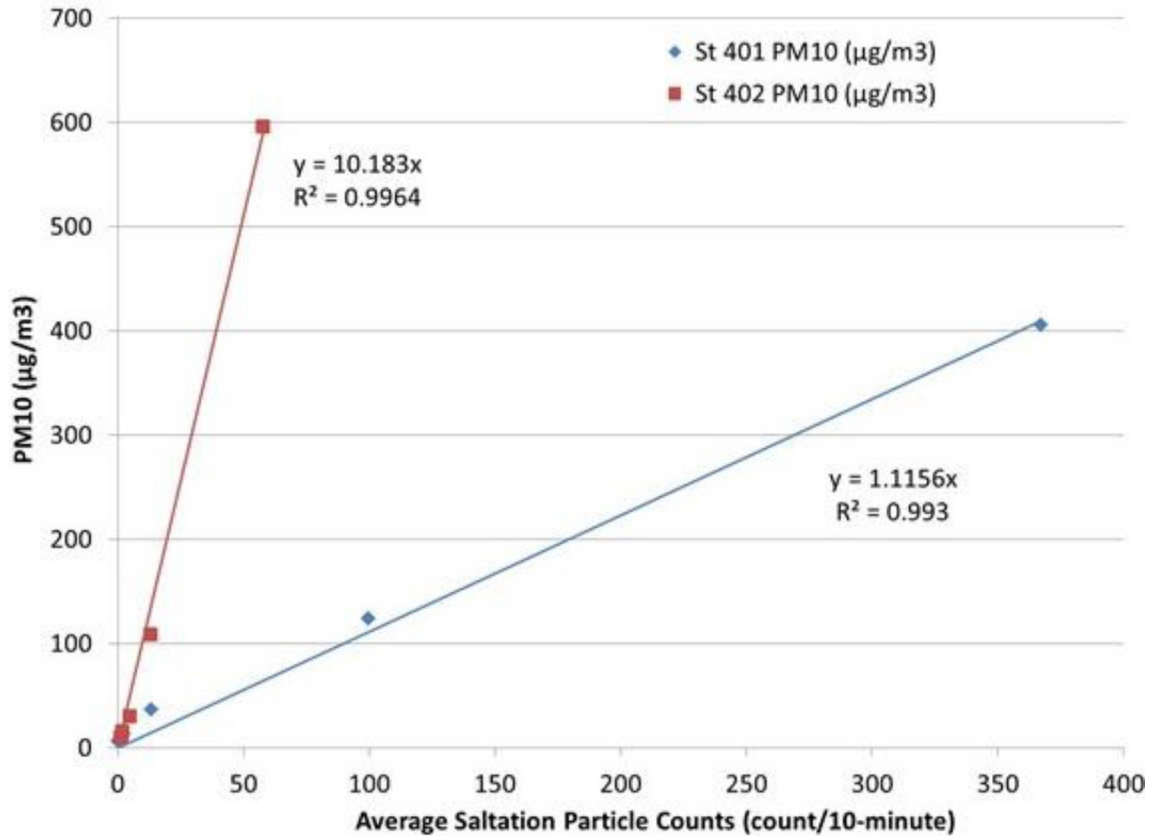


Figure 28. Regression of PM₁₀ against saltation counts by wind speed class.

OBSERVATIONS OF SOIL TRANSPORT BY SUSPENSION

Table 10 summarizes wind speed and the corresponding PM₁₀ concentration by wind speed class for Stations 400, 401, and 402. More than 90 percent of the time, the wind speed at all three stations is below 24 km/hr (15 mph) and the corresponding average PM₁₀ concentrations are below 12 µg/m³. Although PM₁₀ concentrations generally increase as wind speed increases, the PM₁₀ concentrations remain fairly low until winds exceed approximately 32 km/hr (20 mph). At Station 400, PM₁₀ concentrations increase with increasing wind speed and exceed 415 µg/m³ for the strongest winds between 48 and 57 km/hr (30 and 35 mph). At Stations 401 and 402, PM₁₀ concentrations also increased consistently with increasing wind speed, reaching a maximum of 405 µg/m³ and 509 µg/m³, when winds were above 48 and 57 km/hr (30 and 35 mph), respectively.

Table 10. Summary of wind and PM₁₀ data for Stations 400, 401, and 402 for CY2014.

Wind Speed Class (mph)	Duration (hours)	Frequency (%)	Cumulative Frequency (%)	Average Wind Speed (mph)	PM ₁₀ (µg/m ³)
Station 400					
0 – 5	3565.2	41.24%	41.24%	3.02	8.73
5 – 10	3138.0	36.29%	77.53%	6.82	7.54
10 – 15	1274.0	14.74%	92.27%	11.77	8.67
15 – 20	492.7	5.70%	97.96%	16.61	12.71
20 – 25	143.5	1.66%	99.62%	21.54	24.94
25 – 30	31.8	0.37%	99.99%	26.04	54.19
30 – 35	0.7	0.01%	100.00%	30.22	415.42
Total	8645.8				
Station 401					
0 – 5	4157.5	47.76%	47.76%	2.59	6.79
5 – 10	2580.8	29.65%	77.42%	6.88	6.61
10 – 15	1204.0	13.83%	91.25%	11.90	6.49
15 – 20	537.5	6.18%	97.42%	16.80	8.16
20 – 25	160.5	1.84%	99.27%	21.60	13.54
25 – 30	59.2	0.68%	99.95%	26.64	37.09
30 – 35	4.5	0.05%	100.00%	30.71	123.67
>35	0.2	0.00%	100.00%	35.10	405.19
Total	8161.3				
Station 402					
0 – 5	4318.7	52.92%	52.92%	2.53	9.38
5 – 10	2123.3	26.02%	78.93%	6.83	10.11
10 – 15	1059.7	12.98%	91.92%	11.89	10.39
15 – 20	465.2	5.70%	97.62%	16.81	15.82
20 – 25	146.5	1.80%	99.41%	21.71	30.61
25 – 30	45.3	0.56%	99.97%	26.64	108.58
30 – 35	2.7	0.03%	100.000%	31.36	595.69
Total	8733.8				

High wind and correspondingly high PM₁₀ events are relatively rare and generally last for only short periods of time (Figures 29 and 30). Light winds (0 to 8 km/hr [0 to 5 mph]) are most common. Wind speeds in excess of 24 km/hr (15 mph) occur less than 10 percent of the time and wind speeds in excess of 32 km/hr (20 mph) occur less than three percent of the time. The wind speed exceeds 48 km/hr (30 mph) only 0.01 percent (<1 hr) of the year at Station 400, 0.05 percent (<5 hr) of the year at Station 401, and 0.03 percent (<3 hr) of the year at Station 402. All three monitoring stations show similar trends and dependence on wind speed when it comes to PM₁₀ concentration (Figures 31 and 32).

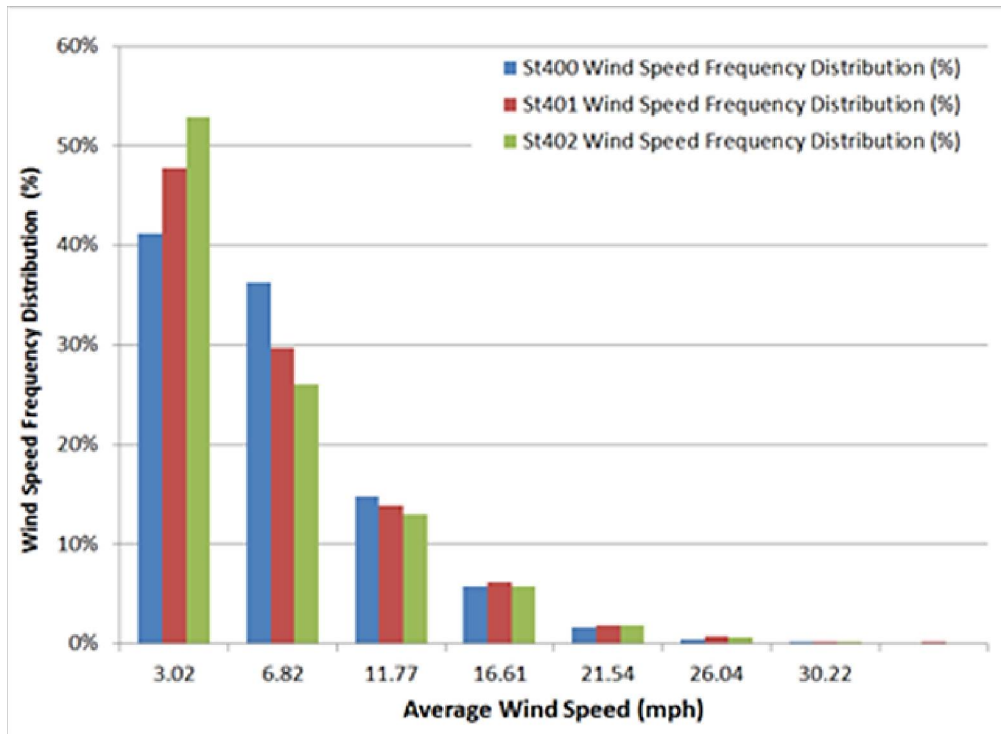


Figure 29. Wind speed frequency by wind class for Stations 400,401, and 402 for CY2014. The portion of time wind speed falls within a given class is plotted against the average wind speed for that class.

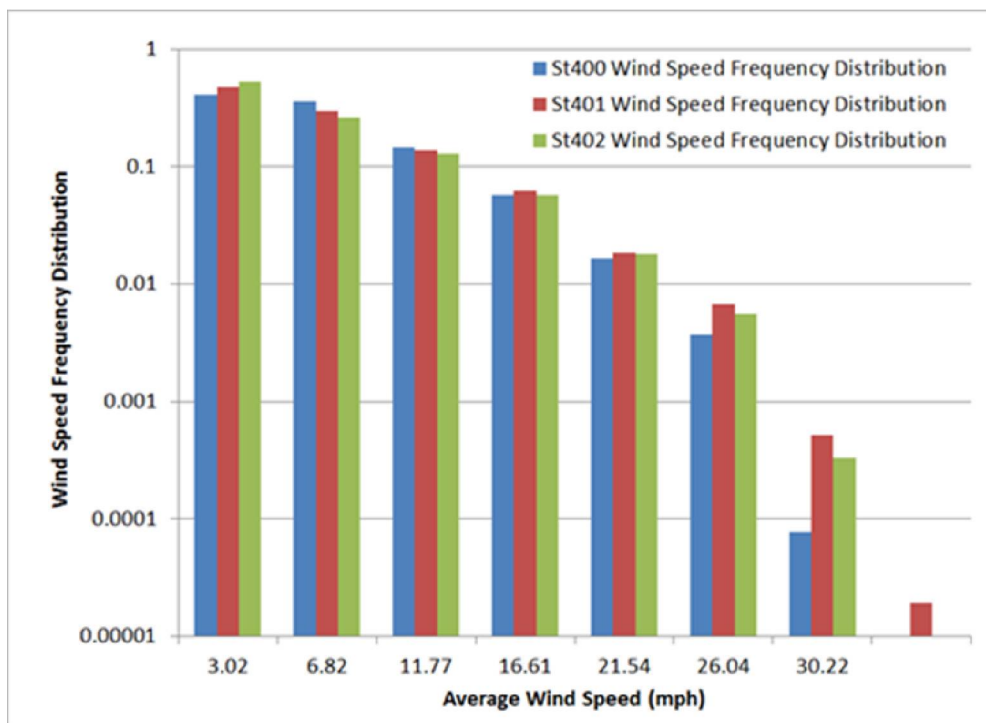


Figure 30. Same as Figure 29 but with logarithmic y-axis.

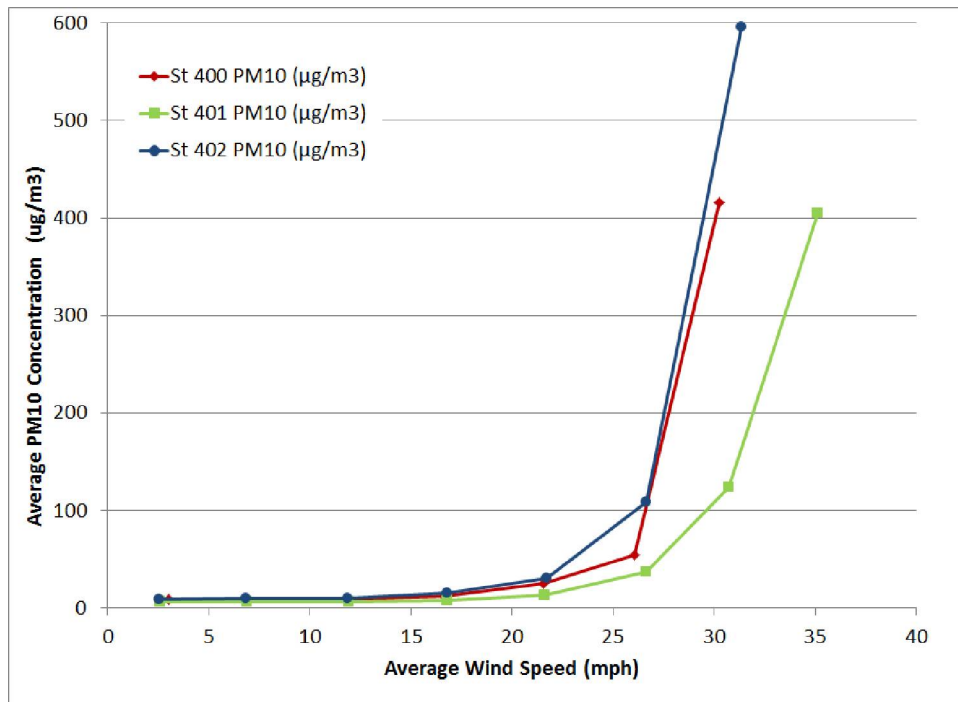


Figure 31. PM₁₀ trends as a function of wind speed for stations 400, 401, and 402 for CY2014.

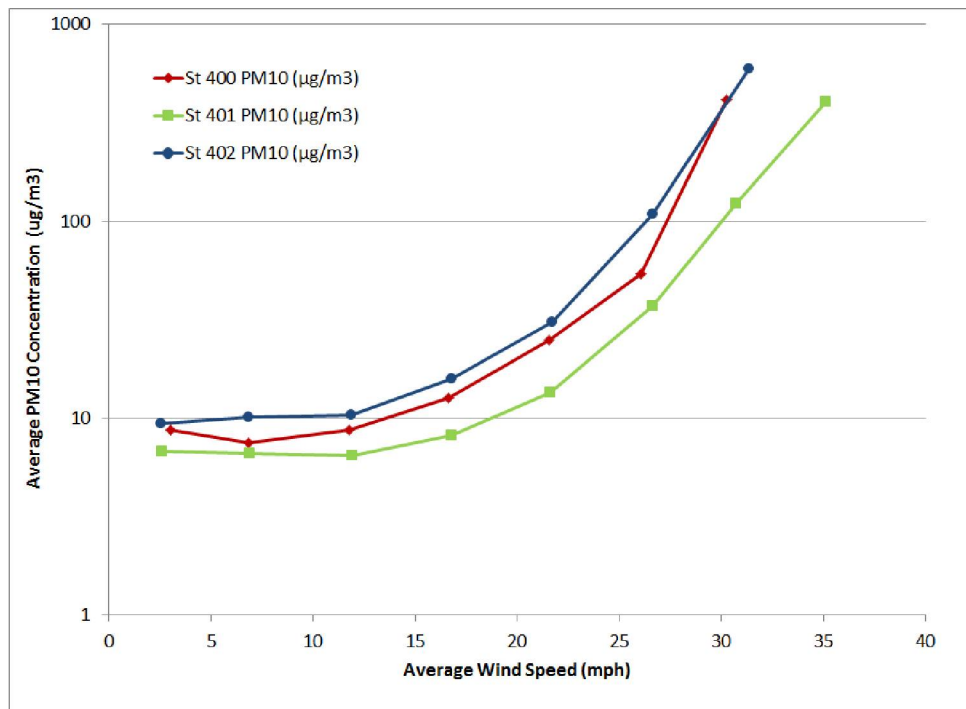


Figure 32. PM₁₀ trends as a function of wind speed for stations 400, 401, and 402 for CY2014. PM₁₀ concentration plotted on a logarithmic scale to illustrate wide dynamic range of PM₁₀ concentrations.

PM₁₀ TO PM_{2.5} RATIO

Wind is the driving mechanism for transport of dust, soil, and potentially contaminated material but it is challenging to decouple and identify dust that is emitted from the Clean Slate Sites from dust that is transported from surrounding areas. The 2013 monitoring report (Mizell *et al.*, 2014) recommended performing a particle size analysis to characterize the dust at each site and enhance interpretation of saltation and suspension data. In CY 2014, this recommendation was followed.

In order to determine the dust contribution between near and far dust sources at monitoring stations at the TTR, the data analysis includes calculation of PM_{2.5} concentration (particles of aerodynamic diameter less than 2.5 micrometers). The PM_{2.5} concentration contains smaller-sized particles that have considerably lower settling velocity and longer residence time in the atmosphere. Mineral dust contains larger-sized fraction particles and usually the PM₁₀ concentration is four to eight times the PM_{2.5} concentration. When mineral dust is emitted and transported by wind, larger particles tend to settle and are not transported large distances, so the ratio of PM₁₀ to PM_{2.5} concentrations generally tends to decrease with transport distance. This ratio can sometimes be used to estimate how far the aerosol has traveled from the source area. Higher PM₁₀ to PM_{2.5} ratios indicate aerosol emitted closer to the measurement site. This type of data analysis is applied to the Clean Slate sites to determine if dust emissions and transport occur close to the monitoring stations or at a greater distance from sites that are likely not to be contaminated. The PM_{2.5} concentration as a function of average wind speed class is shown in Figure 33 and has a very similar trend as Figure 31 for PM₁₀ concentration. However, the PM_{2.5} mass concentrations are lower than the PM₁₀ concentration, which is to be expected because the former are included in the latter.

The ratio between PM₁₀ and PM_{2.5} for increasing wind speed classes is shown in Figure 34. Station 401 shows a significant increase in this ratio from around three for wind speeds under 24 km/hr (15 mph) to over six for wind speeds over 32 km/hr (20 mph). This information is consistent with Figure 16, which shows higher saltation counts at Station 401. This indicates that soil around monitoring Station 401 may be more locally emissive for winds over 32 km/hr (20 mph) when compared with Stations 400 and 402, but the future data from the BSNE traps is needed to examine this possibility further. An increase in the same ratio can be seen for Stations 400 and 402 for wind speeds over 32 km/hr (20 mph), but not to the degree observed at Station 401. This general trend indicates that local transport of dust, proximal to all the monitoring stations, occurs for wind speeds above 32 km/hr (20 mph).

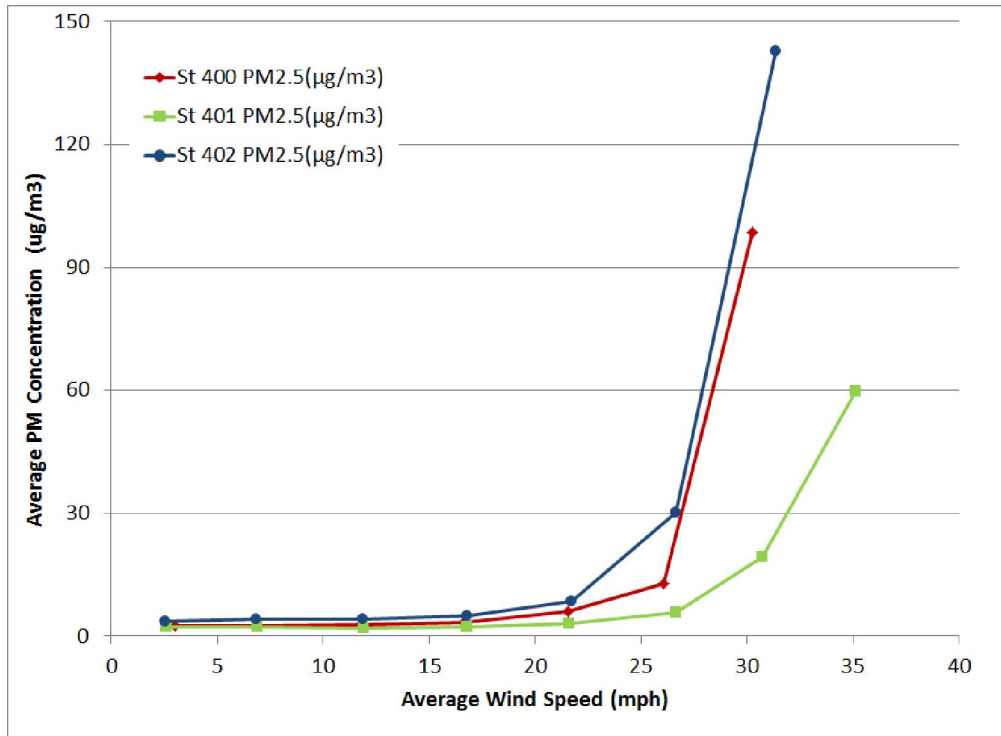


Figure 33. PM_{2.5} as a function of wind speed for stations 400, 401, and 402 for CY2014.

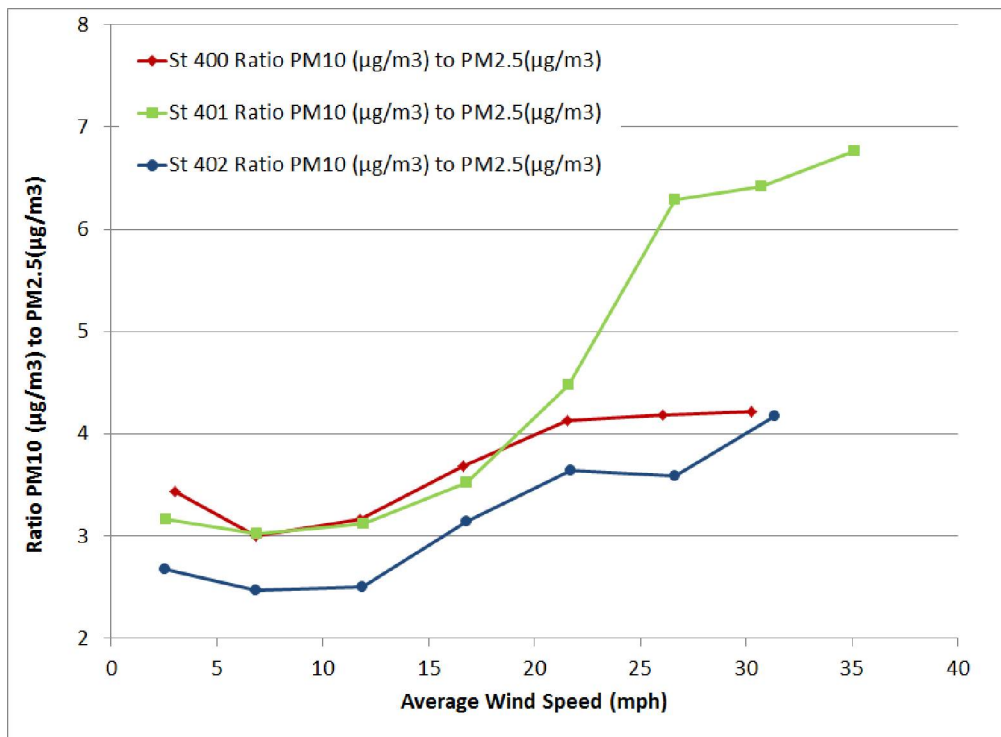


Figure 34. Ratio of PM₁₀ to PM_{2.5} trends as a function of wind speed for stations 400, 401, and 402 for CY2014.

APRIL 25, 2014, WIND EVENT

Most dust transport occurs during high wind events that are short in duration. The strongest wind events usually occur between March and May (see Tables B1-B3 in Appendix B). Figures 35, 36, and 37 examine a strong wind episode accompanied by an increase in PM₁₀ that occurred on April 25, 2014, between 00:00 to 23:50 hrs. All three monitoring stations experienced very similar wind conditions and saw a similar increase in PM₁₀ mass concentrations. On April 25, 2014, winds exhibited peaks at around 12:00 and 16:00 hrs. Although maximum winds approached 65 km/hr (40 mph) on both occasions, the sustained winds around 16:00 were higher at around 43-45 km/hr (27-28 mph). These conditions resulted in PM₁₀ mass concentrations exceeding 500 µg/m³. Strong winds were out of the south before switching to the northwest, at which point they decreased in magnitude. The PM₁₀ concentrations were elevated at all stations above 100 µg/m³ for approximately 70-90 minutes.

The ratio of PM₁₀ to PM_{2.5} increased during the wind event (Figures 35, 36, and 37), indicating that the PM₁₀ has an increasingly larger concentration of particles greater than 2.5 µm in diameter. This coarser PM₁₀ is indicative of a local source because coarser particles settle out from aerosol that is transported over long distance (see previous section for PM₁₀/PM_{2.5} discussion). The increase observed in the PM₁₀/PM_{2.5} ratio during the April 25, 2014, event suggests that the PM₁₀ is increasingly comprised of larger-sized particles that are suspended close to the monitoring stations as the wind speed increases. The PM₁₀/PM_{2.5} ratio remains high even after the PM₁₀ decreases significantly after 18:00 hours, indicating that coarse-sized particles continue to be transported and suspended locally but to a lesser degree because PM₁₀ concentrations decrease from a maximum of approximately 500 µg/m³ to approximately 20 µg/m³ approximately an hour after the maximum is reached.

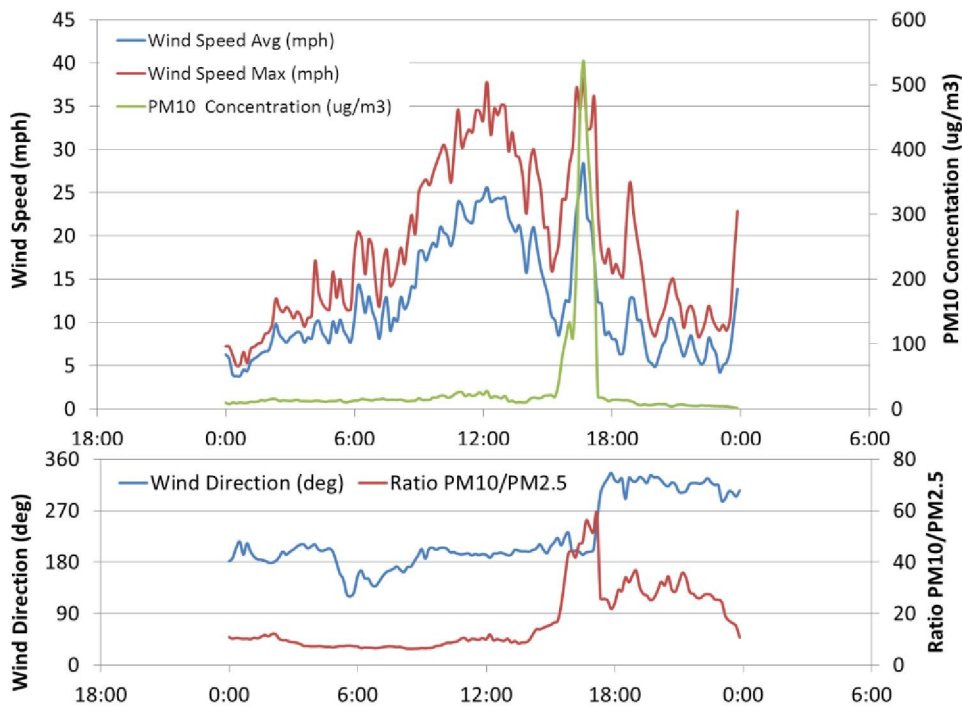


Figure 35. Wind and dust episode April 25, 2014, Station 400.

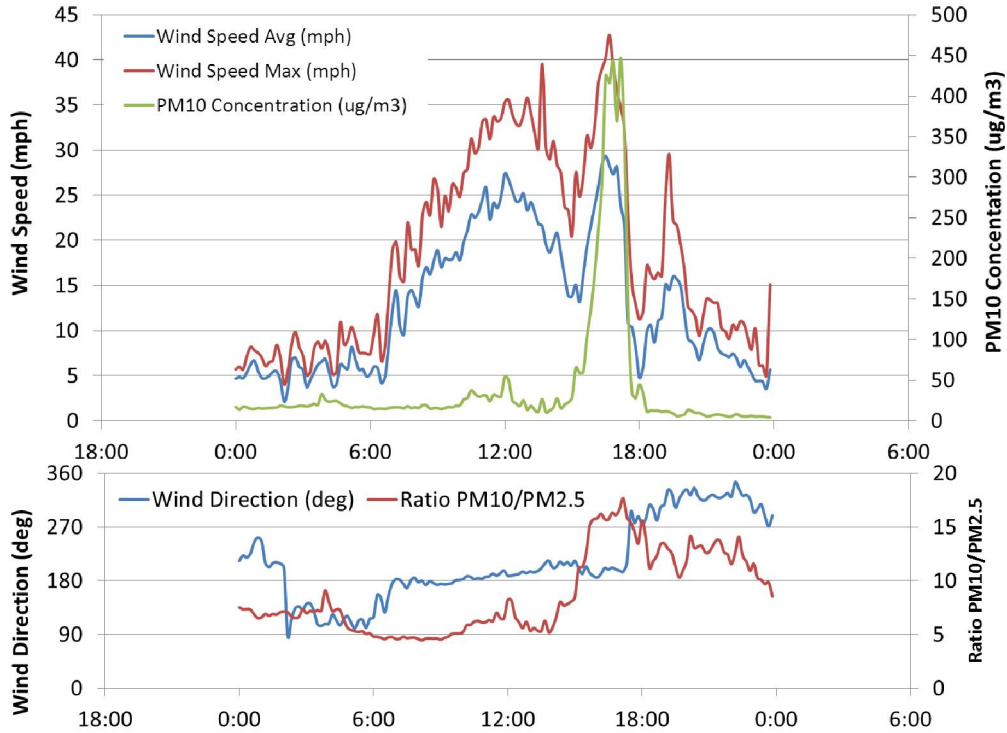


Figure 36. Wind and dust episode April 25, 2014, Station 401.

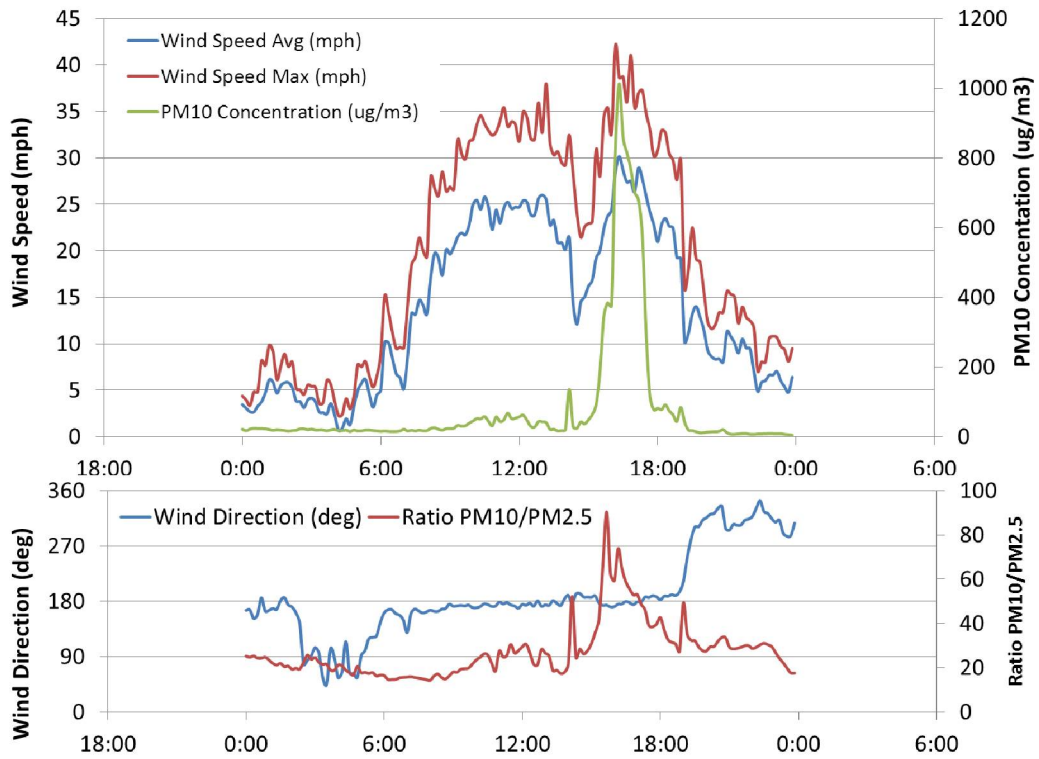


Figure 37. Wind and dust episode April 25, 2014, Station 402.

DISCUSSION

To determine if radiological contaminants are being transported by wind from the Clean Slate sites, dust collected at the monitoring stations is analyzed for gross alpha, gross beta, and gamma spectroscopy, and gamma exposure rate is measured by the PIC instruments. Judgment is required to determine if gross alpha and gross beta analyses and gamma rate measurements indicate contaminant transport by deviating from expected values. In contrast, gamma spectroscopy of dust samples objectively determines the presence or absence of radionuclides of concern. All of the gamma spectroscopy analyses in 2014 indicated the presence of only naturally occurring radionuclides.

Neither background nor baseline values for gross alpha, gross beta and gamma rate have been established for the TTR. Background can vary spatially as a result of many different environmental factors, and in the case of the Clean Slate sites, the current baseline may be expected to differ from background as a result of the Clean Slate tests. Radiological results for CEMP stations in 2014 are used as a basis of comparison for gross alpha, gross beta, and gamma rate for noncontaminated areas in the region. Generally higher gross alpha and gamma-rate values are observed for the TTR stations in comparison to most of the CEMP stations. Nonetheless, the similar gross alpha measurements at the CEMP station at Sarcobatus Flats and the distribution of measurements among the TTR sites themselves (Station 400, most distant from the Clean Slate tests, recorded the maximum gross alpha value in 2014) suggest that gross alpha at the stations reflects background conditions rather than an elevated baseline because of the Clean Slate tests. Similarly, comparison of gamma-rate exposure to the Warm Springs Summit CEMP station and correlation of gamma-rate increases between stations and with precipitation events suggests that natural environmental factors can account for the 2014 measurements. These observations and interpretations lead to the conclusion that none of the radiological analyses indicate that radionuclide migration was captured by the TTR monitoring stations in 2014.

It is important to recognize the spatial limitations of the monitoring network. Although Stations 401 and 402 are located in one of the predominant wind directions, the Clean Slate sites are large and radiologic source and transport conditions certainly vary across it. Migration may also be a discontinuous process, only occurring under specific, infrequent conditions that may not have occurred since the monitoring network has been in operation. These limitations on the spatial and temporal coverage of current monitoring heighten the importance of another objective of the monitoring sites, which is to identify if there are conditions that could allow contaminant transport to occur.

Particle movement by saltation and suspension continues to be recorded at the TTR stations. Specifically, saltation sensors at Clean Slate I and III record the movement of larger particles (usually larger than 50 μm) across the ground surface, particularly when wind speed tops 30 mph. Saltation is found to be strongly correlated with PM_{10} , which indicates that saltation is important for initiating suspension of finer material. The PM_{10} concentrations are generally low until winds exceed 20 mph. The weather data from the stations reveal that less than three percent of the time are winds in excess of 20 mph, but with an exponential-type relationship identified between both saltation and suspension with wind speed, these wind storms are when particles move. An example of this was an April 25, 2014, strong wind event out of the south, which recorded significant dust concentrations at all three monitoring stations.

The combined results of the meteorological and particle monitoring suggest that conditions for wind-borne contaminant migration exist at the Clean Slate sites, but occur infrequently and for brief periods. Radiological monitoring did not detect contaminants at the stations. It remains undetermined whether contaminants at the sites are stabilized such that they are not subject to movement during wind events or whether such movement is occurring but has not reached, has bypassed, or not been captured by the monitoring stations.

CONCLUSIONS

Migration of radionuclide-contaminated soil from the Clean Slate I and III sites was not detected by radiological monitoring at the TTR stations during 2014. There is no evidence of wind-driven transport of radionuclides from the sites to the monitoring stations. The highest mean gross alpha and mean gross beta activities were observed at Station 402, adjacent to Clean Slate I. Values reported for Station 400 (at the SNL ROC) are only slightly lower than the Station 402 values and the maximum individual gross alpha measurement was from Station 400. Gamma spectroscopy analyses for all three sites identified only naturally occurring radionuclides.

The mean gross alpha values for the TTR stations are higher than those observed at CEMP stations in the region, with the exception of Sarcobatus Flats. The mean gross beta measurements at the TTR are lower than the CEMP stations, with the exception of Tonopah. These comparisons suggest that radiation at the TTR monitoring stations is because of natural (terrestrial and cosmic) sources and that the levels of radiation observed are approximately equivalent to levels observed at the surrounding CEMP stations.

Gamma exposure rates as measured by PICs are similar to those measured at the CEMP station at Warm Springs Summit (though higher than rates at other CEMP stations), and within the range observed nationally for background levels of environmental (terrestrial and cosmic) gamma exposure rates in the United States (5.6 to 28.2 $\mu\text{R/hr}$; National Academy of Sciences, 1980). Most intervals of increased gamma values are coincident among the three TTR stations and also coincident with the Warm Springs Summit measurements. Many of these intervals also coincide with precipitation events.

During the first part of CY2014, samples were collected simultaneously with glass-fiber and cellulose-fiber filters at Station 400 to permit a direct comparison of the two sampling media. Results suggest that glass-fiber filters return higher gross alpha and gross beta values as a result of the smaller pore size of the glass-fiber filter. Linear regression indicates that glass-fiber equivalent concentrations cannot reliably be estimated from past samples collected using cellulose filters.

Higher PM_{10} to $\text{PM}_{2.5}$ ratios at the stations during high winds indicate that local transport of dust, proximal to all the monitoring stations, occurs for wind speeds above 32 km/hr (20 mph). A strong correlation between high saltation values and high PM_{10} values indicates that saltation (driven by strong winds) contributes to fine dust emissions. Wind speeds in excess of 32 km/hr (20 mph) occurred less than three percent of the time (roughly 200 hours) at the stations during 2014 and occurred predominantly from the south or northwest. Annual precipitation measured at the stations in 2014 is above the long-term annual average measured at the Tonopah Airport and approximately twice that measured at the stations in 2013. The annual amount varied from 5.18 to 5.76 inches.

RECOMMENDATIONS

1. A size analysis of a representative sample of the soil material on the surface at each of the monitoring stations should be performed. This would facilitate characterization of the amount of PM₁₀ and saltation material available at each site. This information would in turn aid in the interpretation of the saltation and dust transport observations.
2. Establishing background/baseline conditions for the airborne particulate samples and the PIC gamma measurements is important for interpreting the TTR station data. Monitoring data from the Sarcobatus Flats and Warm Spring Summit CEMP stations are important for bracketing the results from the TTR monitoring stations. These locations should be evaluated to identify comparable and contrasting characteristics. An alternative to relying on the CEMP stations for background comparison is to establish an additional monitoring/sample collection station at the TTR in a location that is not downwind of the Clean Slate contamination sites. Such a site would provide control samples presumably from a clean area against which measurements at the contamination areas could be compared.
3. The analysis of PM₁₀ to PM_{2.5} ratios should be continued and combined with data forthcoming from the BSNE traps to determine the proximity of sources for the dust detected at the TTR monitoring stations.
4. Increased areal coverage of the monitoring network, particularly in the other dominant wind direction, would increase confidence in extrapolating the monitoring results across the sites.

REFERENCES

- Dick, J.L., J.D. Shreve, and J.S. Iveson, 1963. Operation Roller Coaster, Interim Summary Report (II). POIR-2500 (Volume 1) Defense Atomic Support Agency predecessor to Defense Threat Reduction Agency, Washington, D.C.
- DOE see U.S. Department of Energy
- Duncan, D., W. Forston, and R. Sanchez, 2000. 1999 Annual Site Environmental Report Tonopah Test Range, Nevada. SAND2000-2229, Sandia National Laboratories, Albuquerque, NM.
- EG&G, 1979. An Aerial Radiological Survey of Clean Slates 1, 2, and 3, and Double Track, Test Range. EGG-1183-1737, Energy Measurement Group, EG&G, Las Vegas, NV.
- Engelbrecht, J.P., I.G. Kavouras, D. Campbell, S.A. Campbell, S. Kohl, D. Shafer, 2008. Yucca Mountain Environmental Monitoring System Initiative, Air Quality Scoping Study for Tonopah Airport, Nye County, Nevada, Letter Report DOE/NV/26383-LTR2008-04.
- Helsel, DR and RM Hirsch. 1995. Statistical Methods in Water Resources. Studies in Environmental Science 49, Elsevier, New York, 529pp.
- Johnson, W.G. and S.R. Edwards, 1996. A historical evaluation of Operation Roller Coaster, Stonewall and Cactus Flats, Nellis Air Force Range and Tonopah Test Range, Nye County, Nevada. NTS Project #9649MA, Historic Evaluation Short Report #SR090996-1, prepared by Desert Research Institute for U.S. Department of Energy, Nevada Operations Office, Las Vegas, Nevada.
- Mizell, S.A., and C. Shadel, in review. Radiological results for samples collected on paired glass- and cellulose-fiber filters at the Sandia complex, Tonopah Test Range, Nevada. Desert Research Institute, Las Vegas, Nevada.
- Mizell, S.A., G. Nikolich, C. Shadel, G. McCurdy, V. Etyemezian, and J. Miller, 2014. Tonopah Test Range Air Monitoring: CY2013 Meteorological, Radiological, and Airborne Particulate Observations. Desert Research Institute Publication No. 45258, DOE/NV/0000939-20.
- National Academy of Sciences, 1980. The Effects on Populations of Exposure to Low Levels of Ionizing Radiation, BEIR III. Washington, D.C.
- NRC see U.S. Nuclear Regulatory Commission.
- NSTec, 2013. Nevada National Security Site Environmental Report 2012. DOE/NV/25946-1856, prepared by National Security Technologies, LLC for the US Department of Energy, National Nuclear Security Administration, Nevada Site Office.
- Proctor, A.E. and T.J. Hendricks, 1995. An aerial radiological survey of the Tonopah Test Range including Clean Slate 1, 2, 3, Roller Coaster, Decontamination area Cactus Springs Ranch Target areas Central Nevada. EGG 11265-1145, The Remote Sensing Laboratory, EG&G Energy Measurements prepared for the US Department of Energy.

- Sandia National Laboratory (SNL), 2012. Calendar Year 2011 Annual Site Environmental Report for Tonopah Test Range, Nevada and Kauai Test Facility, Hawaii. SAND2012-7341P, Sandia National laboratories, Albuquerque, NM.
- UNSCEAR, 2000. Sources and effects of ionizing radiation, Annex B: Exposures from natural radiation sources. United Nations Scientific Committee on the Effects of atomic Radiation. Available May 6, 2013 at:
http://www.unscear.org/unscear/publications/2000_1.html.
- U.S. Department of Energy, 1996. Clean Slate Corrective Action Investigation Plan. Nevada Operations Office, DOE/NV--456.
- U.S. Nuclear Regulatory Commission, 1979. Regulatory Guide 8.12 Health physics surveys for byproduct material at NRC-licensed processing and manufacturing plants, subsection 1.12 Calibration of radiation safety instruments. U.S. Nuclear Regulatory Commission, Office of Standards Development, Washington, D.C.

APPENDIX A: QUALITY ASSURANCE PROGRAM

Although the current data collected for the TTR air monitoring study are considered for informational purposes to support conceptual models or guide investigations, the U.S. Department of Energy National Nuclear Administration Nevada Site Office (DOE/NNSA/NSO) Soils Activity Quality Assurance Plan (QAP) (2012) was used as a guideline for the collection and analysis of radiological data presented in the Radiological Assessment of Airborne Particulates section of this report (page 24). This QAP as well as the Desert Research Institute Quality Assurance Program Manual for the DOE Program (2010) ensures compliance with U.S. Department of Energy Order DOE O 414.1D, "Quality Assurance," which implements a quality management system to ensure the generation and use of quality data. The following items are addressed by the aforementioned QA documents:

- Data Quality Objectives (DQOs)
- Sampling plan development appropriate to satisfy the DQOs
- Environmental health and safety
- Sampling plan execution
- Sample analyses
- Data review
- Continuous improvement

Data Quality Objectives (DQOs)

The DQO process is a strategic planning approach that is used to plan data collection activities. It provides a systematic process for defining the criteria that a data collection design should satisfy. These criteria include when and where samples should be collected, how many samples to collect, and the tolerable level of decision errors for the study. The DQOs are unique to the specific data collection or monitoring activity as well as their defined level of use (informational purpose in this case).

Measurement Quality Objectives (MQOs)

The MQOs are basically equivalent to DQOs for analytical processes. The MQOs provide direction to the laboratory concerning performance objectives or requirements for specific method performance characteristics. Default MQOs are established in the subcontract with the laboratory but may be altered to satisfy changes in the DQOs. The MQOs for the TTR air monitoring study are described in terms of precision, accuracy, representativeness, completeness, and comparability requirements. These terms are defined and discussed in the DOE/NNSA/NSO (QAP).

Sampling Quality Assurance Program

Quality Assurance (QA) in field operations for the TTR air monitoring study includes sampling assessments, surveillances, and oversight of the following supporting elements:

- The sampling plan, DQOs, and field data sheets accompanying the sample package
- Database support for field and laboratory results, including systems for long-term storage and retrieval
- Qualified personnel are available and able to perform required tasks

Sample packages include the following items:

- Sample collectors field notes confirming all observable information pertinent to sample collection.
- An Air Surveillance Network Sample Data Form documenting air sampler parameters, collection dates and times, and total sample volumes collected.
- Chain-of-custody forms that also include some of the elements of the field notes.

This managed approach to sampling ensures that the sampling is traceable and enhances the value of the final data available to the project manager. The sample package also ensures that the field personnel responsible for sample collection have followed proper procedures for sample collection.

Data obtained in the course of executing field operations are entered in the documentation accompanying the sample package during sample collection and in the TTR Study database along with analytical results upon their receipt and evaluation.

Completed sample packages are kept as hard copy in file archives. Analytical reports are kept as hard copy in file archives as well as in dedicated and secure archival systems that are protected and maintained in accordance with the Desert Research Institute's Computer Protection Program.

Laboratory QA Oversight

Although the data for the TTR air monitoring study is for informational purposes the main aspects of the DOE O 414.1D requirements are used as guidelines to evaluate laboratory services through review of the vendor laboratory policies formalized in a Laboratory Quality Assurance Plan (LQAP). The TTR study is assured of obtaining quality data from laboratory services through a multifaceted approach, involving specific procurement protocols, the conduct of quality assessments, and requirements for selected laboratories to have an acceptable QA Program. These elements are discussed below.

Procurement

Laboratory services are procured through subcontracts that establish the technical specifications required of the laboratory to provide the basis for determining compliance with those requirements and for evaluation of overall performance. A subcontract is usually awarded on a "best value" basis as determined by pre-award audits, but because of the specific requirement requested for gamma spectroscopy analysis (24 hour count duration) for the TTR study, the laboratory was procured on a "sole proprietor" basis. The laboratory was required to provide a review package that included the following items:

- All procedures pertinent to subcontract scope
- Environment, Safety, and Health Plan
- LQAP
- Example deliverables (hard copy and/or electronic)
- Proficiency testing (PT) results from the previous year from recognized PT programs
- Résumés
- Accreditations and certifications
- Licenses

Continuing Assessment

A continuing assessment of a selected laboratory involves ongoing monitoring of a laboratory's performance against the contract terms and conditions, of which technical specifications are a part. The following tasks support continuing assessment:

- Tracking schedule compliance
- Reviewing analytical data deliverables
- Monitoring the laboratory's adherence to the LQAP
- Monitoring for continued successful participation in approved PT programs

Data Review

Essential components of process-based QA are data checks, verification, validation, and data quality assessment to evaluate data quality and usability.

Data Checks – Data checks are conducted to ensure accuracy and consistency of field data collection operations prior to and upon data entry into the TTR databases and data management systems.

Data Verification – Data verification is defined as a compliance and completeness review to ensure that all laboratory data and sample documentation are present and complete. Sample preservation, chain-of-custody, and other field sampling documentation shall be reviewed during the verification process. Data verification ensures that the reported results entered in the TTR databases correctly represent the sampling and/or analyses performed and includes evaluation of quality control (QC) sample results.

Data Validation – Data validation is the process of reviewing a body of analytical data to determine if it meets the data quality criteria defined in operating instructions. Data validation ensures that the reported results correctly represent the sampling and/or analyses performed, determines the validity of the reported results, and assigns data qualifiers (or “flags”) if required. The process of data validation consists of the following:

- Evaluating the quality of the data to ensure that all project requirements are met
- Determining the impact on data quality of those requirements if they are not met

- Verifying compliance with QA requirements
- Checking QC values against defined limits
- Applying qualifiers to analytical results in the TTR databases for the purposes of defining the limitations in the use of the reviewed data

Operating instructions, procedures, applicable project-specific work plans, field sampling plans, QA plans, analytical method references, and laboratory statements of work may all be used in the process of data validation. Documentation of data validation includes checklists, qualifier assignments, and summary forms.

Data Quality Assessment (DQA) – DQA is the scientific evaluation of data to determine if the data obtained from environmental data operations are of the right type, quality, and quantity to support their intended use. DQA review is a systematic review against preestablished criteria to verify that the data are valid for their intended use.

2014 Sample QA Results

Assessments of QA were performed by the TTR air monitoring study, including the laboratory responsible for sample analyses. These assessments ensure that sample collection procedures, analytical techniques, and data provided by the subcontracted laboratory complies with TTR study requirements. Data were provided by the University of Nevada, Las Vegas, Radiation Services Laboratory for gross alpha/beta and gamma spectroscopy analysis. A brief discussion of the 2014 results for laboratory duplicates, control samples, blank analyses, and interlaboratory comparison studies is provided along with summary tables within this section.

Laboratory Duplicates (Precision)

A laboratory duplicate is a sample that is handled and analyzed following the same procedures as the primary analysis. The relative percent difference (RPD) between the initial result and the corresponding duplicate result is a measure of the variability in the analytical process of the laboratory, mainly overall measurement uncertainty. The average absolute RPD, expressed as a percentage, was determined for the calendar year 2014 samples and is listed in Table A-1. An RPD of zero indicates a perfect duplication of results of the duplicate pair, whereas an RPD greater than 100 percent generally indicates that a duplicate pair falls beyond QA requirements and is not considered valid for use in data interpretation. These samples are further evaluated to determine the reason for QA failure and if any corrective actions are required. Overall, the RPD values for all analyses indicate very good results with no samples exceeding an RPD of 100 percent.

Table A-1. Summary of laboratory duplicate samples for the TTR air monitoring study in 2014.

Analysis	Matrix	Number of Samples Reported ^(a)	Number of Samples Reported above MDC ^(b)	Average Absolute RPD of those above MDC (%) ^(c)
Gross Alpha	Air	13	11	21.7
Gross Beta	Air	11	11	7.4
Gamma – Beryllium-7	Air	7	7	5.7
Gamma – Lead-210	Air	4	4	23.2

(a) Represents the number of laboratory duplicates reported for the purpose of monitoring precision.

(b) Represents the number of laboratory duplicate result sets reported above the minimum detectable concentration (MDC). If either the original laboratory analysis or its duplicate was reported below the detection limit, the precision was not determined.

(c) Reflects the average absolute RPD calculated for those field duplicates reported above the MDC.

The absolute RPD calculation is as follows:

$$\text{Absolute RPD} = \frac{|FD - FS|}{(FD + FS) / 2} \times 100\% \quad (1)$$

Where: FD = Field duplicate result

FS = Field sample result

Laboratory Control Samples (Accuracy)

Laboratory control samples (LCSs) (also known as matrix spikes) are performed by the subcontract laboratory to evaluate analytical accuracy, which is the degree of agreement of a measured value with the true or expected value. Samples of known concentration are analyzed using the same methods as employed for the project samples. The results are determined as the measured value divided by the true value, expressed as a percentage. To be considered valid, the results must fall within established control limits (or percentage ranges) for further analyses to be performed. The LCS results obtained for 2014 are summarized in Table A-2. The LCS results were satisfactory, with all samples falling within control parameters for the air sample matrix.

Table A-2. Summary of laboratory control samples for the TTR air monitoring study in 2014.

Analysis	Matrix	Number of LCS Results Reported	Number Within Control Limits^(a)
Gross Alpha	Air	8	8
Gross Beta	Air	8	8
Gamma	Air	8	8

(a) Control limits are as follows: 78% to 115% for gross alpha, 87% to 115% for gross beta, 90% to 115% for gamma (¹³⁷Cs, ⁶⁰Co, ²⁴¹Am).

Laboratory Blank Analysis

Laboratory blank sample analyses are essentially the opposite of LCSs discussed above. These samples do not contain any of the analyte of interest. Results of these analyses are expected to be “zero,” or more accurately, below the MDC of a specific procedure. Blank analysis and control samples are used to evaluate overall laboratory procedures, including sample preparation and instrument performance. The laboratory blank sample results obtained for 2014 are summarized in Table A-3. The laboratory blank results were satisfactory with all of the alpha and beta blank samples falling within control parameters for the air sample matrix.

Table A-3. Summary of laboratory blank samples for the TTR air monitoring study in 2014.

Analysis	Matrix	Number of Blank Results Reported	Number within Control Limits^(a)
Gross Alpha	Air	8	8
Gross Beta	Air	8	8
Gamma	Air	8	8

(a) Control limit is less than the MDC.

Interlaboratory Comparison Studies

Interlaboratory comparison studies are conducted by the subcontracted laboratories to evaluate their performance relative to other laboratories providing the same service. These types of samples are commonly known as “blind” samples, in which the expected values are known only to the program conducting the study. The analyses are evaluated and if found satisfactory, the laboratory is certified that its procedures produce reliable results. The interlaboratory comparison sample results obtained for 2014 are summarized in Table A-4.

Table A-4 shows the summary of interlaboratory comparison sample results for the subcontract radiochemistry laboratory. The laboratory participated in the QA Program administered by Mixed Analyte Performance Evaluation Program (MAPEP) for gross alpha, gross beta, and gamma analyses. The subcontractors performed very well during the year by passing all of the parameters analyzed.

Table A-4. Summary of inter-laboratory comparison samples of the radiochemistry laboratory for the TTR air monitoring study in 2014.

Analysis	Matrix	MAPEP Results	
		Number of Results Reported	Number Within Control Limits ^(a)
Gross Alpha	Air	2	2
Gross Beta	Air	2	2
Gamma	Air	2	2

(a) Control limits are determined by the individual inter-laboratory comparison study.

REFERENCES

Desert Research Institute, 2010. *Desert Research Institute Quality Assurance Program Manual for the DOE Program*, October 2010.

U.S. Department of Energy, 2011. *Quality Assurance*. DOE O 414.1D.

U.S. Department of Energy, 2012. *Soils Activity Quality Assurance Plan*. National Nuclear Security Administration, Nevada Site Office report DOE/NV--1478.

APPENDIX B: SUMMARIES OF METEOROLOGICAL DATA

Table B-1. Station 400 Summary of Monthly and Annual Meteorological Data.

Month	Jan	Feb	Mar	Apr	May	Jun	Jul	Aug	Sep	Oct	Nov	Dec	ANNUAL	VALUE
Wind Speed Avg (mph)	6.00	6.61	7.40	8.29	7.80	7.22	7.47	7.31	7.49	6.88	5.93	7.06	AVG	7.12
Wind Speed Max (mph)	27.23	26.59	30.19	29.99	32.15	23.73	28.83	23.68	29.69	25.70	29.59	29.94	MAX	32.15
Wind Speed Gust (mph)	38.73	41.65	47.64	49.61	44.86	38.36	40.77	33.17	43.84	38.21	47.93	42.60	MAX	49.61
*Wind Freq from S	10.9%	47.8%	37.7%	33.6%	32.0%	32.2%	66.5%	61.0%	61.0%	50.5%	36.0%	34.0%	AVG	41.9%
**Wind Freq from NW	79.2%	35.7%	44.8%	50.2%	52.2%	51.7%	11.2%	17.6%	17.0%	30.8%	51.8%	43.2%	AVG	40.5%
Air Temperature Avg (deg F)	37.78	39.37	45.00	52.47	61.17	72.57	77.03	71.05	67.38	57.74	42.72	35.01	AVG	54.94
Air Temperature Min (deg F)	15.15	8.08	21.68	23.93	32.34	43.63	57.92	52.57	39.70	32.70	15.87	11.14	MIN	8.08
Air Temperature Max (deg F)	63.27	68.40	69.60	75.83	88.43	95.92	98.83	91.38	90.50	81.90	73.78	57.97	MAX	98.83
Relative Humidity Avg (%)	39.32	45.55	37.25	27.79	23.77	14.54	32.10	33.83	38.69	27.62	41.20	72.00	AVG	36.14
Relative Humidity Min (%)	8.41	10.80	7.72	5.50	5.84	5.43	6.24	7.04	7.81	7.04	11.50	12.31	MIN	5.43
Relative Humidity Max (%)	99.80	100.00	100.00	100.00	91.10	49.91	95.20	96.80	96.80	70.10	93.10	100.00	MAX	100.00
Total Precipitation (inch)	0.06	0.46	0.11	0.74	0.07	0.00	1.26	0.67	1.21	0.00	0.19	0.41	TOTAL	5.18
Max Daily Precipitation (inch)	0.06	0.25	0.11	0.63	0.07	0.00	0.26	0.40	0.75	0.00	0.19	0.28	MAX	0.75
Soil Temperature Avg (deg F)	41.32	44.04	52.46	60.74	69.28	81.20	83.81	79.45	75.95	65.89	49.13	39.64	AVG	61.91
Soil Temperature Min (deg F)	31.71	29.15	36.69	40.82	48.43	64.53	67.62	63.43	53.01	50.85	35.68	27.46	MIN	27.46
Soil Temperature Max (deg F)	52.20	62.10	71.42	78.21	88.66	99.73	101.10	96.98	95.94	84.74	67.06	53.49	MAX	101.10
Soil Vol. Water Content Avg	0.12	0.12	0.16	0.14	0.14	0.12	0.17	0.20	0.19	0.15	0.14	0.14	AVG	0.15
Soil Vol. Water Content Min	0.11	0.10	0.13	0.12	0.12	0.11	0.11	0.15	0.14	0.13	0.12	0.10	MIN	0.10
Soil Vol. Water Content Max	0.13	0.22	0.22	0.17	0.18	0.14	0.30	0.33	0.33	0.20	0.18	0.21	MAX	0.33
Solar Radiation Avg (ly)	5.91	7.55	10.93	13.68	15.09	16.89	14.21	13.50	11.93	9.48	6.41	4.33	AVG	10.83
Solar Radiation Max (ly)	38.27	41.80	55.91	53.41	58.23	56.60	62.27	52.38	53.33	42.15	38.10	31.39	MAX	62.27
Barometric P. Avg (in Hg)	24.69	24.52	24.56	24.52	24.53	24.50	24.64	24.61	24.55	24.61	24.63	24.57	AVG	24.58
Barometric P. Min (in Hg)	24.28	24.04	24.14	24.09	24.21	24.27	24.49	24.42	24.34	24.22	24.16	24.14	MIN	24.04
Barometric P. Max (in Hg)	25.03	24.72	24.90	24.89	24.87	24.66	24.78	24.81	24.70	24.85	24.93	24.83	MAX	25.03

*Wind Freq. from S (indicates aggregate frequency for winds over 5 mph coming from south direction).

**Wind Freq. from NW (indicates aggregate frequency for winds over 5 mph coming from northwest direction).

Table B-2. Station 401 Summary of Monthly and Annual Meteorological Data.

Month	Jan	Feb	Mar	Apr	May	Jun	Jul	Aug	Sep	Oct	Nov	Dec	ANNUAL	VALUE
Wind Speed Avg (mph)	5.62	6.00	7.43	8.54	8.15	7.28	7.35	6.85	6.63	5.79	5.11	6.69	AVG	6.79
Wind Speed Max (mph)	29.62	30.65	32.56	31.08	35.41	25.45	27.72	25.86	29.10	24.58	25.10	33.73	MAX	35.41
Wind Speed Gust (mph)	37.70	43.33	44.57	47.79	47.93	37.41	39.24	39.68	42.31	35.80	37.26	45.23	MAX	47.93
Wind Freq from S*	4.3%	33.8%	27.9%	27.7%	24.8%	32.2%	58.9%	55.0%	54.8%	46.3%	26.8%	33.0%	AVG	35.5%
Wind Freq from NW**	80.6%	43.8%	46.1%	51.3%	50.0%	46.1%	13.4%	17.3%	18.1%	34.8%	56.4%	47.7%	AVG	42.1%
Air Temperature Avg (deg F)	32.91	35.76	42.82	50.59	59.65	70.74	76.37	69.99	65.86	54.56	38.99	34.60	AVG	52.74
Air Temperature Min (deg F)	5.86	0.59	12.65	18.65	29.66	37.20	50.43	47.41	36.61	24.05	6.62	10.44	MIN	0.59
Air Temperature Max (deg F)	61.86	67.95	69.26	75.79	89.20	96.44	100.20	91.31	91.29	82.06	71.56	60.73	MAX	100.20
Relative Humidity Avg (%)	42.48	47.14	40.64	31.02	27.77	17.28	35.76	39.37	46.07	34.33	46.52	74.61	AVG	40.25
Relative Humidity Min (%)	9.44	12.54	8.65	5.88	6.45	5.48	6.75	8.57	9.00	8.15	15.12	17.00	MIN	5.48
Relative Humidity Max (%)	94.60	94.60	95.70	95.60	89.30	51.14	96.50	97.60	96.40	79.05	94.00	96.80	MAX	97.60
Total Precipitation (inch)	0.02	0.51	0.07	0.39	0.21	0.00	1.18	1.18	1.58	0.00	0.18	0.44	TOTAL	5.76
Max Daily Precipitation (inch)	0.01	0.33	0.06	0.28	0.20	0.00	0.42	0.70	0.99	0.00	0.18	0.22	MAX	0.99
Soil Temperature Avg (deg F)	36.07	40.52	49.52	58.06	67.21	79.04	82.98	76.58	72.92	61.82	46.14	38.41	AVG	59.11
Soil Temperature Min (deg F)	28.41	26.34	36.67	41.63	47.75	66.11	68.45	63.28	55.06	49.48	34.58	27.42	MIN	26.34
Soil Temperature Max (deg F)	46.12	53.67	62.13	71.44	82.27	92.59	96.26	90.27	87.26	74.62	58.62	48.56	MAX	96.26
Soil Vol. Water Content Avg	0.12	0.12	0.19	0.18	0.20	0.13	0.13	0.24	0.23	0.17	0.14	0.15	AVG	0.17
Soil Vol. Water Content Min	0.11	0.11	0.16	0.14	0.16	0.11	0.11	0.17	0.15	0.14	0.13	0.13	MIN	0.11
Soil Vol. Water Content Max	0.13	0.16	0.21	0.24	0.24	0.17	0.28	0.41	0.34	0.22	0.16	0.18	MAX	0.41

*Wind Freq. from S (indicates aggregate frequency for winds over 5 mph coming from south direction).

**Wind Freq. from NW (indicates aggregate frequency for winds over 5 mph coming from northwest direction).

Table B-3. Station 402 Summary of Monthly and Annual Meteorological Data (continued).

Month	Jan	Feb	Mar	Apr	May	Jun	Jul	Aug	Sep	Oct	Nov	Dec	ANNUAL	VALUE
Wind Speed Avg (mph)	5.03	5.62	7.00	8.05	7.87	6.91	6.89	6.36	6.10	5.40	4.79	6.12	AVG	6.34
Wind Speed Max (mph)	25.76	28.75	30.62	32.21	34.91	25.16	26.89	21.93	27.20	24.83	26.96	31.72	MAX	34.91
Wind Speed Gust (mph)	37.41	41.21	43.04	44.06	47.35	37.41	38.43	29.96	39.60	34.27	41.36	43.33	MAX	47.35
Wind Freq from S*	3.5%	32.2%	32.4%	32.9%	31.7%	40.0%	62.4%	49.4%	60.6%	45.6%	28.0%	25.2%	AVG	37.0%
Wind Freq from NW**	84.8%	46.1%	50.6%	54.5%	48.3%	43.3%	13.6%	27.5%	18.3%	37.5%	57.7%	53.2%	AVG	44.6%
Air Temperature Avg (deg F)	33.32	36.41	43.53	51.42	60.41	71.20	76.88	70.73	66.16	54.90	39.57	33.97	AVG	53.21
Air Temperature Min (deg F)	6.01	0.75	13.77	19.08	30.42	38.32	51.67	45.70	36.76	24.59	8.80	7.30	MIN	0.75
Air Temperature Max (deg F)	62.49	69.64	70.16	76.42	90.01	97.27	99.63	91.26	91.85	81.72	72.23	58.21	MAX	99.63
Relative Humidity Avg (%)	40.55	45.58	40.08	28.67	25.41	14.47	32.75	29.49	45.81	32.79	47.64	75.11	AVG	38.20
Relative Humidity Min (%)	7.04	9.36	5.00	2.81	3.21	2.58	3.84	8.90	5.82	5.47	11.09	12.84	MIN	2.58
Relative Humidity Max (%)	98.30	98.40	99.90	100.00	92.40	49.40	97.00	94.70	99.60	81.10	98.50	100.00	MAX	100.00
Total Precipitation (inch)	0.01	0.63	0.08	0.54	0.22	0.00	0.96	0.25	1.88	0.00	0.29	0.50	TOTAL	5.36
Max Daily Precipitation (inch)	0.01	0.36	0.08	0.39	0.21	0.00	0.40	0.25	1.38	0.00	0.29	0.29	MAX	1.38
Soil Temperature Avg (deg F)	34.89	38.82	46.61	57.54	67.33	79.93	82.93	76.87	69.18	57.76	42.53	36.46	AVG	57.57
Soil Temperature Min (deg F)	26.98	24.43	35.07	37.87	43.90	63.12	66.40	66.58	50.54	44.24	30.94	22.66	MIN	22.66
Soil Temperature Max (deg F)	46.96	51.58	58.77	76.08	88.83	101.00	100.40	92.59	87.30	67.98	55.29	48.79	MAX	101.00
Soil Vol. Water Content Avg	0.07	0.07	0.13	0.11	0.13	0.08	0.07	0.13	0.15	0.12	0.11	0.11	AVG	0.11
Soil Vol. Water Content Min	0.07	0.06	0.11	0.09	0.09	0.06	0.06	0.10	0.09	0.10	0.09	0.08	MIN	0.06
Soil Vol. Water Content Max	0.08	0.12	0.15	0.19	0.16	0.10	0.18	0.17	0.29	0.15	0.12	0.14	MAX	0.29
Solar Radiation Avg (ly)	11.06	14.77	20.76	25.90	27.94	31.24	25.50	25.11	22.38	18.23	12.38	8.24	AVG	20.29
Solar Radiation Max (ly)	70.36	72.77	105.10	101.30	107.80	113.30	107.90	92.03	93.67	81.11	81.02	55.31	MAX	113.30
Barometric P. Avg (in Hg)	24.72	24.61	24.38	24.63	24.64	24.61	24.76	24.71	24.68	24.73	24.75	24.70	AVG	24.66
Barometric P. Min (in Hg)	23.34	19.26	22.90	23.51	24.32	24.39	24.61	24.56	24.46	24.33	24.30	24.26	MIN	19.26
Barometric P. Max (in Hg)	26.46	26.54	26.08	25.01	24.99	24.78	24.90	24.87	24.82	24.97	25.06	24.95	MAX	26.54

*Wind Freq. from S (indicates aggregate frequency for winds over 5 mph coming from south direction).

**Wind Freq. from NW (indicates aggregate frequency for winds over 5 mph coming from northwest direction).

APPENDIX C: DAILY AVERAGE METEOROLOGICAL AND ENVIRONMENTAL DATA FOR TTR MONITORING STATIONS 400, 401, AND 402 DURING CY2014

Tonopah Test Range Station 400 2014

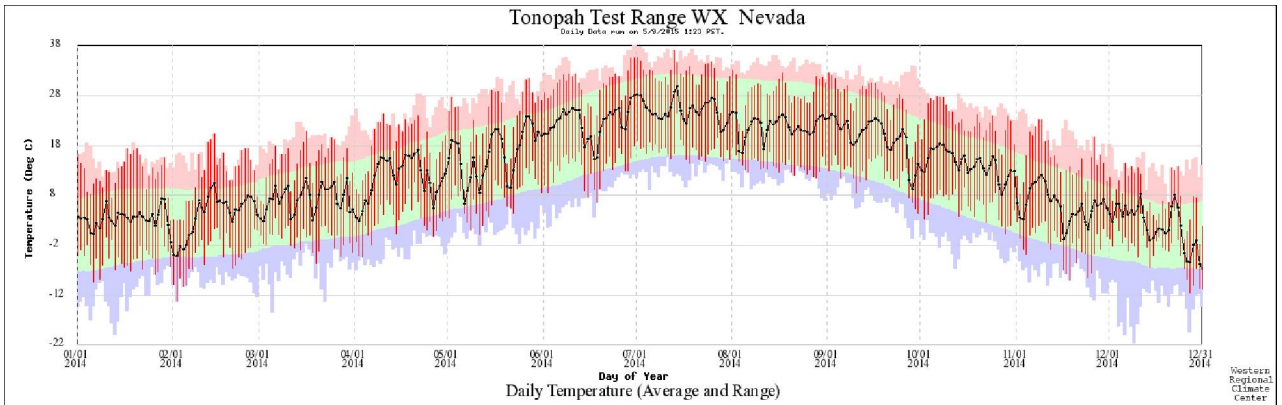


Figure C-1. Graphical summary of temperature data collected by the TTR 400 station from January 1, 2014, until December 31, 2014. Underlying pastel colors represent the period-of-record extremes (red and blue) and averages (green).

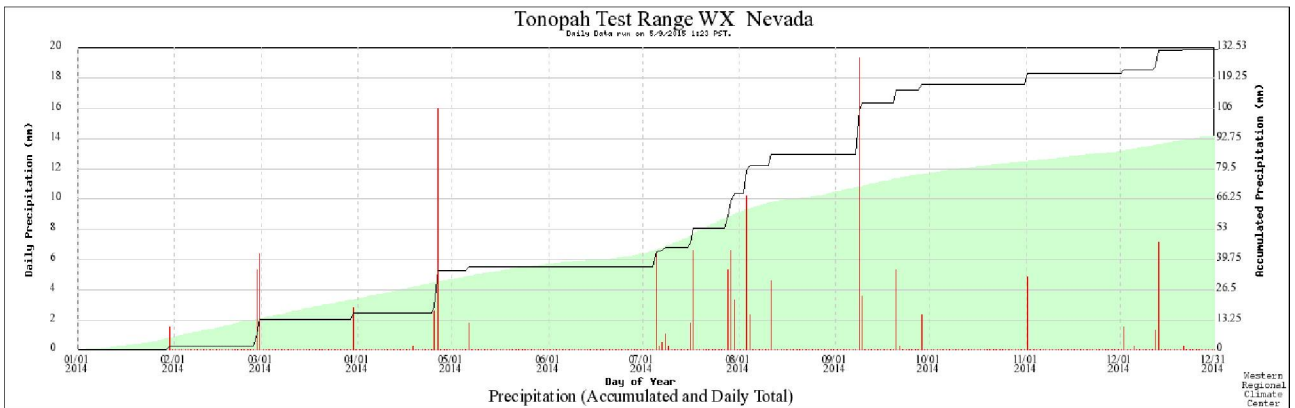


Figure C-2. Graphical summary of precipitation data, daily total (red bars) and accumulated (black line), collected by the TTR 400 station from January 1, 2014, until December 31, 2014. Underlying light green shaded area represents the station period-of-record average precipitation accumulation.

Tonopah Test Range Station 400 2014

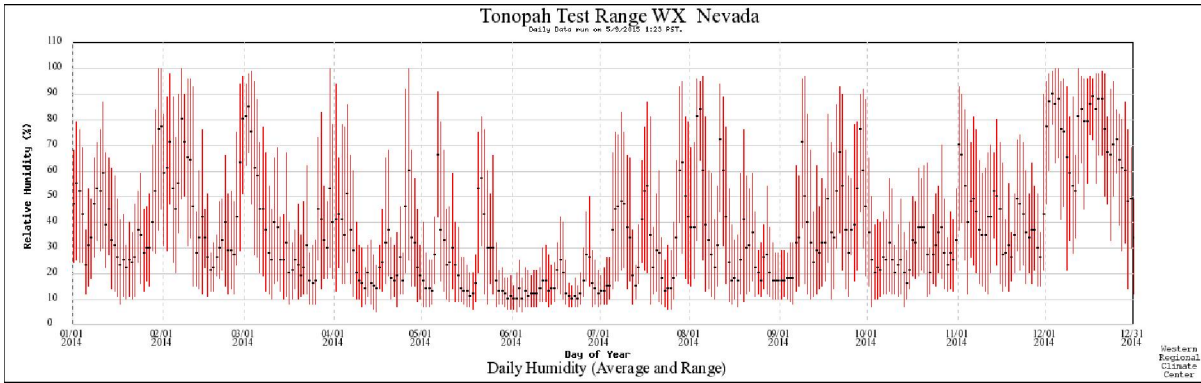


Figure C-3. Graphical summary of the humidity data, daily maximum, minimum (red bar) and average (black mark), collected by the TTR 400 station from January 1, 2014, until December 31, 2014.

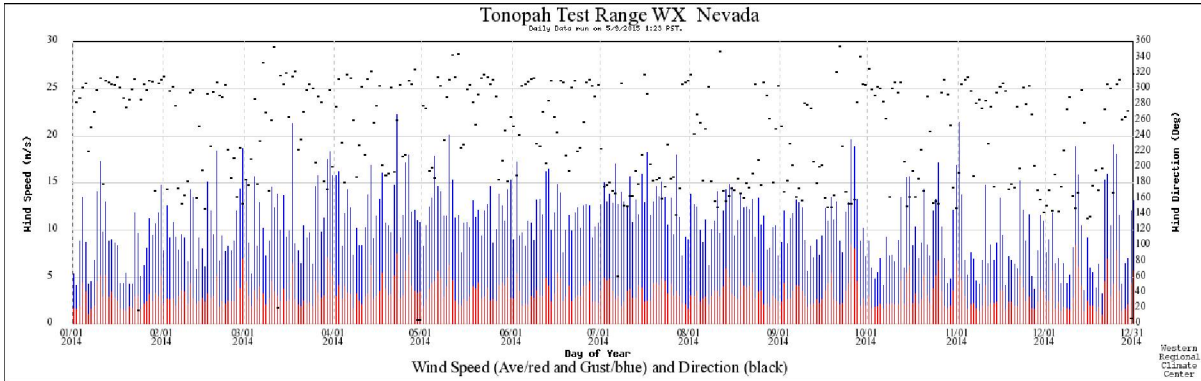


Figure C-4. Graphical summary of wind speed (daily average-red, daily peak gust- blue) and direction (black marks) data collected by the TTR 400 station from January 1, 2014, until December 31, 2014.

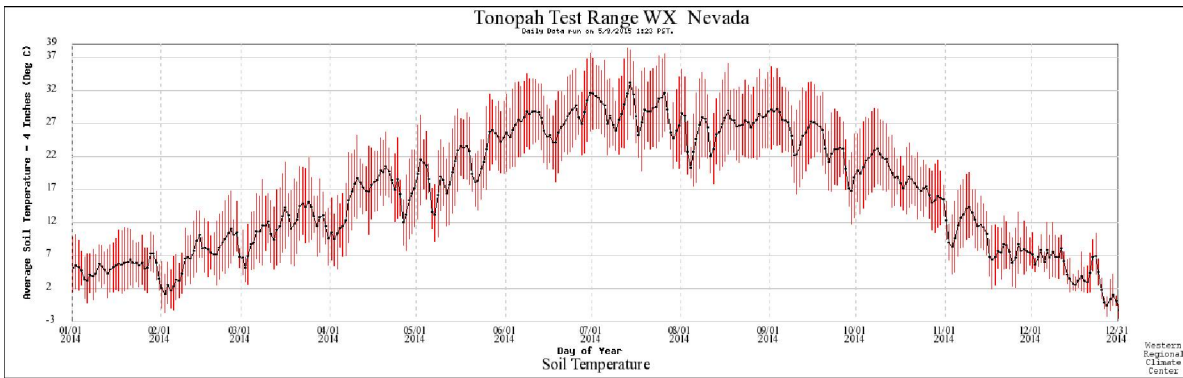


Figure C-5. Graphical summary of soil temperature data, daily maximum, minimum (red bar) and average (black line), collected by the TTR 400 station from January 1, 2014, until December 31, 2014.

Tonopah Test Range Station 400 2014

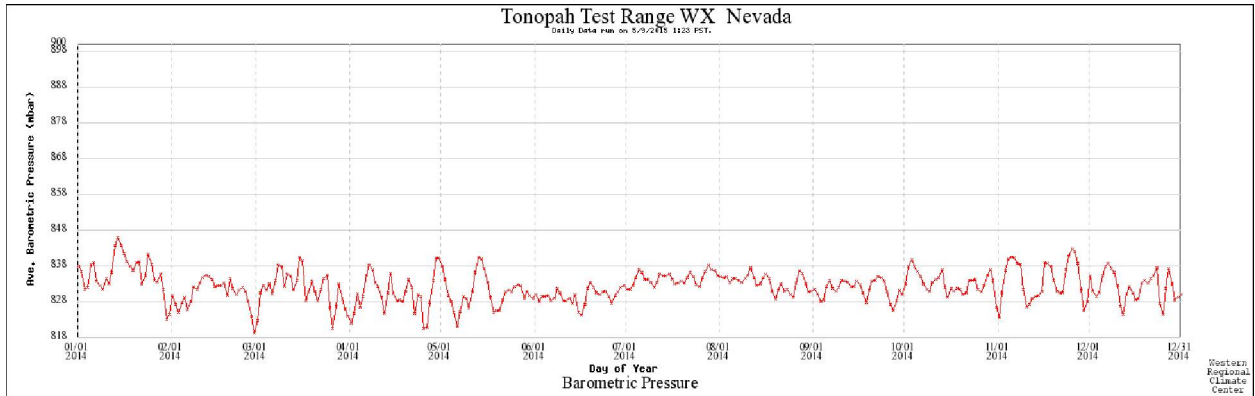


Figure C-6. Graphical summary of the daily average barometric pressure data collected by the TTR 400 station from January 1, 2014, until December 31, 2014.

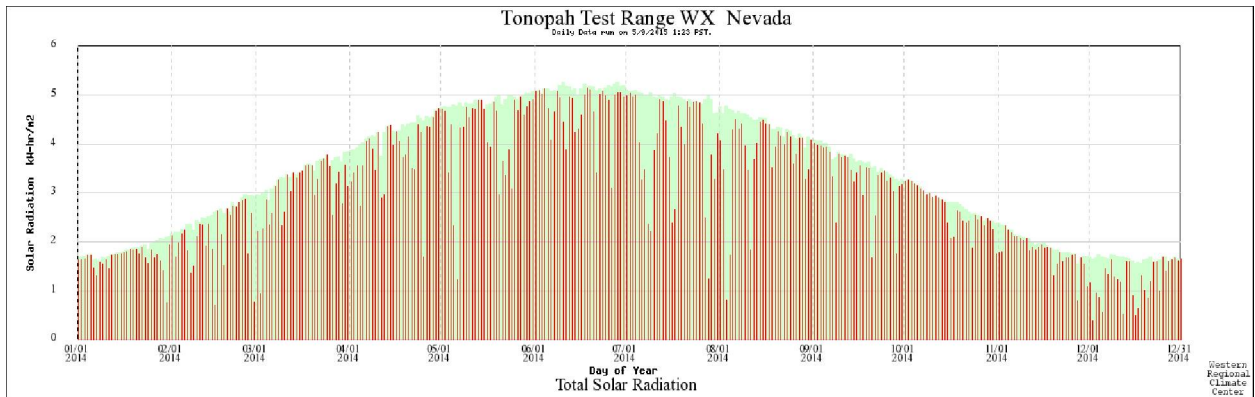


Figure C-7. Graphical summary of daily total solar radiation (red bar) data collected by the TTR 400 station from January 1, 2014, until December 31, 2014. Underlying light green shaded area represents the station period-of-record maximum daily solar radiation.

Clean Slate 3 Station 401 2014

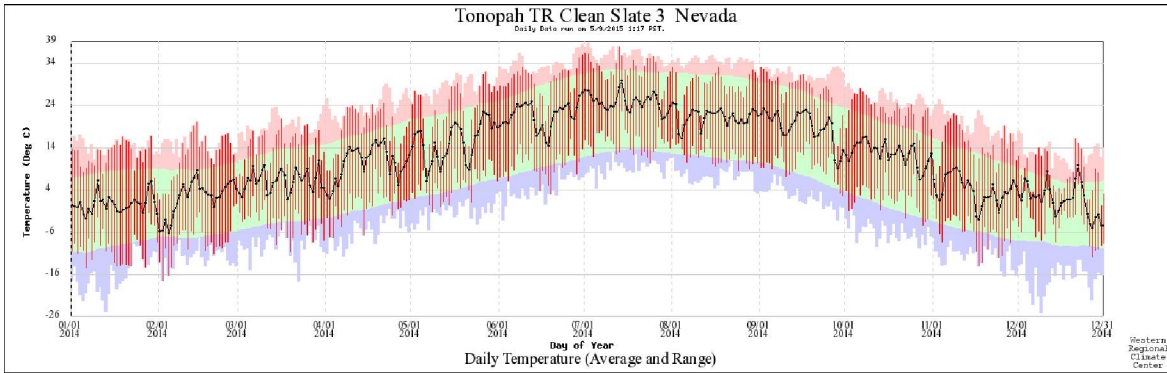


Figure C-8. Graphical summary of temperature data collected by the Clean Slate 3 station from January 1, 2014, until December 31, 2014. Underlying pastel colors represent the period-of-record extremes (red and blue) and averages (green).

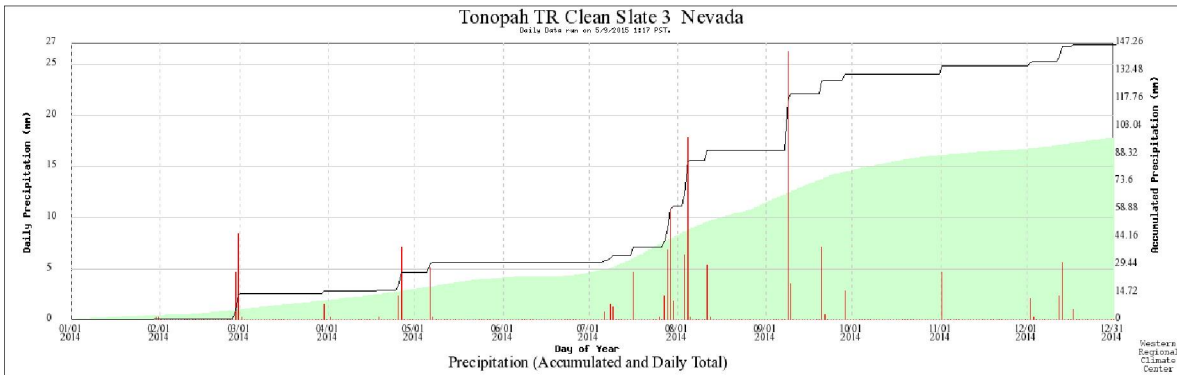


Figure C-9. Graphical summary of precipitation data, daily total (red bars) and accumulated (black line), collected by the Clean Slate 3 station from January 1, 2014, until December 31, 2014. Underlying light green shaded area represents the station period-of-record average precipitation accumulation.

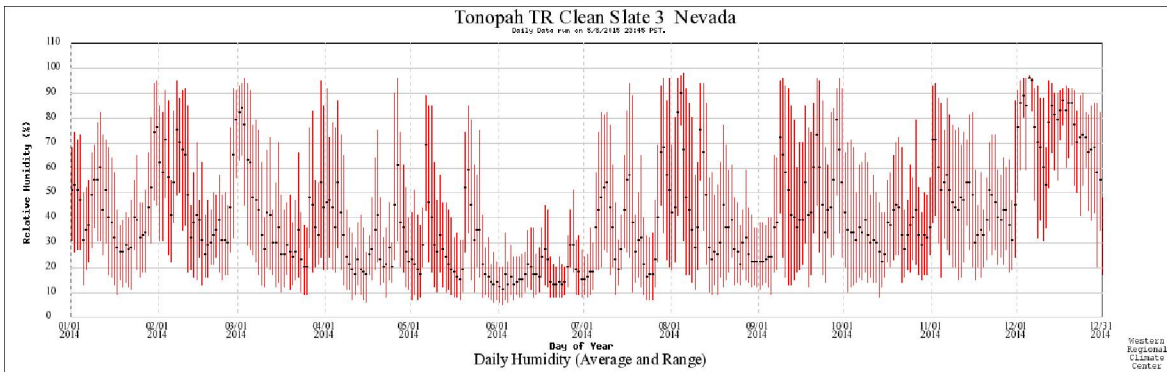


Figure C-10. Graphical summary of the humidity data, daily maximum, minimum (red bar) and average (black mark), collected by the Clean Slate 3 station from January 1, 2014, until December 31, 2014.

Clean Slate 3 Station 401 2014

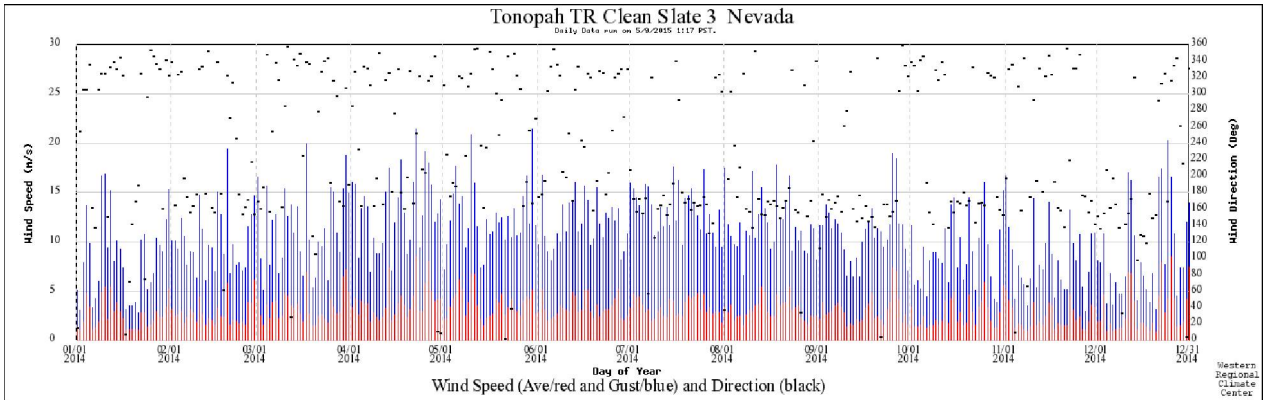


Figure C-11. Graphical summary of wind speed (daily average, red; daily peak gust, blue) and direction (black marks) data collected by the Clean Slate 3 station from January 1, 2014, until December 31, 2014.

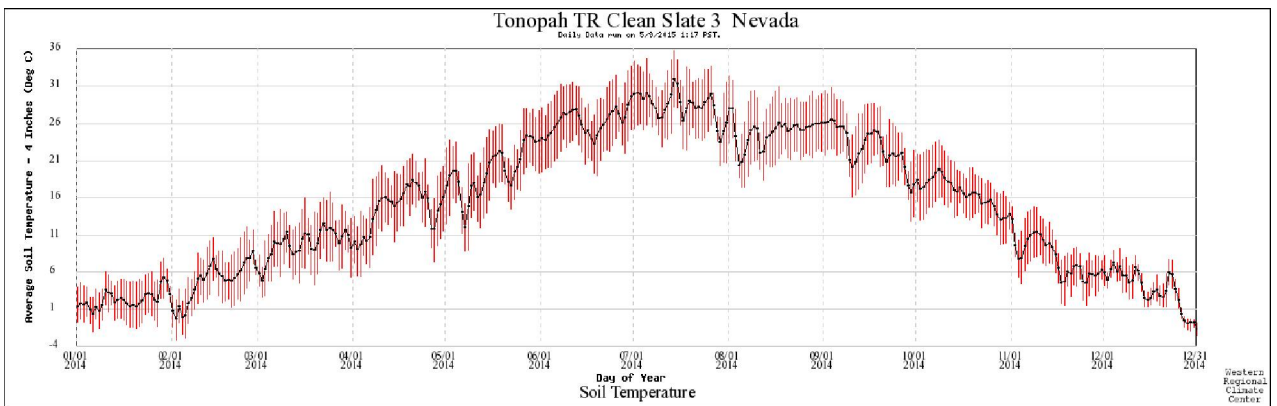


Figure C-12. Graphical summary of soil temperature data, daily maximum, minimum (red bar) and average (black line), collected by the Clean Slate 3 station from January 1, 2014, until December 31, 2014.

Clean Slate 1 Station 402 2014

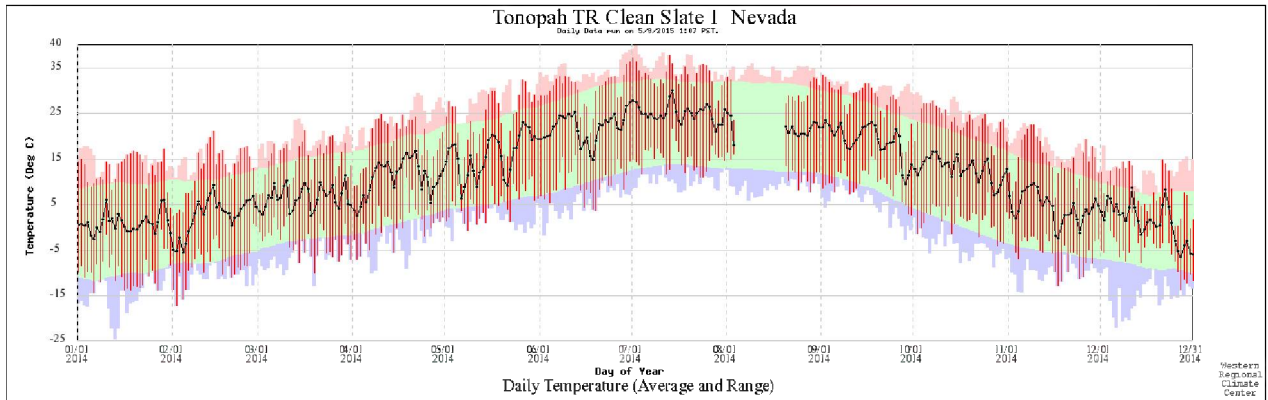


Figure C-13. Graphical summary of temperature data collected by the Clean Slate 1 station from January 1, 2014, until December 31, 2014. Underlying pastel colors represent the period-of-record extremes (red and blue) and averages (green). The data gap in August was because of equipment failure at the station.

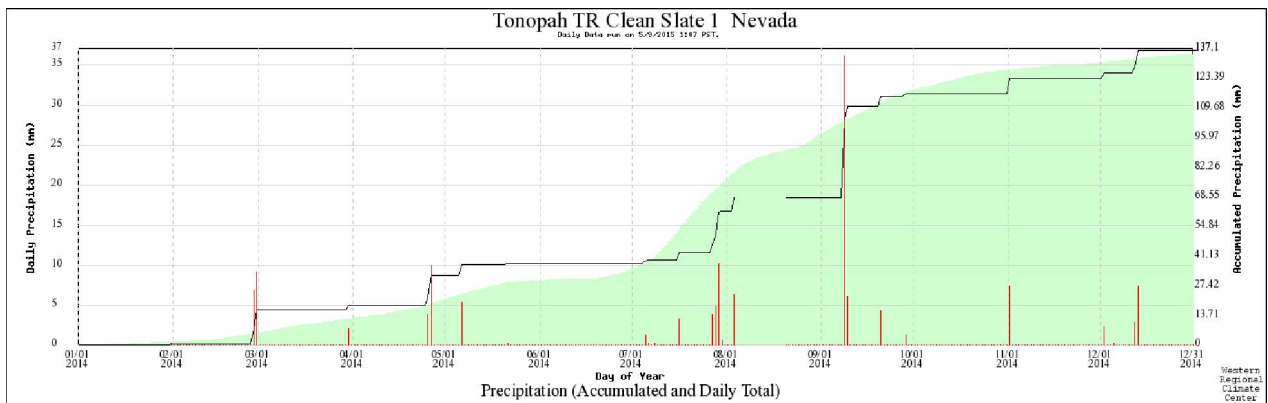


Figure C-14. Graphical summary of precipitation data, daily total (red bars) and accumulated (black line), collected by the Clean Slate 1 station from January 1, 2014, until December 31, 2014. Underlying light green shaded area represents the station period-of-record average precipitation accumulation. The data gap in August was because of equipment failure at the station.

Clean Slate 1 Station 402 2014

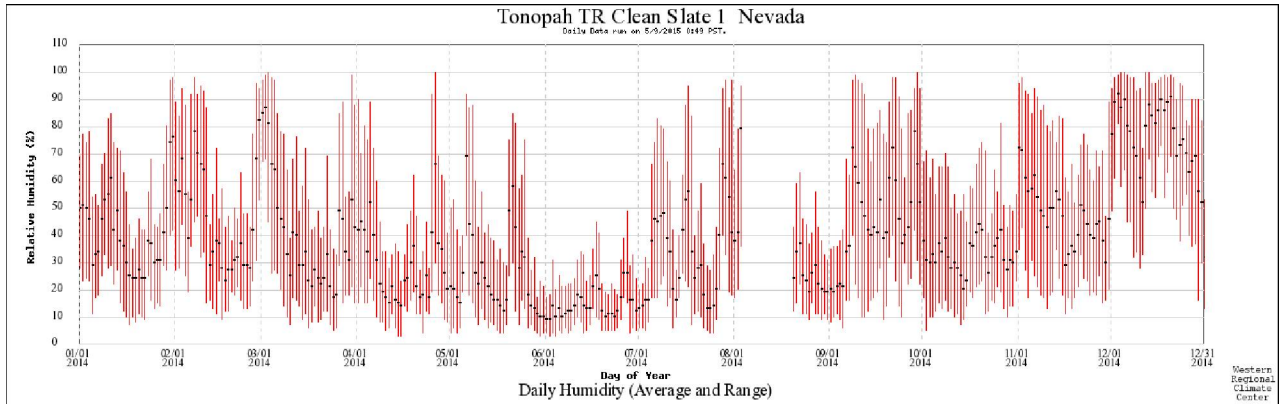


Figure C-15. Graphical summary of the humidity data, daily maximum, minimum (red bar) and average (black mark), collected by the Clean Slate 1 station from January 1, 2014, until December 31, 2014. The data gap in August was because of equipment failure at the station.

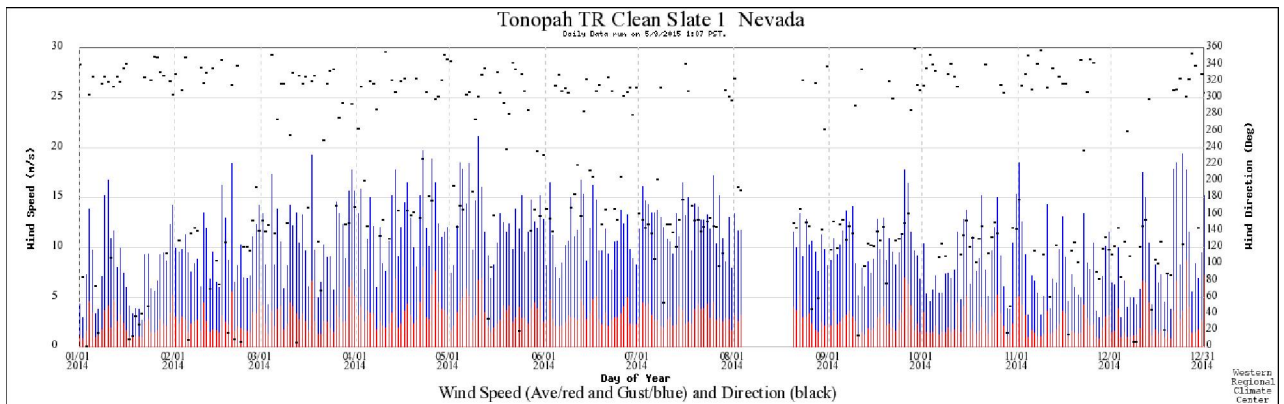


Figure C-16. Graphical summary of wind speed (daily average-red, daily peak gust- blue) and direction (black marks) data collected by the Clean Slate 1 station from January 1, 2014, until December 31, 2014. The data gap in August was because of equipment failure at the station.

Clean Slate 1 Station 402 2014

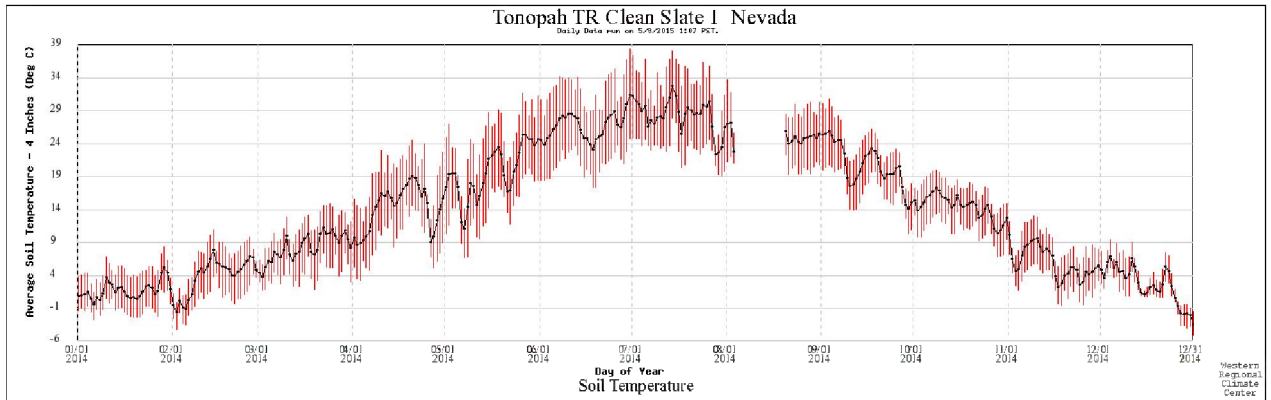


Figure C-17. Graphical summary of soil temperature data, daily maximum, minimum (red bar) and average (black line), collected by the Clean Slate 1 station from January 1, 2014, until December 31, 2014. The data gap in August was because of equipment failure at the station.

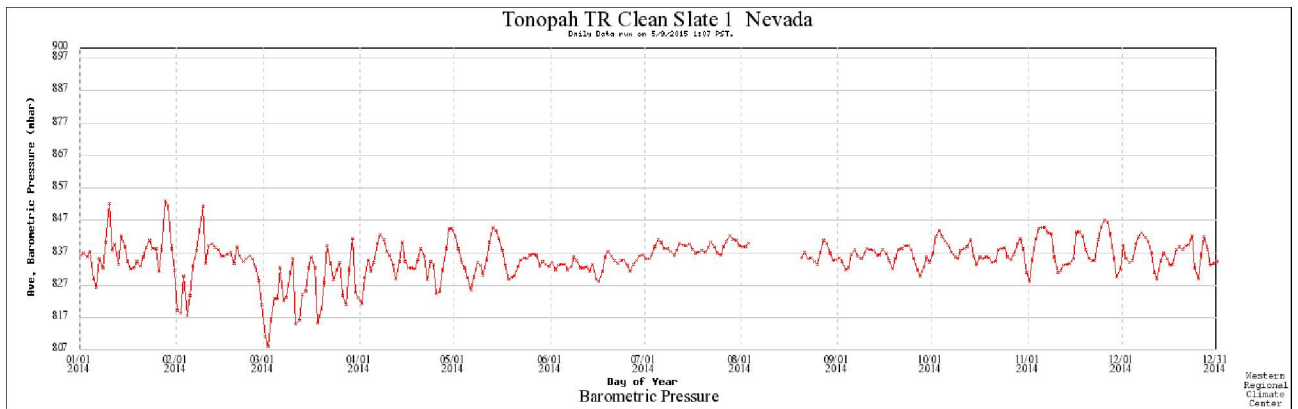


Figure C-18. Graphical summary of the daily average barometric pressure data collected by the Clean Slate 1 station from January 1, 2014, until December 31, 2014. The data gap in August was because of equipment failure at the station.

Clean Slate 1 Station 402 2014

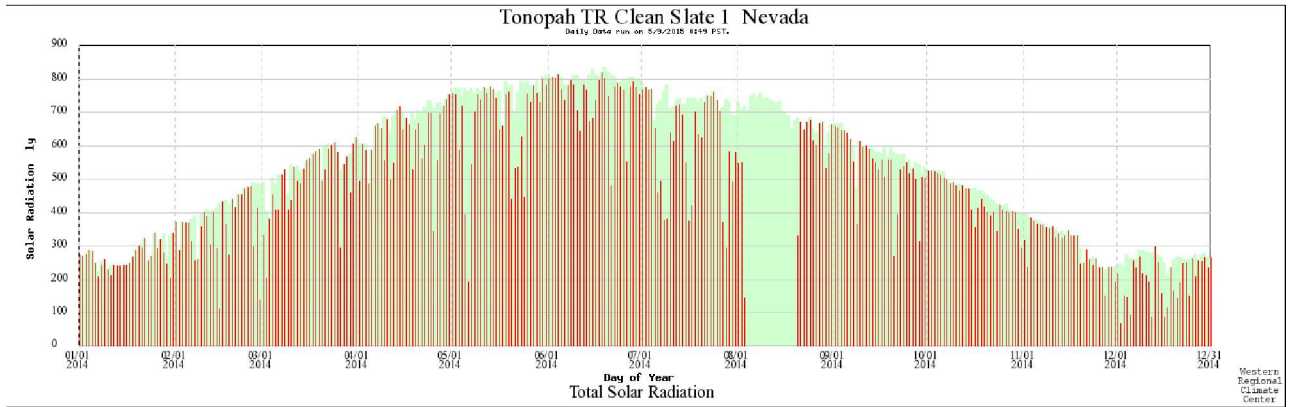


Figure C-19. Graphical summary of daily total solar radiation (red bar) data collected by the Clean Slate 1 station from January 1, 2014, until December 31, 2014. Underlying light green shaded area represents the station period-of-record maximum daily solar radiation. The data gap in August was because of equipment failure at the station.